ISTANBUL TECHNICAL UNIVERSITY ★ GRADUATE SCHOOL

A PEAK CURRENT CONTROLLED DIMMABLE SEPIC LED DRIVER WITH LOW FLICKER

M.Sc. THESIS

Kerim ÖRÜKLÜ

Department of Electrical Engineering

Electrical Engineering Programme

JANUARY 2022

ISTANBUL TECHNICAL UNIVERSITY ★ GRADUATE SCHOOL

A PEAK CURRENT CONTROLLED DIMMABLE SEPIC LED DRIVER WITH LOW FLICKER

M.Sc. THESIS

Kerim ÖRÜKLÜ
504181056

Department of Electrical Engineering

Electrical Engineering Programme

Thesis Advisor: Asst. Prof. Deniz YILDIRIM

JANUARY 2022

ISTANBUL TEKNİK ÜNİVERSİTESİ ★ LİSANSÜSTÜ EĞİTİM ENSTİTÜSÜ

DÜŞÜK FLİCKERLİ TEPE AKIM KONTROLLÜ AYARLANABİLİR SEPIC LED SÜRÜCÜ

YÜKSEK LİSANS TEZİ

Kerim ÖRÜKLÜ
504181056

Elektrik Mühendisliği Anabilim Dalı

Elektrik Mühendisliği Programı

Tez Danışmanı: Dr. Öğr. Üyesi Deniz YILDIRIM

OCAK 2022

Kerim ÖRÜKLÜ, a M.Sc. student of İTU Graduate School student ID 50418106, successfully defended the thesis/dissertation entitled "A PEAK CURRENT CONTROLLED DIMMABLE SEPIC LED DRIVER WITH LOW FLICKER", which he prepared after fulfilling the requirements specified in the associated legislations, before the jury whose signatures are below.

Thesis Advisor :	**Asst. Prof. Deniz Yıldırım** İstanbul Technical University	.....
Jury Members :	**Prof. Dr. Güven Kömürgöz Kırış** Istanbul Technical University	.....
	Asst. Prof. Nihan Altıntaş Yildiz Technical University	.....

Date of Submission : 02.01.2022
Date of Defense : 18.01.2022

To my family and friends,

FOREWORD

At first, I would like to express my special thanks to my advisor, Asst. Prof. Deniz YILDIRIM, for his guidance and endless support during my master thesis and education. I believe that his knowledge shared with me about Power Electronics will contribute a lot to me in academia and in my professional life.

In addition, I would like to thank my friends and colleagues, Umutcan POLAT for his support, and Oğuzkağan ALIÇ who help me a lot with the experimental work. Also, I would like to thank Asst. Prof. Lale Erdem ATILGAN for helping us with the tests in Lighting Technology Laboratory at Istanbul Technical University.

Finally, I must thank to my family, Salih ÖRÜKLÜ and Hamide ÖRÜKLÜ, for their great effort and support during my entire life.

January 2022 Kerim ÖRÜKLÜ

TABLE OF CONTENTS

Page

ABBREVIATIONS

LED	**:** Light Emitting Diode
SEPIC	**:** Single Ended Primary Inductor Converter
IC	**:** Integrated Chip
THD	**:** Total Harmonic Distortion
PF	**:** Power Factor
PFC	**:** Power Factor Correction
IES	**:** Illuminating Engineering Society
IEC	**:** International Electrotechnical Commission
CCM	**:** Continuous Conduction Mode
DCM	**:** Discontinuous Conduction Mode
PWM	**:** Pulse Width Modulation
RMS	**:** Root Mean Square
SMPS	**:** Switch Mode Power Supply
PCMC	**:** Peak Current Mode Control
NOEL	**:** No Observable Effect Level
Mod%	**:** Modulation (%)

SYMBOLS

C	**:** Capacitance
L	**:** Inductance
R	**:** Resistance
V	**:** Volt
I	**:** Current
D	**:** Duty Cycle
T	**:** Period
P	**:** Active Power
S	**:** Apparent Power
φ	**:** Phase Angle Between the Current and Voltage
η	**:** Efficiency
t	**:** Time
f	**:** Frequency

LIST OF TABLES

Page

LIST OF FIGURES

Page

A PEAK CURRENT CONTROLLED DIMMABLE SEPIC LED DRIVER WITH LOW FLICKER

SUMMARY

Nowadays, a considerable part of the energy consumption in the world has been formed by lighting sources used in buildings, industry, transportation, and commercial. Yet, there has been a rapid decrease in traditional energy resources. Therefore, an energy efficient lighting system could be a solution to global energy problem. Light-emitting diodes (LEDs) have been taken much attention lately and expected to replace with classical lamps due to their special characteristics like high efficiency, long lifetime, environment friendly, robustness, and small size. However, a driver circuit is required to operate LEDs and constant current drivers can improve the LEDs performance. Hence, studies on LED driver circuits and its control method have recently been increased both in industry and in academia.

In some applications, it is desirable to have control on LED brightness. This can be done by a current-control method that adjust the current flowing through LEDs. But, there are recommended practices while modulating current in High-Brightness LEDs for mitigating health risk to viewers in IEEE Std. 1789-2015. Most of the driver circuit have put on the market without any flicker measurements and checking these recommended practices about percent flicker and flicker index. All light sources may have flicker with various levels. However, the flicker generally exists in LED lighting when AC to DC conversion is present. Because of the full-wave bridge rectification in AC-DC LED drivers, LED lamps will have a peak-to-peak current ripple at twice the line frequency (100 Hz or 120 Hz). Hence, the flicker is mainly dependent on the driver circuit for LED lighting. Health risks and biological effects of flicker to the viewers such as headache, eyestrain, and seizures cannot be ignored and should be taken into consideration when designing a LED driver. A flicker-free LED driver can improve the visual performance and offer a human health friendly lighting.

In this thesis, a peak-current control method is proposed for 30-Watt Single Ended Primary Inductor Converter (SEPIC) LED driver with adjustable output current. The proposed control strategy is based on measuring MOSFET peak current value using a shunt resistor. When this voltage reaches peak threshold value, controller turns off switch. The output current is adjusted to desired levels by changing this peak threshold value. Both simulation and implementation of the driver have been carried out. 220V rms, 50 Hz AC main is used as input of the driver. Pulse Width Modulation (PWM) signals are generated by using UC3842 and TL3845 Integrated-Chips (IC). Flicker measurements are taken from the output current curve. To validate proposed peak current control method, a 33.6 Watt, 112 V / 0.3 A SEPIC LED driver prototype is constructed and tested. Analysis and measurements have been carried out for different output current levels. Peak efficiency is obtained as 88.4% at nominal output current. Furthermore, 5.806% and 6.540% of percent flicker have been obtained at 300mA and 100mA, respectively.

It has been found that the proposed Peak-Current-Mode-Controlled SEPIC LED driver offers LED brightness control for the consumer comfort, a high efficient system for energy efficiency, and a low-risk level of flicker for human health.

DÜŞÜK FLİCKERLİ TEPE AKIM KONTROLLÜ AYARLANABİLİR SEPIC LED SÜRÜCÜ

ÖZET

Günümüzde dünyadaki enerji tüketiminin önemli bir kısmını binalarda, sanayide, ulaşımda ve ticari alanlarda kullanılan aydınlatma kaynakları oluşturmaktadır. Öte yandan, geleneksel enerji kaynakları hızla azalmaya devam etmektedir. Bu nedenle, enerji verimli bir aydınlatma sistemi, küresel enerji sorununa bir çözüm getirebilir. Işık yayan diyotlar (Light Emitting Diodes- LEDs), yüksek verimlilik, uzun ömür, çevre dostu, sağlamlık ve küçük boyutları gibi özellikleri nedeniyle son zamanlarda büyük ilgi görmektedir ve LED'lerin klasik lambaların yerini alması beklenmektedir. Ancak LED' leri çalıştırmak için bir sürücü devresine ihtiyaç vardır ve akım kontrollü sürücüler LED'in performansını artırabilir. Bu nedenle, son zamanlarda LED sürücü devreleri ve bu devrelerin kontrol yöntemleri ile ilgili çalışmalar akademide ve sanayide daha fazla ilgi görmektedir.

LED'ler doğru akım (Direct Current- DC) ile çalışmaktadırlar. LED' in Akım-Gerilim (I-V) eğrisi diyotun çalışma eğrisine benzemektedir. LED'e uygulanan gerilim eşik gerilimine ulaşıncaya kadar LED üzerinden bir akım akmaz. Bu eşik gerilimine ulaştıktan sonra akım akmaya başlar. Yüksek Parlaklı LED'lerin (High-Brightness LEDs) çalışma gerilimi genellikle 2.5 V ve 4 V arasında değişirken, bu LED'lerin çalışma akımları 50 mA ve 300 mA arasında değişmektedir. Fakat daha kuvvetli bir aydınlatma elde etmek için LED'ler seri, paralel veya seri/paralel diziler halinde bağlanabilirler. Bu durumda, yük olarak birbirine seri olarak bağlanmış birden fazla LED düşünülürse, LED'leri çalıştırmak için uygulanması gereken minimum gerilimin LED' lerin gerilim düşümlerinin toplamına eşit olması veya bu gerilimden yüksek olması gerekmektedir. Genellikle gereken doğru gerilim AC şebekeden tam-dalga-köprü-doğrultucu ve doğrultucu önünde bir kapasite yardımıyla elde edilir. Türkiye'de AC şebeke etkin gerilimi (Root Mean Square-RMS) 220 Volt iken, şebeke frekansı 50 Hertz'dir. Şebeke gerilimi doğrultulduktan sonra, bir sürücü yardımıyla LED'in nominal çalışma akımı ve gerilimi elde edilmeye çalışılır. LED' e giden akımı bir direnç yardımıyla sınırlama veya doğrusal gerilim ayarlayıcı ile LED'e giden akımı kontrol etme gibi LED sürücü yöntemleri vardır. Ancak bu yöntemlerin enerji verimliliği oldukça düşüktür. Bu yüzden, LED sürücülerinde verimliliği artırma noktasında yüksek kontrol kabiliyetleri ile anahtarlamalı güç kaynakları (Switching Power Supplies) tercih edilebilir.

Genelde, şebekeden beslenen bir AC-DC LED sürücü devresinde sırası ile bir AC-DC dönüştürücü, ardından DC-DC dönüştürücü ve en son olarak LED gelir. Bu yapıda en çok karşılaşılan problemlerden ilki, AC-DC dönüştürücüden hemen sonra gelen büyük elektrolitik kapasite sebebiyle kaynaktan çekilen giriş akımının toplam harmonik bozunumu (Total Harmonic Distortion-THD) yüksek olması ve girişte güç faktörünün düşük olmasıdır. Şebeke güç kalitesini düşürmemek için, genellikle güç elektroniği devreleri içeren LED sürücüleri gibi elektronik aygıtlar tarafından çekilen şebeke

akımı harmonikleri Uluslararası Elektroteknik Komisyonu (International Electrotechnical Commission-IEC) tarafından IEC61000-3-2 standardına göre sınırlandırılmıştır. Bu standarda göre aydınlatma aygıtları C kategorisinde içinde bulunmaktadır. Güç faktörünü 1' e yaklaştırmak ve akımı olabildiğince şebeke gerilimine özdeş tutmak için Güç Faktörü Düzelten (Power Factor Correction- PFC) sürücü devreleri bulunmaktadır. Çoğunlukla GFD devrelerde, doğrultma işleminden sonra gelen büyük elektrolitik kapasite devreden kaldırılarak, giriş akımının giriş gerilimini takip etmesini sağlayan kontrol yöntemleri uygulanmaktadır. Bu sayede, şebeke kalitesini bozmayan güç faktörü yüksek LED sürücüleri tasarlanmış olur. Ayrıca, ortalama ömrü 5000 saat olarak bilinen elektrolitik kapasitenin kaldırılması sürücünün de ömrünü uzatmaktadır. Tahmin edilen ömrü 50000 saat olan LED'ler, elektrolitik kapasitelerden tam 10 kat daha uzun ömürlüdür. Aslında, LED ve LED sürücüsü bir paket halinde düşünülürse, bu paketin ömrü sürücü devresi tarafından belirlenmektedir. Elektrolitik kapasitenin devreden kaldırılması, bu yapıya daha uzun bir ömür sağlayabilir.

Lakin GFD sürücülerde elektrolitik kapasitenin devreden kaldırılması beraberinde "flicker" diye adlandırılan, aydınlatma cihazlarında karşılaşılan bir sorunu daha belirgin bir hale getirmektedir. Flicker Türkçe olarak "kırpışma" veya "titreme" adlandırılmaktadır. Flicker Aydınlatma Mühendisliği Topluluğu (Illuminating Engineering Society- IES) tarafından "anlık parlaklık değişimleri" olarak tanımlanmıştır. Yüzde flicker [Percent Flicker- Modulation (%)] ve Flicker indeks (Flicler Index) bu değişimi ölçmek için en sık kullanılan metriklerdir. Flicker olayı izleyiciler- yani insanoğlu tarafından çıplak gözle fark edilebilir veya fark edilemez seviyelerde gerçekleşmektedir. "Görünür flicker" frekans aralığı 3 Hz' den 70 Hz'e kadar tanımlanmış olsa da insandan insana göre bu aralık farklılık gösterebilir. 70 Hz üzeri flicker frekansları "görünmez flicker" olarak tanımlanmaktadır. Görünmez flicker gözle görülemeyecek kadar hızlı olmasına rağmen, insan retinasının 100 Hz ila 160 Hz frekansları aralığındaki ışık modülasyonunu çözebildiği saptanmıştır. Görünen ve görünmeyen flickerin insan sağlığı üzerinde potansiyel riskleri olabilir. Bunlardan bazıları: baş ağrısı, göz yorgunluğu, görme bozukluğu, migren, vertigo, epilepsi ve nöbet gibi insan sağlığını olumsuz etkileyen ciddi biyolojik etkilerdir ve göz ardı edilemez. Bu etkilerden, epileptik nöbet birkaç saniyelik görünür flickere maruz kalma sonucu hemen gerçekleşebilir. Ayrıca, uzun süreli görünmez flickere maruz kalma sonucu baş ağrıları, görme performansında düşüklük gibi insan sağlığı üzerinde olumsuz etkileri görülebilir.

AC-DC LED sürücülerinde doğrultma işleminden sonra aslında tam bir doğru gerilim elde edilmez. Elde edilen gerilim, bir DC bileşen ve şebeke frekansının iki katı yani Türkiye için 100 Hz olan bir AC bileşenden oluşmaktadır. Bu 100 Hz'lik AC bileşen, LED üzerine uygulanan gerilime de yansımaktadır. Tepeden tepeye (Peak-to-Peak) AC gerilim dalgalanma büyüklüğüne göre, LED' in akımı daha büyük oranlarda dalgalanma yapacaktır. LED'in parlaklığının, LED'in üzerinden geçen akım ile doğru orantılı olduğu düşünülürse, akımdaki 100 Hz'lik AC dalgalanma aslında LED'in 100 Hz'lik frekansla flicker yapmasına sebep olacaktır. IEEE Güç Elektroniği Topluluğu tarafından (IEEE Power Electronics Society) IEEE 1789-2015 standardı kapsamında, Yüksek Parlaklık LED'lerde akım değişiminin izleyicilere yönelik sağlık riskini azaltmak için önerilen uygulamalar vardır. Önerilen uygulamaya göre, 100 Hz'lik flicker frekansındaki Yüzde Flicker %8'in altında olması gerekirken, Flicker indeks 0.1'in altında olmalıdır. Sürücü devrelerinin çoğu, herhangi bir Flicker ölçümü yapmadan ve Flicker yüzdesi ve Flicker indeksi ile ilgili bu önerilen uygulamaları

kontrol etmeden piyasaya sürülmektedir. Flickerin izleyiciler üzerindeki biyolojik etkileri göz ardı edilemez ve bir LED sürücüsü tasarlanırken bu etkiler göz önünde bulundurulmalıdır. Flickersiz bir LED sürücü görsel performansı iyileştirebilir, insan sağlığı için daha sağlıklı bir aydınlatma sağlayabilir. Literatürde çalışmalar LED'i sürecek olan akımı olabildiğince doğru akıma yaklaştırma yönündedir.

Bu tezde, çıkış akımı ayarlanabilir 30 Watt SEPIC LED sürücüsü için bir tepe akım kontrol yöntemi önerilmiştir. Sürücü girişi olarak 220V rms, 50 Hz AC şebeke kullanılmıştır. Yarı iletken anahtar sürme kolaylığı ve devre çıkışındaki polaritenin giriş ile aynı olması sebebiyle DC-DC dönüştürücü olarak SEPIC (Single Ended Primary Inductor Converter) seçilmiştir. Çıkış akımının ayarlanabilir olması için Tepe Akım Modu kontrol (Peak-Current-Mode-Control) yöntemi seçilmiştir. Önerilen kontrol stratejisi, bir şönt direnç kullanarak devredeki anahtarın tepe akım değerinin ölçülmesine dayanmaktadır. Bu akım değeri, tepe eşik değerine ulaştığında kontrolcü anahtarı kapatmaktadır. Tepe eşik değeri değiştirilerek çıkış akımı istenilen seviyelere ayarlanmaktadır. Anahtar tepe akımı her anahtarlama periyodunda ölçüldüğünden, anahtarın yanmasına sebep olacak aşırı akımlar önlenmiş olur ve sistem ani değişimlere kapalı döngü kontrol (Closed Loop Control) yöntemiyle hızlı cevap vermektedir. Darbe Genişlik Modülasyonu (Pulse Width Modulation- PWM) sinyalleri, UC3842 ve TL3845 akım kontrol entegreleri kullanılarak üretilmiştir. Önerilen sürücünün hem simülasyonu hem de uygulaması yapılmıştır. Simulasyonda anahtarlama frekansı 100 kHz, uygulamada ise 40 kHz seçilmiştir.

Simülasyonun ilk kısmında önerilen kontrol yöntemi, güç faktörü kötü olan klasik bir AC-DC LED sürücü üzerinde denenmiştir. Önerilen kontrol yöntemi ile 50 mA ve 300 mA arasında akım kontrolü yapılabildiği kanıtlanmıştır. Ayrıca, ölçülen flicker metriklerinin önerilen limitlerin içinde kaldığı tespit edilmiştir.

Simülasyonun ikinci kısmında, güç faktörünü iyileştirmek hedeflenmiştir. Doğrultucudan sonra gelen kapasite devreden kaldırılmıştır ve AC girişten bir referans alınarak akımın giriş gerilimini takip etmesi sağlanmıştır. Güç faktörü 0.98' yakın tutulurken, çıkışta 100 mA ve 300 mA arasında akım ayarı yapılmıştır. Devre 300 mA altında çalıştırılırken, yüzde flicker önerilen limitlerin biraz üzerinde ölçülmüştür ancak flicker indeks hep 0.1 limitinin altında kalmıştır.

Önerilen kontrol yöntemi doğrulamak için, 33.6 Watt, 112 V, 300 mA bir SEPIC LED sürücü devresi kurulmuştur. Farklı çıkış akım seviyeleri için analiz ve ölçümler yapılmıştır. Maksimum verim, devre nominal çıkış akımında çalışırken %88.4 olarak bulunmuştur. Elde edilen sonuçlar, 100mA ve 300 mA arasında akım kontrol yapılabileceğini ve sürücünün %80'in üzerinde bir verimle çalıştırılabileceğini göstermektedir. Ayrıca 300mA ve 100mA'da sırasıyla %5.806 ve %6.540 oranında yüzde flicker elde edilmiştir. Bu tezde önerilen kontrol yönteminin başka sürücü devrelerinde rahatlıkla kullanılabilir olduğunu hatırlatmakta fayda vardır. Sonuç olarak, önerilen Tepe-Akım-Modu-Kontrollü SEPIC LED sürücünün, tüketici konforu için LED parlaklık kontrolü, enerji verimliliği için yüksek verimli bir sistem ve insan sağlığı için düşük riskli bir flicker seviyesi sunduğu tespit edilmiştir.

1. INTRODUCTION

Nowadays, light emitting diodes (LEDs) are preferred in general lighting applications due to their high luminous efficacy, long lifetime, robustness, and small size [1], [2]. Halogen bulbs, fluorescent and compact fluorescent lamps (CFL) and high intensity discharge (HID) lamps are some of the other lighting technologies used in the industrial, commercial and residential lighting [3]. Lighting applications forms a large part of electricity consumption in the world. Hence, the most important subject when designing a lighting system is to reduce energy consumption and increase efficiency like in any other electrical system/application. Therefore, LED's have been replaced with classical bulbs in recent years since they use less electricity and generates less thermal dissipation. Moreover, LED's are environment friendly because they do not contain any mercury like the fluorescent lamps [3], [4].

However, the driver circuit plays remarkable role in dominating the energy efficiency. The overall system efficiency can be increased with an appropriate driver circuit [4]. The efficiency of conventional LED drivers including resistor based current limiters, charge pumps, and linear regulators is low [5]. The high efficiency can be acquired by switched mode power supplies with a high control accuracy that make them unique as high-power LED drivers [5]. Classical LED drivers can be subdivided into single-stage and two-stage LED drivers [4], [6]. Single stage driver is a DC/DC converter with constant output current which can accomplished power factor correction. Two-stage driver has PFC circuit that is responsible for high power factor and DC/DC converter, separately. With the advancing technologies, integrated-stage topologies which can merge PFC stage and DC/DC stage into one stage by sharing active power switches and control circuits are designed to overcome the large size and high cost of the two stage converters [4]. High efficiency, high reliability, and fast output dynamics can be acquired by integrated stage converters. Besides, a current loop is mostly included to control stage of DC/DC converter to obtain constant current control, since the LED luminosity depends on the current flowing through LED lamp. Furthermore, a current balance stage will be needed when multiple arrays of LED are adopted [4], [7].

Many circuit topologies and control algorithms have been developed to improve system power factor for LED drivers. Passive power factor correction and active power factor correction circuit topologies are well explained in [8] for researchers interested in PFC circuits. Among them, well known active power factor correction switch mode power supplies that are buck, boost, buck-boost, Flyback and fourth-order CUK, SEPIC and Zeta converters etc. can be used as LED drivers while keeping the PF close to unity. These converters can operate in continuous conduction mode (CCM), discontinuous conduction mode (DCM), and boundary conduction mode (BCM). In addition, SMPS used for LED drivers can be classified according to the converter whether is isolated/non-isolated or step-up/step-down.

Furthermore, PFC LED drivers can be categorized according to control techniques such as current mode control and voltage mode control. Several known methods related with current mode control are average current control, peak current control, and I^2 average current control. As well as, there are digital PFC control techniques that are expected to replace the analog PFC control techniques due to development in digital circuits [8].

Another key point when driving LEDs is that the light modulation that is also called as flicker, flutter, and shimmer. Flicker is defined as "variations of luminance in time" [9]. Percent flicker [Modulation (%)] and flicker index are the most commonly used metrics to quantify this variation [9], [10]. All light sources may flicker with various levels. However, the flicker exists in LED lighting when AC to DC conversion is present. In that case, LED lamps will have a peak-to-peak current ripple at twice the line frequency (100 Hz to 120 Hz). Hence, the flicker is mainly dependent on the driver circuit for LED sources. Visible (3 Hz to 70 Hz) and invisible flicker can have potential risks on human health. Health risk and biological effects of flicker cannot be ignored. Headache, eyestrain, and seizures are some of them. The detailed information about flicker and its biological effects are explained in related section and in [9].

1.1 Literature Review

In literature [2], an average current controlled PFC SEPIC LED driver is proposed for 30-Watt , 12 V/ 2.5 A LED. Universal input voltage 85-265 V AC, 50 Hz is used. High power factor and THD are obtained within the input voltage range. However, the

results are obtained from the simulation and the proposed driver circuit is not implemented.

In literature [11], a peak current mode control strategy is proposed for Power Factor Correctors that are used to drive high-brightness LEDs. With a special selection of the compensation slope, minimum THD levels and high power factor are obtained. 45-Watt, 14-16 V / 3 A PFC Fly-back topology is prototyped and tested. For the implementation of control strategy, current-mode-controller UC3843 is used. Proposed control method has kept PF close to unity even when the line frequency is increased from 60 Hz to 800 Hz. This has been achieved by cycle-by-cycle of input current. Even so, the converter has not been designed for dimming function.

In literature [7], A voltage mode controlled 240 Watt SEPIC LED driver with an output voltage of 24 V is proposed to be used in automotive and railway LED applications. Input voltage of the converter varies between 16 V and 36 V. The closed loop stability of the converter has been analyzed using average switch model under possible input voltage and load conditions. Although, the load has been chosen as resistor instead of LED.

In literature [12], Single stage high power factor 6 Watt SEPIC LED driver is proposed. SEPIC inductors are realized in the same core. The compatibility of input current harmonic spectrum to IEC 61000-3-2 standard is examined. However, an open loop control method is preferred.

In literature [13], a single stage single switch LED driver based on the integrated SEPIC circuit and Class-E resonant converter is proposed to be used for street lighting system in. High power factor is obtained by operating the SEPIC converter in discontinuous conduction mode. Soft switching is achieved by resonant converter, so that switching losses are reduced, system efficiency is improved. 100 Watt, 50 V laboratory prototype is built. Low THD, high power factor and around 91% of efficiency have been obtained in full load condition.

In literature [14], a PWM dimmable digital LED driver is proposed to control the brightness of LED. PIC16F877A microcontroller is used to generate 1.95 kHz PWM signal for dimming. LED current and luminous flux have been measured at different duty cycles of PWM signal. But, the LED power was very low around 1 Watt.

In literature [5], a flicker-free AC-DC LED driver is proposed to increase the lifetime of LED drivers by removing electrolytic capacitor from the driver circuit. Because, the lifetime of an electrolytic capacitor is much less than the lifetime of LEDs. However, when the electrolytic capacitor is removed, the current at the output will pulsate twice the line frequency. AC component of this pulsating current that causes light flicker is absorbed by the proposed bidirectional buck/boost converter. Therefore, there will be only a dc component to drive the LEDs and light flicker will be absent. 33.6 Watt, 48 V / 0.7 A prototype is constructed with around 90% efficiency by the proposed AC-DC driver. The driver circuit consists of an electrolytic capacitor-less PFC fly-back and a bidirectional buck/boost converter. As for the control variable, the average value of the driving current is taken to regulate output flux of the LEDs. UC3843 controller is preferred.

In literature [15], a ripple cancellation method is introduced to remove the twice the line frequency LED current ripple in conventional offline single-stage PFC LED drivers. If the ripple is cancelled from the output current, there will be only a pure dc current to drive LEDs. Flicker-free LED driving will be achieved by this method. In proposed method, an opposite twice line frequency ripple voltage is intentionally generated by another converter (called as Ripple Cancellation Converter) to compensate the ripple at output current. A 35-W, 50V/0.7 A Flyback and 10-W, 50V/0.2 A Buck-Boost LED drivers have been implemented by proposed control technique. Around 85% efficiency has been obtained by both converters. Moreover, the percent flicker is obtained as 5.4% from the sensed light output in proposed buck-boost LED driver.

1.2 Purpose of Thesis

The main contribution of this thesis is to adjust brightness of LED and flicker-free operation by proposing a peak current mode control method. Consequently, the consumers can adjust LED brightness as demanded, where LED current is adjusted by a control voltage. Furthermore, it is aimed to bring solution to flicker producing LED lighting sources, which are driven by a driver and likely to produce harmful effects on human health. A comprehensive measurement of percent flicker and flicker index have been introduced by using LED driving current. In the power stage of driver design, SEPIC converter is preferred since the switch is easy to drive and there is no reverse

polarity at the output. In the control stage of the driver, closed loop control is preferred by using Current-Mode-Controllers UC3842 and TL3845.

1.3 Outline of Thesis

In Chapter 1, literature review and purposes of the thesis are expressed in detail. The other parts of the thesis are organized as follows.

In Chapter 2, SEPIC converter is introduced and analyzed in continuous conduction mode. The special selection of the active and passive components of the converter and their mathematical calculations are represented. Voltage mode control and current mode control techniques are compared comprehensively. Moreover, expected features from a LED driver are listed and peak current mode control method is chosen as the optimum control technique.

In Chapter 3, electrical characteristics of LED are explained. Flicker issue in LED lighting is investigated in-depth and biological effects of flicker are discussed. Flicker limits are given for both percent flicker and flicker index. Finally, a peak-current-mode-controlled SEPIC LED driver is proposed to adjust brightness of the LED. Proposed control methodology is introduced mathematically. Two LED driver circuits: with power factor correction and without power correction are represented by proposed method.

In Chapter 4, simulation results of complete LED driver including power and control circuits are given and discussed. Simulations of the PFC and without PFC drivers are held in PSIM. Output current control of the LED string by proposed control method is validated. Power factor comparison is carried out. In addition, flicker limits of the related circuits are revealed. In Chapter 5, proposed PCMC SEPIC LED driver is carried out in practice.

In Chapter 6, the results obtained in Chapter 4 and 5 are discussed, and the motivation of this thesis is summarized.

2. CIRCUIT OPERATION ANALYSIS of CCM SEPIC CONVERTER

In this chapter, passive elements and semiconductor devices used in SEPIC converter are explained first. The related voltage and current waveforms such as inductor currents, switch current, and switch voltage of the SEPIC converter that operates in continuous conduction mode are presented. Each component parameter calculation, switching device selection and important design criterias are given. State-space averaging technique is introduced and applied to the SEPIC converter. Voltage and current mode control methods are explained for Switch-Mode-Power-Supplies. Peak-current-mode-control method advantages in LED drivers mentioned.

SEPIC converter consists of a single switch, a diode (D), two-inductors (L_1, L_2), a coupling capacitor (C_c), and an output capacitor (C_{OUT}) as shown in Figure 2.1. The DC voltage at the input of the converter can be rectified from the AC mains or it can be directly a dc voltage source such as PV panels, batteries. Inductors can be realized in the same core that is called as coupled inductor. The load is represented as R in usual.

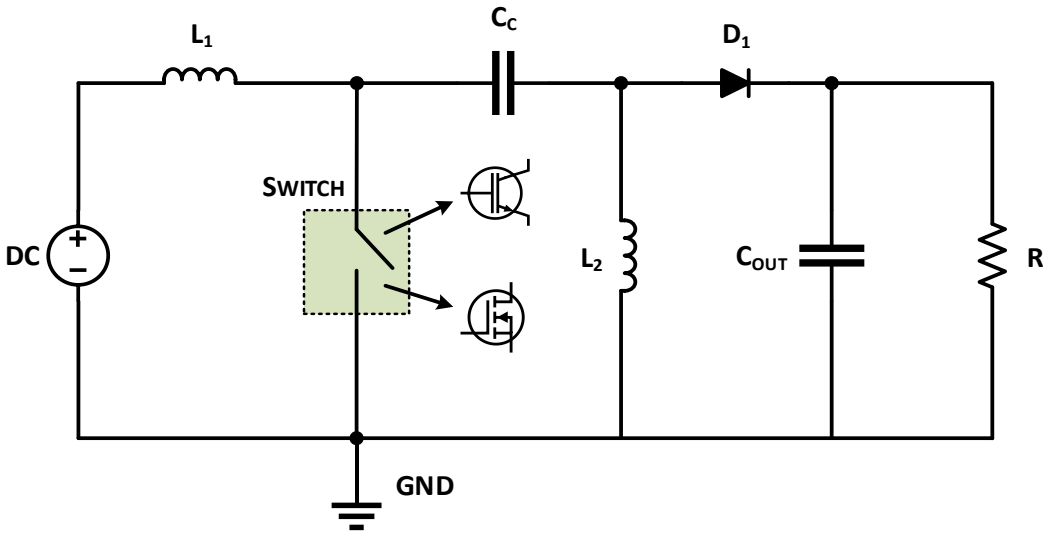

Figure 2.1 : General DC-DC SEPIC converter.

The general principle of the converter lies on switching the semiconductor device at a certain frequency. This switch can be a MOSFET or IGBT depending on the application needs. The switching frequency and the power ratings of the converter are

the two important parameters when choosing the switching device. After the brief information about the circuit elements, CCM operation of the SEPIC converter is explained in next section.

2.1 CCM Operation of SEPIC

When the switch is replaced by a MOSFET, the voltages and currents belong to SEPIC converter elements are indicated in Figure 2.2. As the name "Continuous conduction mode" implies, the inductor currents never reach the zero point at any time. Continuous conduction mode operation basically includes two stage which are the switch on and switch off intervals. The boundary conduction mode and the discontinuous conduction mode occurs when the inductor peak-to-peak current ripple is equal to or greater than average inductor current in a DC-DC converter. In DCM mode, there is a third interval, which both MOSFET and diode are off.

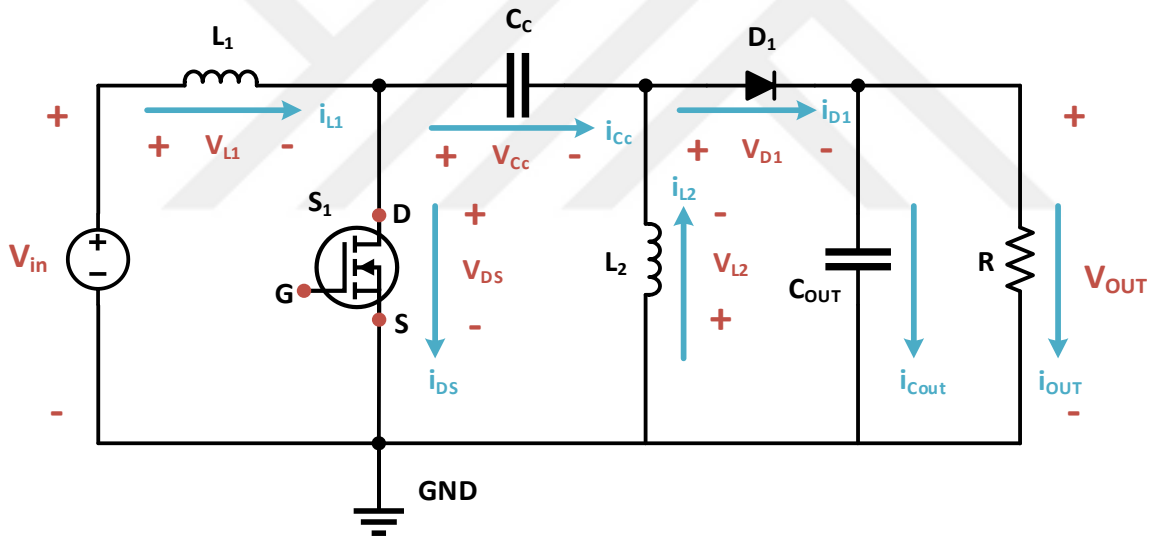

Figure 2.2 : SEPIC converter.

A pulse-width modulation signal is applied to gate-source pin of the MOSFET to turn on/off the switch. When the PWM signal is high, MOSFET is closed. If the PWM signal is low, MOSFET is open since there is no voltage applied to gate-source pin. For the two operation intervals in CCM, the equivalent circuits are represented in Figure 2.3.

The MOSFET is turned on/closed in the first interval DT_s, where D is the duty cycle. The input voltage is applied to inductor L_1. The inductor current i_{L1} starts to increase with a slope of V_{in}/L_1 until the end of this interval. The capacitor voltage V_{Cc} is applied

to inductor L_2. Likewise, the i_{L2} starts to increase. The MOSFET current will be equal to sum of the two inductors' current $(i_{L1} + i_{L2})$. The diode D_1 is off and the output capacitor C_{out} supplies the load.

The MOSFET is turned off/open, in the second interval $(1 - D)T_s$. Both inductor current starts to decrease with a slope of $(-V_{OUT}/L_{1,}L_2)$, since $-V_{OUT}$ is applied to the inductors. During this stage, the diode D_1 is conducting and the current flowing through the diode is the sum of the two inductors' current. The diode current feeds the output section both capacitor and load. One period (T_s) of operation is now completed by the second interval finishes and the first interval begins again. This repetitive procedure goes on like T_s , $2T_s$, $3T_s$ and so on. After the explanations of operation mechanism, the important waveforms of the circuit elements are illustrated in Figure 2.4 and Figure 2.5.

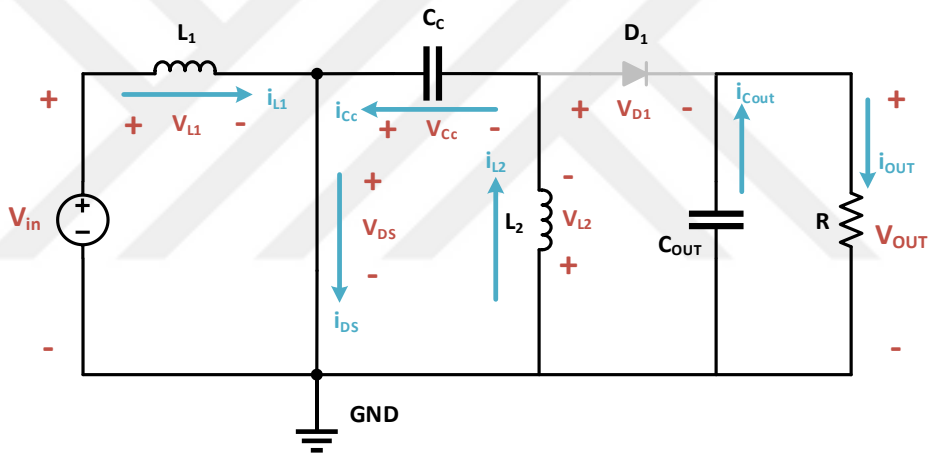

(a) Interval DTs

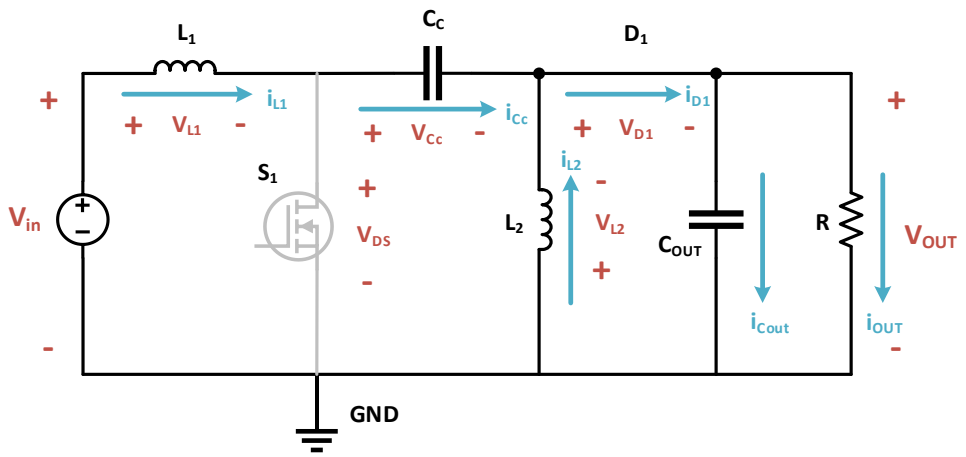

(b) Interval (1-D)Ts

Figure 2.3 : Operations stages of CCM SEPIC converter: a)Switch on. b)Switch off.

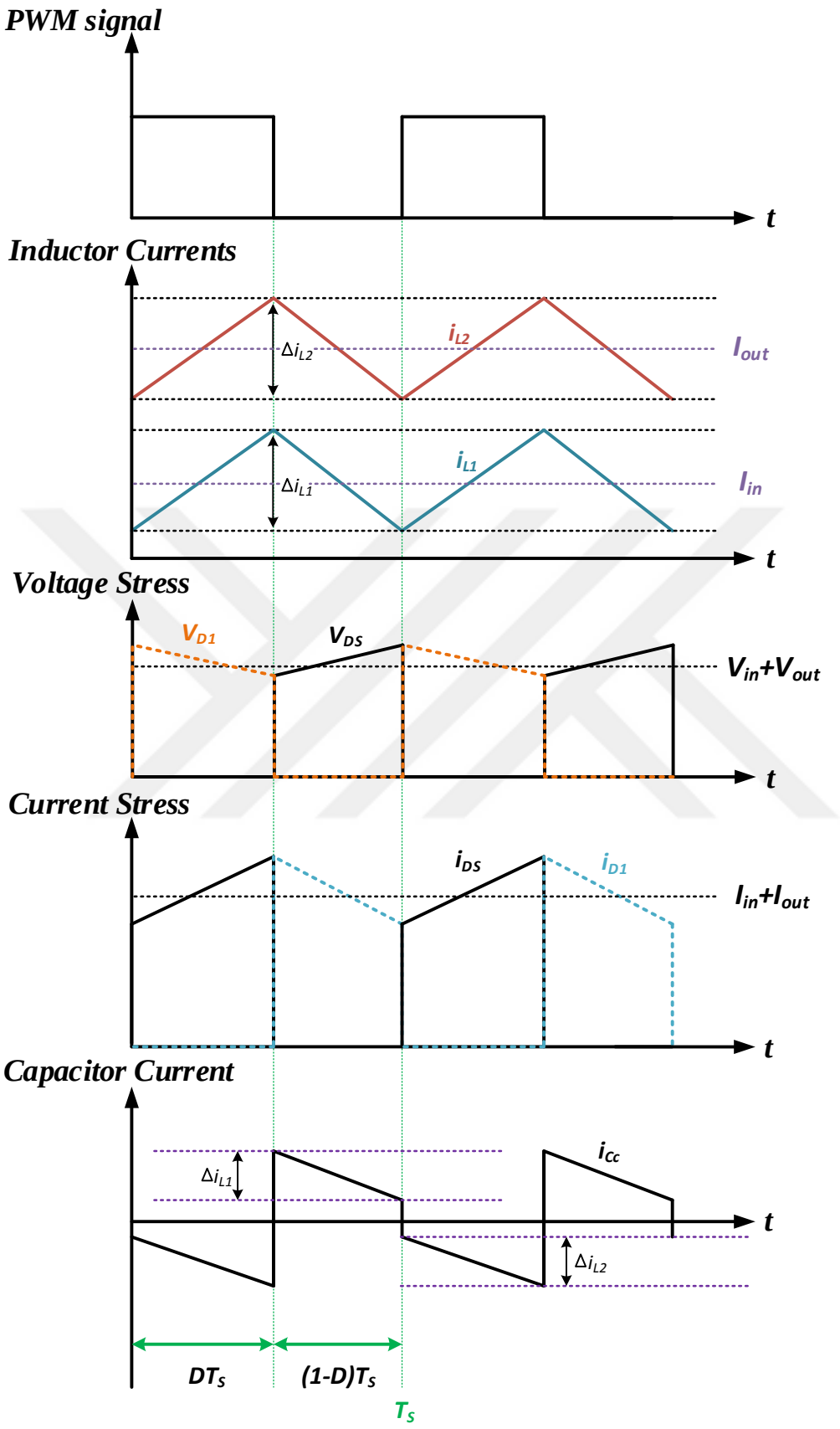

Figure 2.4 : The important waveforms of CCM SEPIC Converter.

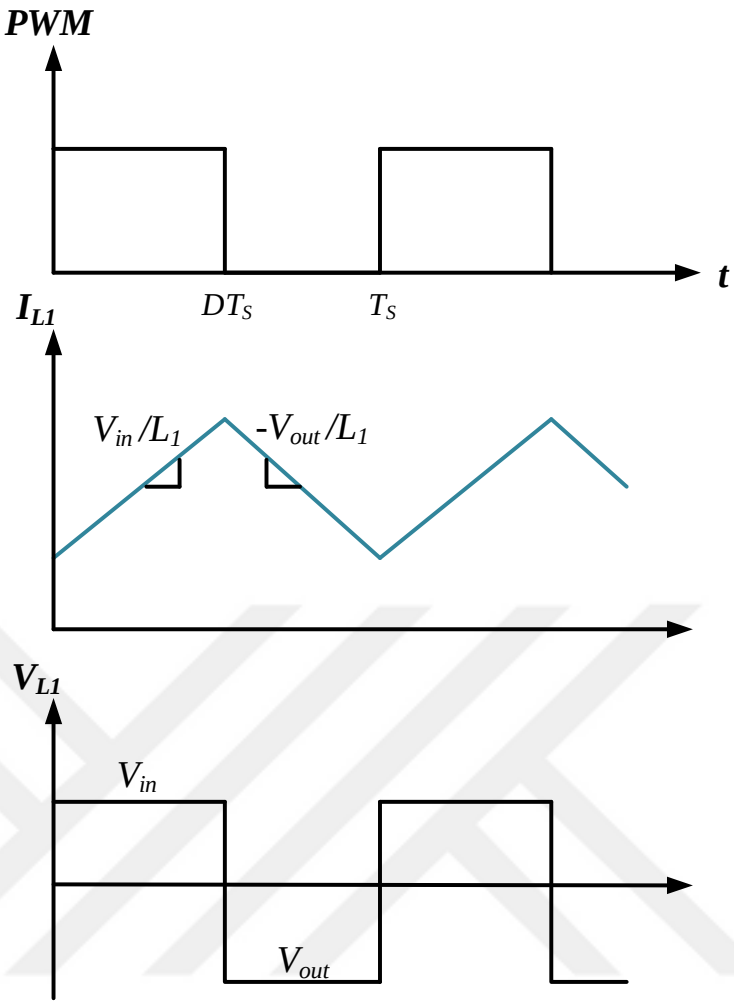

Figure 2.5 : Voltage and current change of inductor L_1.

To sum up the energy flow and switching device stress in a single period [16]:

In interval DT_s;

- The energy flows from the input voltage source to the inductor L_1 and stored in it.
- A part of the energy stored in coupling capacitor C_c flows to the inductor L_2 and stored in it.
- A part of the energy stored in output capacitor C_{OUT} flows to the load and feeds it.
- MOSFET current is the sum of the two inductors' current $(i_{L1} + i_{L2})$ and its voltage is zero.
- Diode voltage is the sum of the input voltage and output voltage $(V_{in} + V_{OUT})$ and its current is zero since there is no conducting path.

In interval $(1-D)T_s$;

- The input energy and the energy stored in inductors L_1, L_2 flow to the coupling capacitor C_c and the output section C_{OUT} and the load.
- MOSFET voltage is the sum of the input voltage and output voltage $(V_{in}+V_{OUT})$ and its current is zero since there is no conducting path.

2.2 SEPIC Converter Design

With the following assumptions,

- Capacitor ESR is zero.
- Inductor resistance zero.
- Switches are ideal.
- Diode forward voltage drop is zero.
- MOSFET on resistance is zero.
- Input source is ideal.

calculations of the inductor and capacitor values will be given. Proper switch selection and details about the circuit will be introduced.

2.2.1 Duty cycle considerations

The average inductor voltages and the capacitor currents are zero over a period according to inductor volt-second balance and capacitor charge balance. In Figure 2.5 at bottom graphic, if the volt-second balance law is applied to the inductor L_1:

$$V_{L_1} = \frac{1}{T_s}\int_0^{T_s} v_{L_1} dt = 0 \tag{2.1}$$

$$V_{in}DT_s - V_{out}(1-D)T_s = 0 \tag{2.2}$$

$$V_{in}D + V_{out}D = V_{out} \tag{2.3}$$

$$D = \frac{V_{out}}{V_{in}+V_{out}} \tag{2.4}$$

The key parameter D as duty cycle is found. Duty cycle determines the relationship between the input and output voltages. The output voltage could be lower, higher than, or equal to input voltage by adjusting the duty cycle. The relationship between the input and output voltage can be given as:

$$\frac{V_{out}}{V_{in}} = \frac{D}{1-D} \tag{2.5}$$

According to capacitor charge balance, the average current flowing through the C_c must be zero.

$$\frac{1}{T_s}\int_0^{T_s} i_{C_c} dt = 0 \tag{2.6}$$

The DC current will not flow through the coupling capacitor. Therefore, the output current will be provided by inductor L_2 and will be equal to average current of L_2.

$$I_{L2} = I_{out} = \frac{V_{out}}{R} \tag{2.7}$$

Assuming that all elements in the converter are ideal, the input power should be equal to the output power. In practice, there will be losses. The average current of inductor L_1 is also the input current of the converter in Equation 2.8.

$$I_{in}V_{in} = I_{L1}V_{in} = I_{out}V_{out} \tag{2.8}$$

2.2.2 Inductor and current ripple selection

As mentioned earlier, the inductor currents start to increase with a slope of V_{in}/L_1 and V_{in}/L_2 in the first interval. In this interval, di_{L1} is the change in the amount of current and dt is the change in the time. In Equation 2.9, replacing them by Δi_{L1} and DT_s will make the calculations easier.

$$L_1 \frac{di_{L1}}{dt} = V_{in} \tag{2.9}$$

$$L_1 \frac{\Delta i_{L1}}{DT_s} = V_{in} \tag{2.10}$$

$$L_1 = L_2 = \frac{V_{in} D T_s}{\Delta i_{L1}} = \frac{V_{in} D}{\Delta i_{L1} f_s} \tag{2.11}$$

Where, $\Delta i_{L1}$is called as peak-to-peak current ripple of L_1 and should be around 40% of the average input current [17]. The inductance values can be determined from this equation choosing the proper switching frequency and Δi_{L1} according to design criteria. Very small inductor peak-to-peak current ripple may cause unsteady operation or very large values may increase EMI [18].

The peak currents of the inductances must be selected lower than the saturation current [7], [17]. They can be calculated via:

$$I_{L1(peak)} = I_{L1} + \frac{\Delta i_{L1}}{2} = I_{out} \frac{V_{out}}{V_{in}} \left(1 + \frac{40\%}{2}\right) \tag{2.12}$$

$$I_{L2(peak)} = I_{L2} + \frac{\Delta i_{L2}}{2} = I_{out} \left(1 + \frac{40\%}{2}\right) \tag{2.13}$$

2.2.3 Coupling capacitor, output capacitor and voltage ripple selection

In steady state, the voltage over the coupling capacitor will be the input voltage. In this case, the voltage rating of the C_c should be greater than the input voltage. When selecting this capacitor, the RMS current of C_c must be considered as well. When the MOSFET is closed, the current of the inductor L_2 flows through the capacitor. When the MOSFET is open, the current of the inductor L_1 flows through the capacitor. Then, the RMS current of the coupling capacitor is calculated by following formula [17], [19]:

$$I_{Cc} = \sqrt{{I_{L2}}^2 D + {I_{L1}}^2 D'} = \sqrt{{I_{out}}^2 D + \left(I_{out} \frac{D}{D'}\right)^2 D'} \tag{2.14}$$

The rms currrent of C_c can be found by substituting Equation 2.5 into Equation 2.14.

$$I_{Cc} = I_{out} \sqrt{\frac{D}{1 - D}} = I_{out} \sqrt{\frac{V_{out}}{V_{in}}} \tag{2.15}$$

Instantaneous current through the coupling capacitor is defined as:

$$I_{Cc} = C_c \frac{dV_{Cc}}{dt} \tag{2.16}$$

Over a period, dV_{Cc} is the change in the amount of voltage and dt is the change in the time. The by replacing the ΔV_{Cc} and T_s instead of these quantities, C_c value is expressed as;

$$C_c = \frac{I_{Cc} T_s}{\Delta V_{Cc}} \tag{2.17}$$

Where, ΔV_{Cc} is called as peak-to-peak voltage ripple on C_c. It can be calculated also by using Equation 2.18 [17], [18], [20]. C_c value can be found by limiting the voltage ripple on the coupling capacitor.

$$C_C = \frac{I_{OUT} D}{\Delta V_{Cc} f_{sw}} \tag{2.18}$$

The output capacitance value can be found by:

$$C_{out} = \frac{I_{OUT} D}{\Delta V_{out} f_{sw}} \tag{2.19}$$

Where, ΔV_{out} is called as peak-to-peak output voltage ripple. C_{out} can be determined by limiting the voltage ripple on the output capacitor. If the output capacitor ESR is considered in the design, the output voltage ripple consists of V_{ESR} and V_{Cout} and it is represented in Figure 2.6.

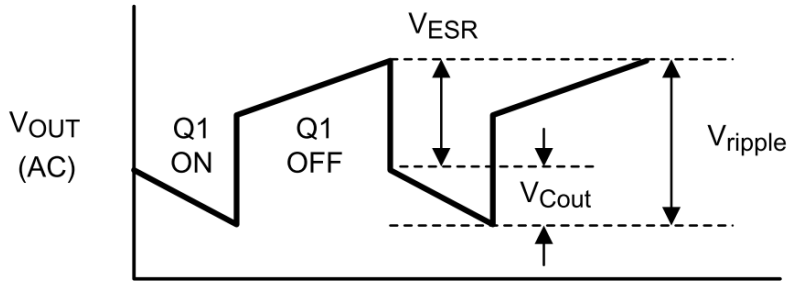

Figure 2.6 : Peak-to-peak output voltage ripple [17].

When the MOSFET is closed, output capacitor supplies the load. Hence, large ripple currents can occur on the output capacitor according to output power [17]. The output

capacitor must be capable of handling this RMS current flowing through on it. The RMS current on the C_{out} is given as:

$$I_{Cout} = I_{out}\sqrt{\frac{V_{out}}{V_{in}}} \tag{2.20}$$

When the MOSFET is open, both inductor currents supply the load and output capacitor ESR will see the ripple of V_{ESR}. Assuming that V_{ESR} and V_{Cout} have the same effect on the output voltage ripple, they can be calculated respectively via:

$$\text{ESR} \leq \frac{0.5V_{ripple}}{I_{L1(peak)} + I_{L2(peak)}} \tag{2.21}$$

$$C_{out} \geq \frac{I_{OUT}D}{\Delta V_{out} f_{sw} 2} \tag{2.22}$$

When selecting the output capacitor, the RMS current, ESR and capacitance should be taken into consideration carefully [17].

2.2.4 MOSFET and diode selection

In Figure 2.3, during the second interval, the drain-source voltage of the MOSFET will see the sum of the input voltage and output voltage [17]. While, the MOSFET current will be the sum of the input current and output current during the first interval. So, the MOSFET must be selected to withstand following current and voltage stresses.

$$\begin{aligned} V(D'T_s) &= V_{Mosfet} = V_{in} + V_{out} \\ I(DT_s) &= I_{Mosfet} = I_{in} + I_{out} \end{aligned} \tag{2.23}$$

As similar, the stress calculations are the same for the diode. The diode current at forward biased will be the $I_{in} + I_{out}$, when MOSFET is not conducting. The voltage drop on the diode at reverse biased will be $V_{in} + V_{out}$, when MOSFET is conducting [19]. As for the average diode current, it is equal to output current as in equation 2.24 [18].

$$I_{D1,avg} = I_{out} \tag{2.24}$$

2.3 State-Space Averaging of SEPIC

The state equations of a network should be explained before the state space averaging concept.

2.3.1 The state-space description and state equations of a system

The state equations of a network should be explained before the state space averaging concept. The state-space description is a simple way to define a system by differential equations. Considering a linear network, linear combinations of the system independent inputs and the state variables help to express the derivatives of the state variables [21]. The physical state variables in a typical converter circuit are usually the "inductor currents" and "capacitor voltages". The state equations of a system can be written in a matrix form as Equation 2.25.

$$\begin{cases} K\dfrac{dx(t)}{dt} = Ax(t) + Bu(t) \\ y(t) = Cx(t) + Eu(t) \end{cases} \tag{2.25}$$

Where, x(t) is the state vector that contains state variables such as the inductor currents i_L and capacitor voltages V_C. U(t) is the input vector that contains the independent inputs such as the input voltage source V_{in}, the diode forward voltage V_D. K is the matrix that contains values of the capacitances and inductances in the circuit. Now, the K$(dx(t)/dt)$ matrix simply becomes the inductor voltages and the capacitor currents in the circuit. The derivatives of the state variables which are the inductor voltages and capacitor currents are expressed by a linear combinations of the state variables x(t) and the independent input u(t) by Equation 2.25 [21]. The derivatives of the state variables can be indicated also as $\dot{x}$ in the equations, in that case $K\dot{x}$ is also acceptable. The A and B matrices consist of constants. The y(t) is the output vector that can contain any dependent signal even the signal is not actually a physical output such as the input current, switch current. Moreover, the output current and the output voltage could be an element of y(t). The C and E matrices consist of constants. The vector y(t) should be also expressed as linear combinations of x(t) and u(t).

As mentioned earlier, the SEPIC converter operating in CCM have two stages. During the first and second interval state equations can be derived by following formula:

$$Interval\ DT_s: \begin{cases} K\dfrac{dx(t)}{dt} = A_1x(t) + B_1u(t) \\ y(t) = C_1x(t) + E_1u(t) \end{cases} \tag{2.26}$$

$$Interval\ (1-D)T_s: \begin{cases} K\dfrac{dx(t)}{dt} = A_2x(t) + B_2u(t) \\ y(t) = C_2x(t) + E_2u(t) \end{cases} \tag{2.27}$$

Likewise, other PWM converters operating in CCM such as Boost, Buck-Boost, Zeta, Buck etc. can be modeled by state equations as in Equation 2.26 and 2.27. If there is a third interval that occurs in DCM mode, this interval should be also added to state equations. In order to get averaged state- space model, state equations are averaged over a switching period T_s. The averaged inductor voltages and the capacitor currents are zero over a period according to inductor volt-second balance and capacitor charge balance. So, the state-space averaged model can be shown as;

$$\begin{aligned} 0 &= AX + BU \\ Y &= CX + EU \end{aligned} \tag{2.28}$$

Where the averaged matrices are expressed by;

$$\begin{aligned} A &= DA_1 + (1-D)A_2 \\ B &= DB_1 + (1-D)B_2 \\ C &= DC_1 + (1-D)C_2 \\ E &= DE_1 + (1-D)E_2 \end{aligned} \tag{2.29}$$

So, the steady-state solution of the converter can be found by solving Equation 2.28.

2.3.2 State-space averaged model of SEPIC

Let's define the state-space averaged model for the SEPIC converter operating in CCM shown in Figure 2.3. The equations for the first interval and second interval are shown in Equation 2.30 and 2.31 according to KVL and KCL, respectively.

$$DT_s \begin{cases} L_1 \dfrac{di_{L1}}{dt} = V_{in} \\ L_2 \dfrac{di_{L2}}{dt} = V_{Cc} \\ C_c \dfrac{dV_{Cc}}{dt} = -i_{L2} \\ C_{out} \dfrac{dV_{Cout}}{dt} = -\dfrac{V_{Cout}}{R} \end{cases} \tag{2.30}$$

$$(1-D)T_s \begin{cases} L_1 \dfrac{di_{L1}}{dt} = V_{in} - V_{Cc} + V_{L2} \\ L_2 \dfrac{di_{L2}}{dt} = -V_{OUT} \\ C_c \dfrac{dv_{Cc}}{dt} = i_{L1} \\ C_{out} \dfrac{dv_{Cout}}{dt} = (i_{L1} + i_{L2}) - \dfrac{V_{Cout}}{R} \end{cases} \tag{2.31}$$

These equations can be written in a simple form as state equations.

$$\dot{x} = Ax + Bu \qquad y = Cx + Eu \tag{2.32}$$

Where, x is the state vector $\begin{bmatrix} i_{L1} \\ i_{L2} \\ V_{Cc} \\ V_{Cout} \end{bmatrix}$, u is the input vector $[V_{in}]$, y is the output vector $[V_{OUT}]$.

As for the first interval and second interval, the state equations become as following equations, respectively.

$$\dot{x} = \overbrace{\begin{bmatrix} 0 & 0 & 0 & 0 \\ 0 & 0 & 1/(L_2) & 0 \\ 0 & -1/(C_c) & 0 & 0 \\ 0 & 0 & 0 & -1/(RC_{out}) \end{bmatrix}}^{A_1} \begin{bmatrix} i_{L1} \\ i_{L2} \\ V_{Cc} \\ V_{Cout} \end{bmatrix} + \overbrace{\begin{bmatrix} 1/(L_1) \\ 0 \\ 0 \\ 0 \end{bmatrix}}^{B_1} [V_{in}]$$

$$\dot{x} = \overbrace{\begin{bmatrix} 0 & 0 & -1/(L_1) & -1/(L_1) \\ 0 & 0 & 0 & -1/(L_2) \\ 1/(C_c) & 0 & 0 & 0 \\ 1/(C_{out}) & 1/(C_{out}) & 0 & -1/(RC_{out}) \end{bmatrix}}^{A_2} \begin{bmatrix} i_{L1} \\ i_{L2} \\ V_{Cc} \\ V_{Cout} \end{bmatrix} + \overbrace{\begin{bmatrix} 1/(L_1) \\ 0 \\ 0 \\ 0 \end{bmatrix}}^{B_2} [V_{in}]$$

$$[V_{OUT}] = \overbrace{[0 \quad 0 \quad 0 \quad 1]}^{C_1} \begin{bmatrix} i_{L1} \\ i_{L2} \\ V_{Cc} \\ V_{Cout} \end{bmatrix} + \overbrace{[0]}^{E_1} [V_{in}]$$

$$[V_{OUT}] = \overbrace{[0 \quad 0 \quad 0 \quad 1]}^{C_2} \begin{bmatrix} i_{L1} \\ i_{L2} \\ V_{Cc} \\ V_{Cout} \end{bmatrix} + \overbrace{[0]}^{E_2} [V_{in}]$$

The averaged matrices and state equations becomes as follows:

$$A = \begin{bmatrix} 0 & 0 & -D'/(L_1) & -D'/(L_1) \\ 0 & 0 & D/(L_2) & -D'/(L_2) \\ D'/(C_c) & -D/(C_c) & 0 & 0 \\ D'/(C_{out}) & D'/(C_{out}) & 0 & -1/(RC_{out}) \end{bmatrix}$$

$$B = \begin{bmatrix} 1/(L_1) \\ 0 \\ 0 \\ 0 \end{bmatrix}, \qquad C = [0 \quad 0 \quad 0 \quad 1]$$

$$\dot{x} = \overbrace{\begin{bmatrix} 0 & 0 & -D'/(L_1) & -D'/(L_1) \\ 0 & 0 & D/(L_2) & -D'/(L_2) \\ D'/(C_c) & -D/(C_c) & 0 & 0 \\ D'/(C_{out}) & D'/(C_{out}) & 0 & -1/(RC_{out}) \end{bmatrix}}^{A} \begin{bmatrix} i_{L1} \\ i_{L2} \\ V_{Cc} \\ V_{Cout} \end{bmatrix} + \overbrace{\begin{bmatrix} 1/(L_1) \\ 0 \\ 0 \\ 0 \end{bmatrix}}^{B} [V_{in}]$$

$$y = \overbrace{[0 \quad 0 \quad 0 \quad 1]}^{C} \begin{bmatrix} i_{L1} \\ i_{L2} \\ V_{Cc} \\ V_{Cout} \end{bmatrix}$$

The steady-state solutions can be found by some algebraic manipulations on averaged state equation.

$$\begin{aligned} X &= -A^{-1}BU \\ Y &= -CA^{-1}BU \end{aligned} \tag{2.33}$$

SEPIC is a fourth-order nonlinear system, thus the linear model of the converter is needed in order to design feedback controller and analyze converter stability [22]. SSA helps to model the SEPIC or other PWM converters by linear components [23]. The good thing about the state-space averaging, a small-signal averaged model of a PWM converter can be obtained any time after the SSA [21]. Besides, the SSA model of

SEPIC allows to analyze the converter behavior, describe a mathematical model for the controller design and find the transfer function of the converter [24].

2.4 Control Methods for Switch Mode Power Supplies

For the Switch Mode Power Supplies (SMPS), there are two main control techniques which are:

1) Voltage-mode control
2) Current-mode control

2.4.1 Voltage-mode control

In Figure 2.7, basics of voltage-mode control are represented. The duty ratio is controlled by comparing the error voltage V_e with a constant ramp (sawtooth) waveform V_R. The PWM signal status is defined by Equation 2.34.

$$\mathrm{Q} = \begin{cases} 0, & V_e < V_R \\ 1, & V_e > V_R \end{cases} \tag{2.34}$$

In this method, the converter output is directly controlled by choice of the duty ratio [21]. In voltage-mode-controlled converters, the main advantage is the single voltage feedback loop [25], [26]. A single feedback loop makes the analysis and design of the converter easier. Also, the stable modulation is provided by high amplitude ramp waveform [26]. Besides, cross-regulation for multiple output supplies is better compared to current-mode control because of the low-impedance at the output [25] . Nevertheless, the disadvantages of this method can be listed as below:

1) The voltage-mode control has a slower response. Because, any change in the input voltage or load resistance is first sensed as an output voltage change and then corrected by the feedback loop [25], [26].
2) An extra pole is added to the feedback loop by the RC filter at the output.
3) The loop gain varies with the input voltage and compensation becomes more complicated [26].

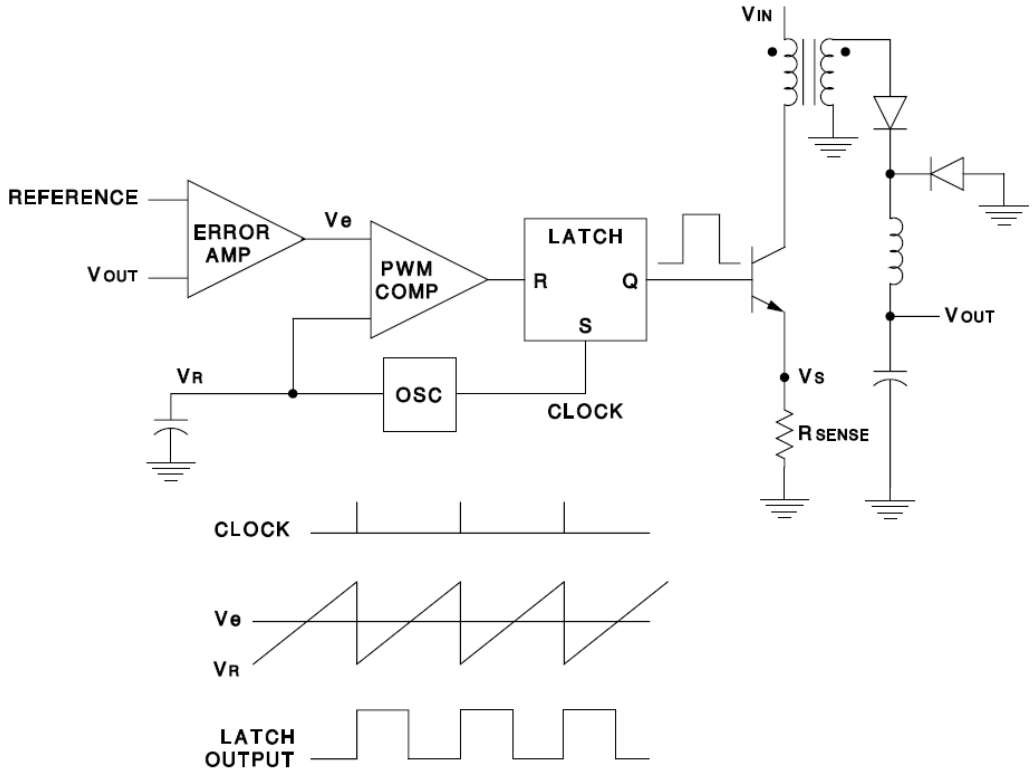

Figure 2.7 : Voltage mode control [26].

2.4.2 Current-mode control

In Figure 2.8, basics of current-mode control are illustrated. Current mode control is also introduced as "Current Programmed Mode" in [21]. This multi-loop system consists of a voltage feedback for outer loop and current feedback for inner loop. A set-reset flip-flop (SR latch), an oscillator and a current sensor are the elements of inner loop [25]. As the name set-reset implies, the latch is responsible for set and reset operation of the Q. The current sensor senses the inductor or switch current via a current transformer or a resistor [25]. In more complicated converters, this sensed current could be the sum of several inductor currents [21]. The outer loop determines a threshold value for the inner current loop and sets a current reference in response to the output voltage variations [25].

In Figure 2.8, The ramp waveform in voltage-mode control is replaced by the switch signal V_s which is sensed by a resistor R_{SENSE}. The node called as V_s is actually proportional to the switch current. This signal is then compared with the error signal V_e, which will be the current reference and control input signal. The detailed operation of current-mode control can be explained on waveforms shown in Figure 2.8.

Voltage pulses at a fixed frequency is generated by the clock. The clock frequency will be also the switching frequency f_s of the converter. When the clock pulse goes high, the latch output will be high and turn on the switch [21], [25]. A switching period T_s begins with this pulse. The switch current or the inductor current start to increase linearly with a certain slope during the switch closed position. V_s increases proportionally to the switch current. At one point, this voltage will reach the threshold level. Once V_s gets equal to V_e, the PWM comparator output voltage will go high and resets the latch. This will cause the latch output low and the switch turned off. The switch remains open until the next clock pulse. To sum up, the converter output is controlled by choice of the peak switch current which follows the control input signal [21]. In current-mode control, duty cycle is not directly controlled since it depends on the control input, inductor currents, output voltage and input voltage [21].

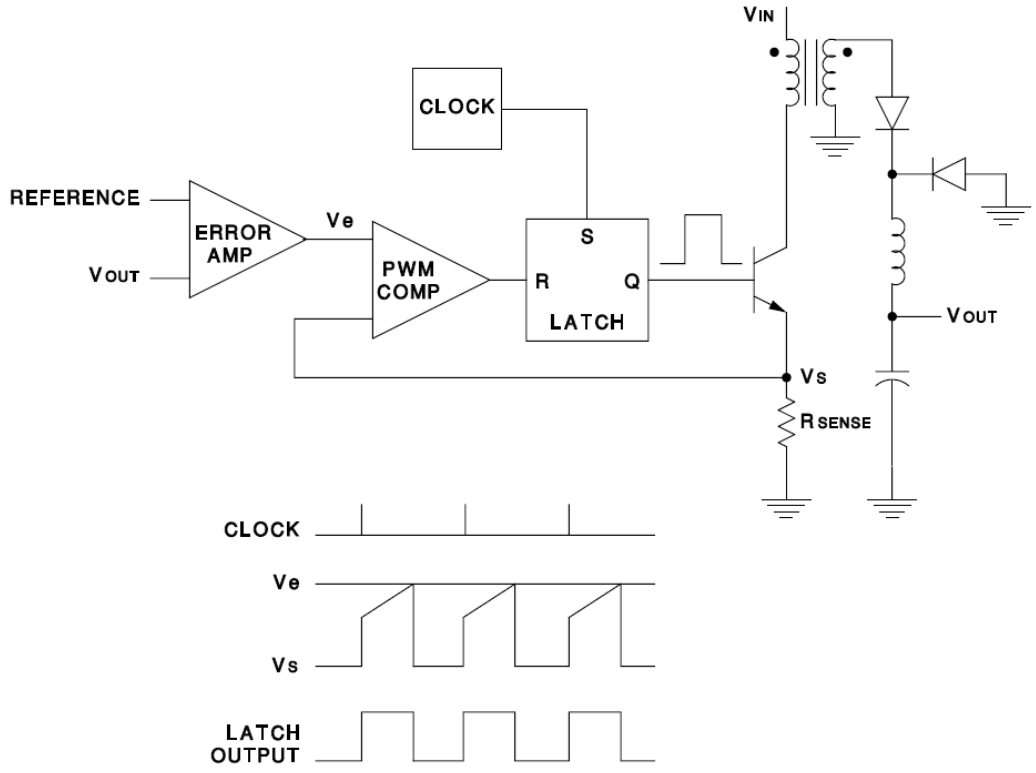

Figure 2.8 : Current mode control [26].

In practice, the purpose of the current-mode control is to control the instantaneous peak inductor current or switch current on the converter. But as in Equation 2.35, the average inductor current will be almost equal to peak inductor current if the inductor peak-to-peak current ripple is small.

$$I_L \approx I_{L,peak} - \frac{\Delta i_L}{2} \tag{2.35}$$

Thus, the peak inductor current control is also the indirect control of the average inductor current. In buck and buck derived topologies like in Figure 2.8, the inductor is on the output side and the average inductor current is equal to the output current [27]. Therefore, current mode control will be naturally the output current control in this type of topologies. As for the boost converter, the inductor is on the input side. In that case, the average inductor current is the input current flows into the converter. Hence, current-mode control controls the input current in such topologies. It can be useful in high power factor pre-regulators. The input current can be shaped into a desired sinusoidal waveform easily [27]. The other advantages of current-mode control can be listed as follows:

1. It has a fast response to changes in the input voltage. Line regulation is improved [26], [28].
2. Inherent current limiting is achieved. Limiting the maximum switch current cycle-by-cycle prevents switch failures from excessive currents [21].
3. The feedback loop contains only a single pole.

However, several disadvantages of the peak current-mode control are given as follows:

1. Poor Noise Immunity; in Figure 2.8 the rising slope of the switch current is compared with the current reference determined by the outer loop. The switch is controlled by this reference current. The current ramp is usually quite small compared to the reference current. Therefore, this method is less immune to noise. A noise spike generated every time the switch turns on -typically caused by transformer winding capacitance and output diode recovery current- can cause the switch to turn off suddenly [26], [27]. This will result in sub-harmonic oscillations with much larger ripple [25]. A stable operation can be ensured by adding an RC filter to suppress these susceptible noises when sensing current. Circuit layout is also important for successful operation.
2. Slope Compensation; duty cycles above 50% cause the converter operates unstable. An external ramp equal to inductor current down-slope is added to comparator input to eliminate this instability [25]–[27].
3. Two-feedback loop; that makes the converter analysis more difficult.

4. Topology problems; in general peak-current-mode-control controls the inductor current. When the inductor is in the output, it is most effective for the output current control. However, much of the advantage of this method for output current control is lost with boost and flyback topologies where the inductor is not on the load side. Hence, the PCMC method is well suited for boost and flyback like topologies for the input current control [25], [27].

Advantages and disadvantages of both methods are discussed. Optimum control technique can be preferred for the application needs. As for the LED driver application, SEPIC LED driver should have following aspects:

- ✓ LED brightness is determined by the current flowing through the LED. Therefore, an output current control is needed. LED current must be limited.
- ✓ Over voltage protection of the LED.
- ✓ The fastest dynamic response is needed.
- ✓ Excessive current failures on switching devices must be prevented.
- ✓ For LED drivers, the DC voltage at the input of the converter is usually rectified from AC mains (220V RMS) that results in very high DC voltage. Assuming that the total output voltage of the LED nearly 100V, the duty cycle of the converter will be below 0.5. Hence, no slope compensation is needed.
- ✓ A Low-cost application with fewest components.

Peak current mode control technique can satisfy above-mentioned features for LED drivers.

3. SEPIC LED DRIVER

In this chapter, electrical characteristics of High-Brightness LEDs are introduced. The necessity of the driver circuit is emphasized. A significant quantity flicker for LEDs is explained. A peak-current-mode-controlled SEPIC LED driver is proposed. Many noteworthy parameters in LED drivers are mentioned.

3.1 Electrical Characteristics of LED

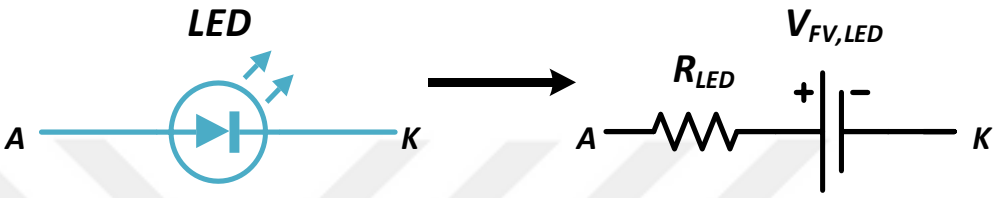

Figure 3.1 : Equivalent circuit of a single LED.

Equivalent circuit of a single LED is shown in Figure 3.1. The voltage-current characteristic of the LED is similar to diode. LED does not conduct until the applied voltage between anode and cathode node is equal to or greater than forward voltage of the LED. Forward voltage of the LEDs is differed by the color of LED. Typical drive voltage for High Brightness LEDs is about 2.5V to 4V. The operation current of the LED is generally about 50-300 mA [29]. But, the produced illumination is considerably weak by a single LED chip. Thus, multiple LED chips are generally connected in series and/or parallel in order to obtain the enough lighting levels [1], [30].

Two different LED string are tested to understand V-I curve of the LEDs. First one is 9 Watt LED shown in Figure 3.2. It has two parallel branches and each branch has 8 series connected LED chips. Its curve is given in Figure 3.3.

The second one is 15 Watt LED shown in Figure 3.4. This LED has also two parallel branches, but each branch has 15 series connected LED chips. Its curve is given in Figure 3.5

LEDs are tested in laboratory. The data taken from the lab are given in Table A.1 and Table A.2 in appendices.

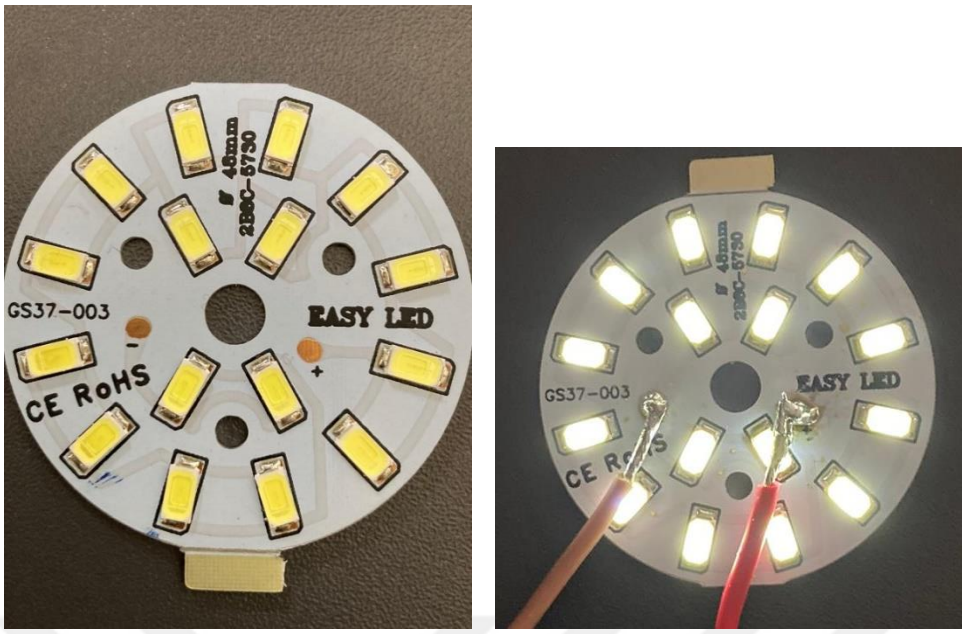

Figure 3.2 : 9 Watt LED.

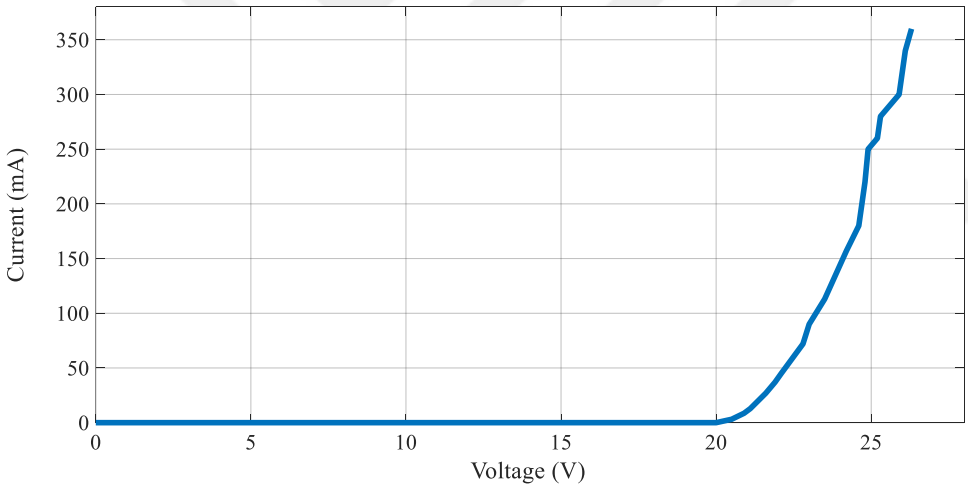

Figure 3.3 : V-I curve of the 9 Watt LED string.

Figure 3.4 : 15 Watt LED.

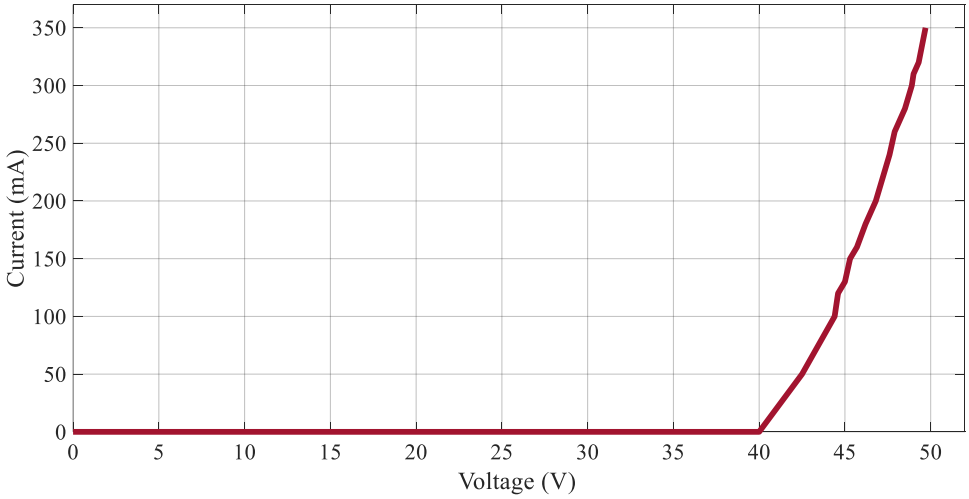

Figure 3.5 : V-I curve of the 15 Watt LED string.

As can be seen from the two examples, the LED string does not conduct until the total forward voltage of the LEDs met with the applied voltage. After that point, current starts to increase exponentially. And, the relationship between current and voltage of a LED is expressed by following formula [4] :

$$I_F = I_s\left(e^{\frac{qV_F}{KT}} - 1\right) \tag{3.1}$$

Where, I_F is the LED current, I_s is the reverse saturation current, q is the electron charge, K is the Boltzmann constant, and T stands for junction absolute temperature.

There is an inversely proportional relationship between the temperature and the voltage of the LED. As the temperature increases, the voltage of the LED decreases as shown in Figure 3.6.

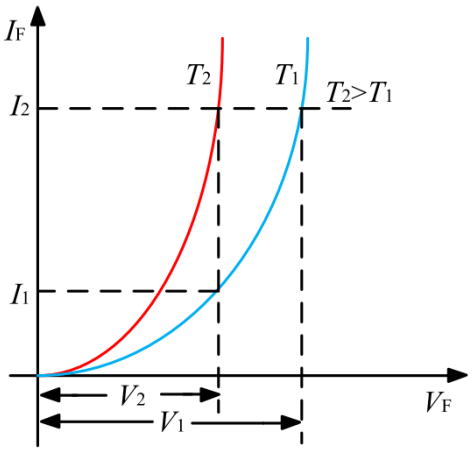

Figure 3.6 : Relationship between temperature and voltage of the LED [4].

The temperature of the LED can increase if the LED is supplied by a voltage source for a long time. In this case, LED current will increase quickly that also results in temperature growth. Eventually, the LED is burned if the heat is not controlled. This phenomenon can be prevented by using a constant current source when driving a LED. Then, the temperature growth will only results in voltage drop that does not harm LED string [4].

LEDs are required a proper driver circuit and direct current (DC) operation for aforementioned features. In general, this DC voltage is rectified from an AC power supply by an uncontrolled full wave bridge rectifier. Then, a DC-DC converter regulate the output voltage/current depending on the power demand of the LED string. If multiple LED chips are connected in series, the output voltage of the DC-DC converter must supply at least total forward voltage of LED's, regardless from voltage variations in AC power supply [31]. Therefore, in switch mode drivers, a voltage feedback or/and current feedback which is mostly included into control stage provide a stable operation to LED string. Among the current mode control techniques, peak current mode control is a good choice by means of current regulation, over-voltage protection. In Figure 3.7, general current mode-controlled AC-DC LED driver circuit is represented. There are other LED driver techniques such as resistive current limiting also called as linear LED driver, pulse width modulation dimming. The suitable driver circuit can be chosen for various application needs like automotive lighting, street lighting, household lighting, and commercial lighting and many others.

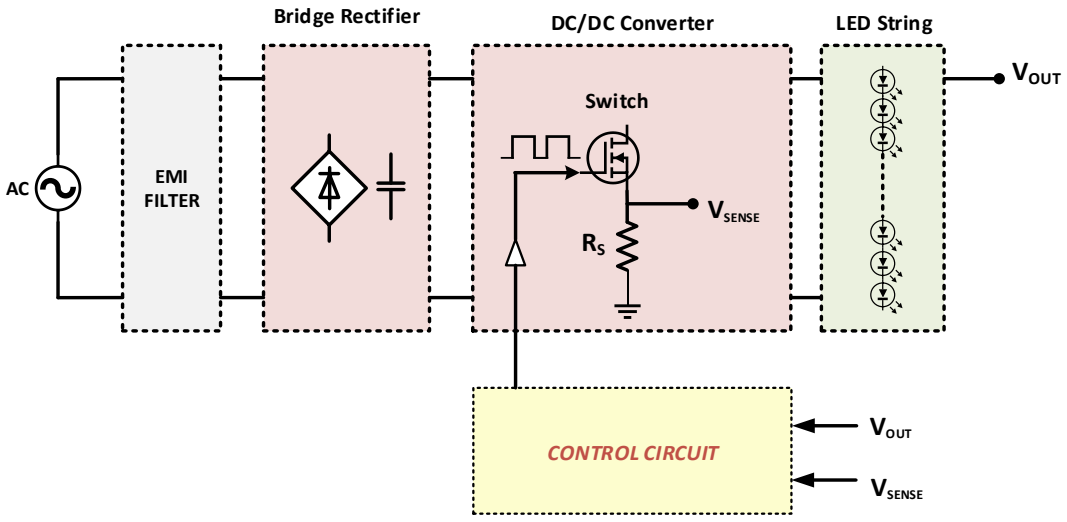

Figure 3.7 : General current mode-controlled LED driver representation.

3.2 Flicker in LED Lighting

The flicker in LED lighting is mostly related with the driver circuit. Therefore, the flicker and its biological effects on human health are introduced before the driver circuit.

Light modulation is called as flicker, flutter, and shimmer [9]. However, flicker is the most commonly used term and defined as "variations of luminance in time" in Illuminating Engineering Society's (IES) Lighting Handbook [32]. Percent flicker [Modulation (%)] and flicker index are the most commonly used metrics to quantify this variation[9], [10]. For the mathematical expressions, a light output curve is shown in Figure 3.8.

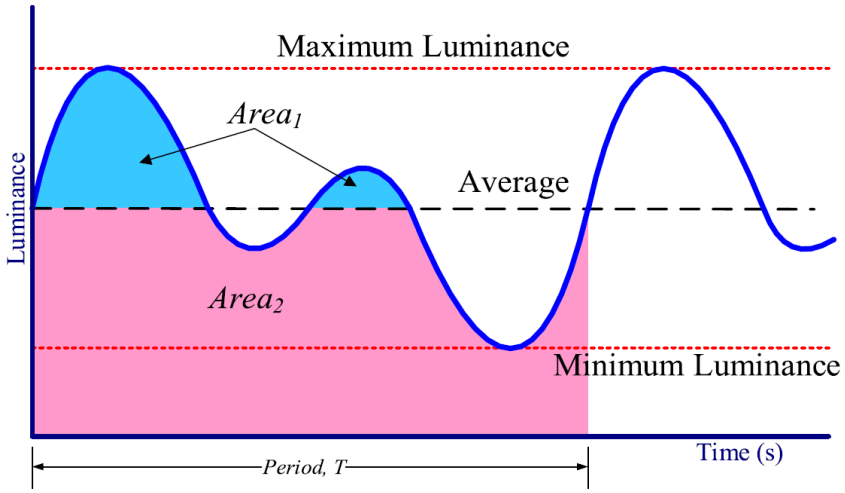

Figure 3.8 : Random light output curve [33].

Flicker index is defined as area above the average light divided by the total area of the light output curve for a single period by following formula according to Figure 3.8 [9].

$$Flicker\ Index = \frac{Area\ 1}{Area\ 1 + Area\ 2} \tag{3.2}$$

Percent Flicker, also called as peak-to-peak contrast, modulation depth and Modulation (%) is defined as follows according to Fig 3.8 [9].

$$Percent\ Flicker\ or\ Mod\% = 100\frac{L_{MAX} - L_{MIN}}{L_{MAX} + L_{MIN}} \tag{3.3}$$

With the assumption of LED current is approximately proportional to luminous flux output of the LED, then the modulation of the light will be equal to modulation in LED current [9]. All light sources may flicker with various levels. However, the flicker especially exists in LED lighting when the DC voltage is rectified from AC mains. In this case, LED lamps will have a peak-to-peak current ripple at twice the line frequency; 100 Hz in Europe and 120 Hz in America [9]. Therefore, the flicker is mainly dependent on the driver circuit.

Visible and invisible flicker can have potential risks on human health. Health risk and biological effects of flicker to the viewers such as headache, eyestrain, and seizures cannot be ignored. This effects may immediately result from a few seconds' exposure such as the risk for epileptic seizures or may result in long-term exposure such as the headache, malaise and reduced visual performance [9]. Visible flicker frequencies range from 3 Hz to 70 Hz. Nevertheless, the range may change person to person. The human visual system may not perceive above visible flicker frequencies. That is called as invisible flicker, may nonetheless have effects like headache and eyestrain. Although the invisible flicker is too fast to be seen, measurements of the electroretinogram (A record of the electrical activity of the retina, used in medical diagnosis and research) shows that the human retina can resolve the modulation of light in the frequency range 100 Hz to 160 Hz and up to 200 Hz.

In Figure 3.9, it is recommended to operate in the shaded area to minimize visual discomfort and give low risk for headaches and photosensitive epileptic seizures [9]. According to recommendations, the modulation should be less than 0.025*f at below 90 Hz frequencies, while modulations should be less than 0.08*f at or above 90 Hz frequencies. However, there is not any restriction in modulation above 1250 Hz [9].

The above recommendations can assure low risk region for flicker frequencies. Nonetheless, to achieve No Observable Effect Level (NOEL), the flicker modulation (%) should be as follows [9]:

- Modulation (%) is less than 0.01*frequency below 90 Hz
- Modulation (%) is less than 0.0333*frequency between 90 Hz and 3000 Hz
- There is not any restriction above 3 kHz.

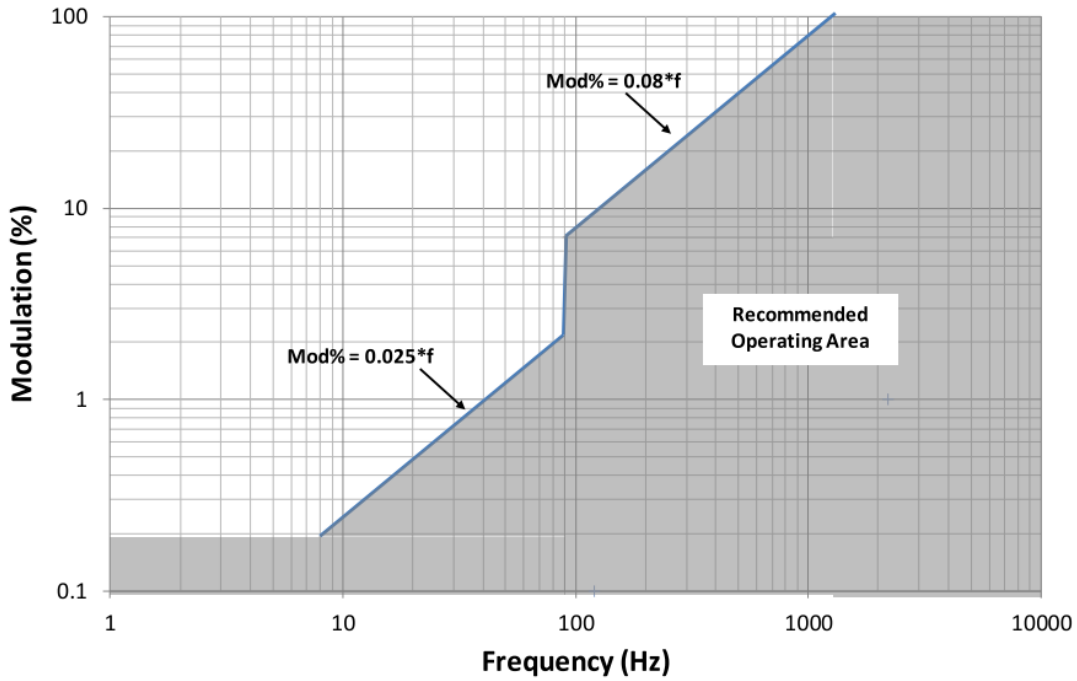

Figure 3.9 : Recommended operating area as a function of frequency and modulation (%) [9].

Moreover, to prevent seizure, the flicker modulation (%) should be kept less than 5% at below 90 Hz for any lighting source [9]. An example is given just to clarify calculations for flicker free LED lightning considering the LED driver circuit represented in Figure 3.7. Assume that the line frequency is 50 Hz. Then, the flicker frequency ($f_{flicker}$) will be 100 Hz that is twice the line frequency. If the recommended practices applied for 100 Hz, the required limits are summarized as in Table 3.1.

Table 3.1 : Recommended percent flicker at 100 Hz for human health.

Biological Effect	Recommended Operation	Percent Flicker
Low-Risk Level	$Mod\% < 0.08 f_{flicker}$	8%
NOEL	$Mod\% < 0.0333 f_{flicker}$	3.33%

As for the flicker index, the data points taken from the several studies on flicker index have been turned into a graphical representation shown in Figure 3.10 [34]. According to this figure, the light sources are separated whether they produce imperceptible flicker, acceptable flicker, low to moderate flicker, or moderate to bad flicker. Later, an orange line has been drawn to see the difference whether the light source produce no flicker (Allowed) or problematic flicker (Not Allowed).

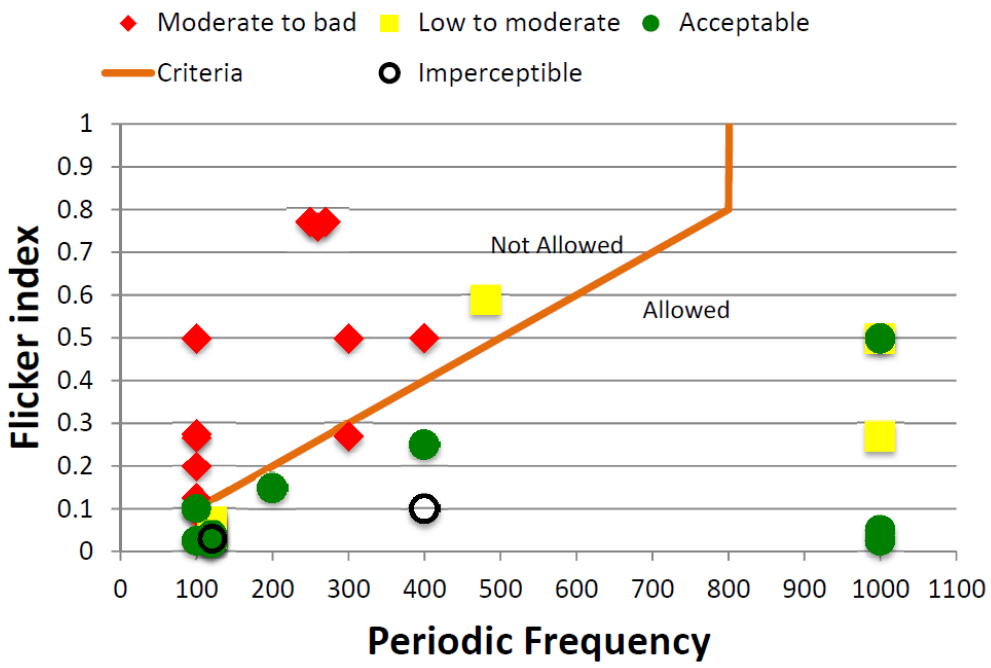

Figure 3.10 : Flicker index vs flicker frequency [34].

In general lighting, it is recommended to operate at region fall below the orange line in Figure 3.10 by the lighting specifiers [34]. For example, the flicker index should be less than 0.1 at 100 Hz and less than 0.4 at 400 Hz. At flicker frequencies greater than 800 Hz, it is unlikely to produce harmful effects. Also, it is not recommended to operate at flicker frequencies below 100 Hz. So, the recommended flicker index at 100 Hz flicker frequency for human health should be less than 0.1.

In figure 3.11, three familiar waveforms which are triangle, sine and square are given to understand flicker calculations. Y axis is assumed to be the output current from a LED source. The magnitudes of the currents are given randomly just to understand calculations. The frequency of the waveforms is 120 Hz. Average values of the waveforms is identical.

The observations from the waveforms can be listed as:

1. Percent flicker is the same despite the waveforms are different from each other. Because it is related with the maximum and minimum value of the waveform according to Equaiton 3.3.
2. Flicker index are different for each waveform and square waveform has the highest flicker index.

3. Measurement of the flicker index is more complex than percent flicker. Because, some certain areas must be calculated according to formula 3.2. The integral operation or basic geometry skills can help to calculate flicker index. However, accurate calculation of flicker index can be tough when the waveform is more complicated.

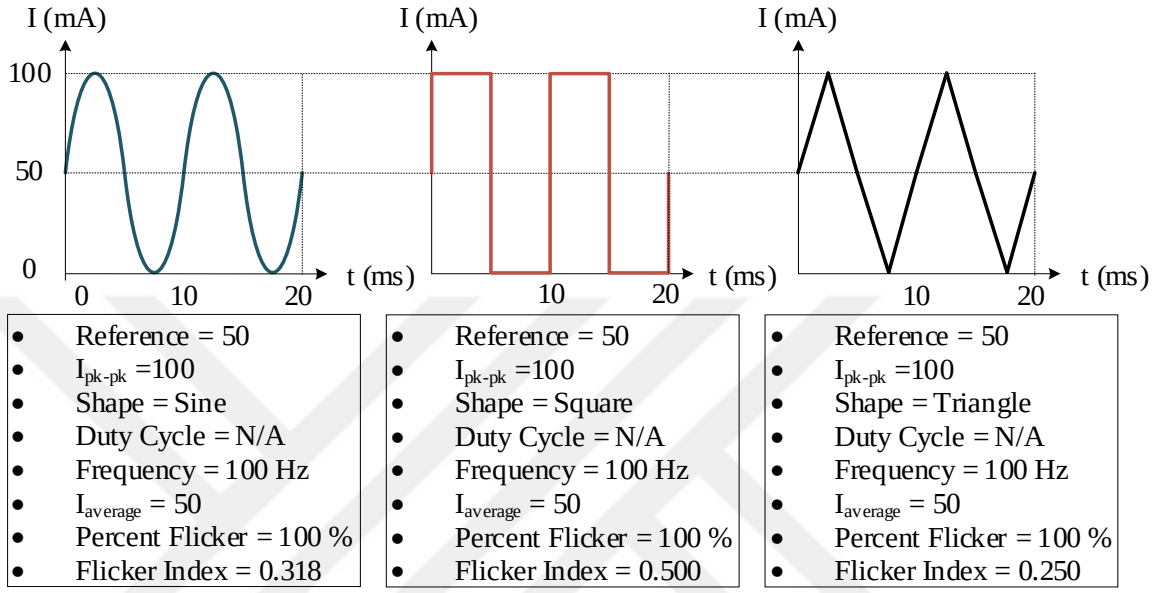

Figure 3.11 : Flicker metrics for basic periodic waveforms [34].

It is more accurate to measure the actual light output variation of the LED source, even though the measuring the LED current variations can help us to measure flicker [35]. Photo sensors are capable of measuring visible light and the waveform of the light output can be captured by an oscilloscope. Moreover, holding your smart phone camera to the LED source can show the existence of flicker in light source [10].

3.3 LED Brightness Control by the Peak-Current-Mode-Controlled SEPIC LED Driver

General peak current mode controlled SEPIC LED driver diagram is given in Figure 3.12. The system consists of a voltage feedback for outer loop and current feedback for inner loop. The MOSFET current is sensed by a resistor (R_{SENSE}) in series to the MOSFET, and then compared with the current reference (I_{REF}) by PWM comparator. By controlling the reference current, the output current can be adjusted.

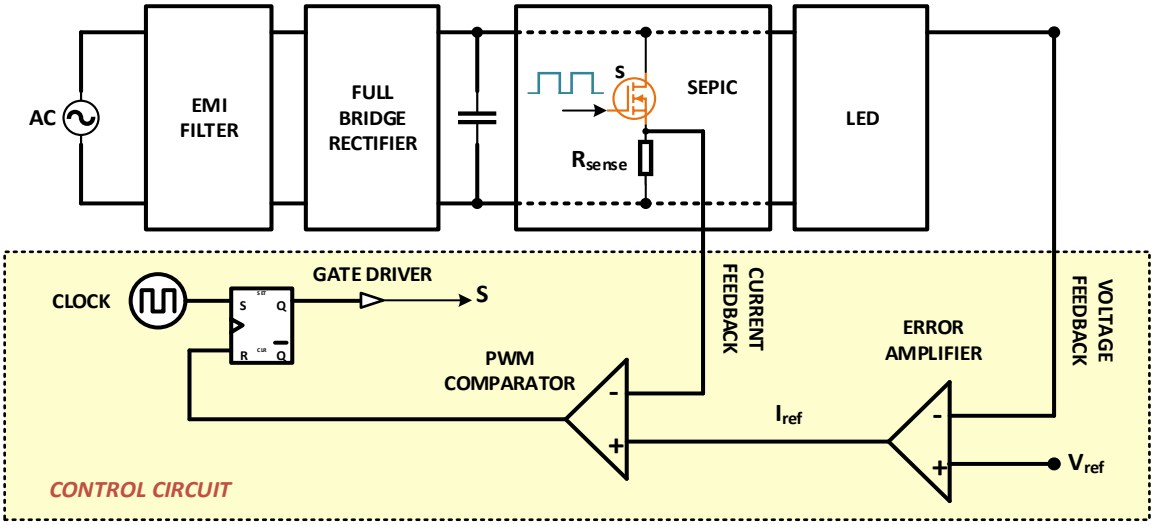

Figure 3.12 : Peak-current-mode-controlled SEPIC LED driver.

Low cost current mode controller UC3842 IC can be used for peak current mode control. This IC can provide a robust current control. For current sensing and limiting, related internal structure of the UC3842 IC is presented in Figure 3.13 (see all internal structure of UC3842 IC taken from the datasheet in appendix).

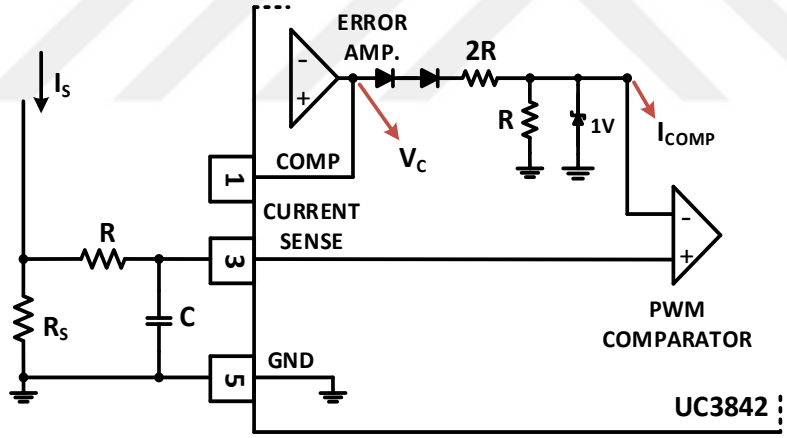

Figure 3.13 : Current sensing and limiting.

Error amplifier output voltage is also called as control voltage V_c which is followed by two diodes, two resistors and a zener diode in Figure 3.13. The diode pair has totally a forward voltage of 1.4 V, 0.7 V for each. The voltage at the inverting leg of the PWM comparator I_{COMP} will be equal to the voltage across the resistor R, which is 1/3 of the voltage after the diode's voltage drop from V_c. So, the peak voltage across R_{SENSE} is controlled by the E/A output, according to following formula [28]:

$$V_{R_{SENSE}}(PEAK) = \frac{V_C - 1.4V}{3} \tag{3.4}$$

The zener diode limits this peak voltage to 1V [28], [36]. Applying the Ohm's law, peak current on R_{SENSE} can be calculated according to formula:

$$I_{R_{SENSE}}(PEAK) = \frac{V_{R_{SENSE}}(PEAK)}{R_{SENSE}} = \frac{V_C - 1.4V}{3R_{SENSE}} \tag{3.5}$$

The controller turns off the switch when the voltage across R_{SENSE} reaches its peak value. If the sensing resistor is chosen as 1 Ω, the peak current that can pass through the switch will be 1A because of the zener diode limitation.

In this thesis, a variable DC voltage source as control input voltage is used to adjust output current, brightness of the LED. As the control voltage V_c decreases, peak voltage across the R_s decreases. Smaller peak voltages will push the MOSFET turn off earlier, and will result in smaller duty cycles. Therefore, the output current can be regulated by adjusting V_c properly. Outer feedback loop will be disabled because of the V_c is controlled by an external dc voltage source. Normally, the voltage feedback is used for overvoltage protection. But in the proposed control strategy, amount of the current flowing through the LED string naturally determines the output voltage and prevents overvoltage. In addition, to prevent huge spikes in current waveform while sensing the current, simple RC filter is used [28], [36]. The proposed peak-current-mode controlled SEPIC LED driver without PFC and with PFC are shown in Figures 3.14 and 3.15, respectively.

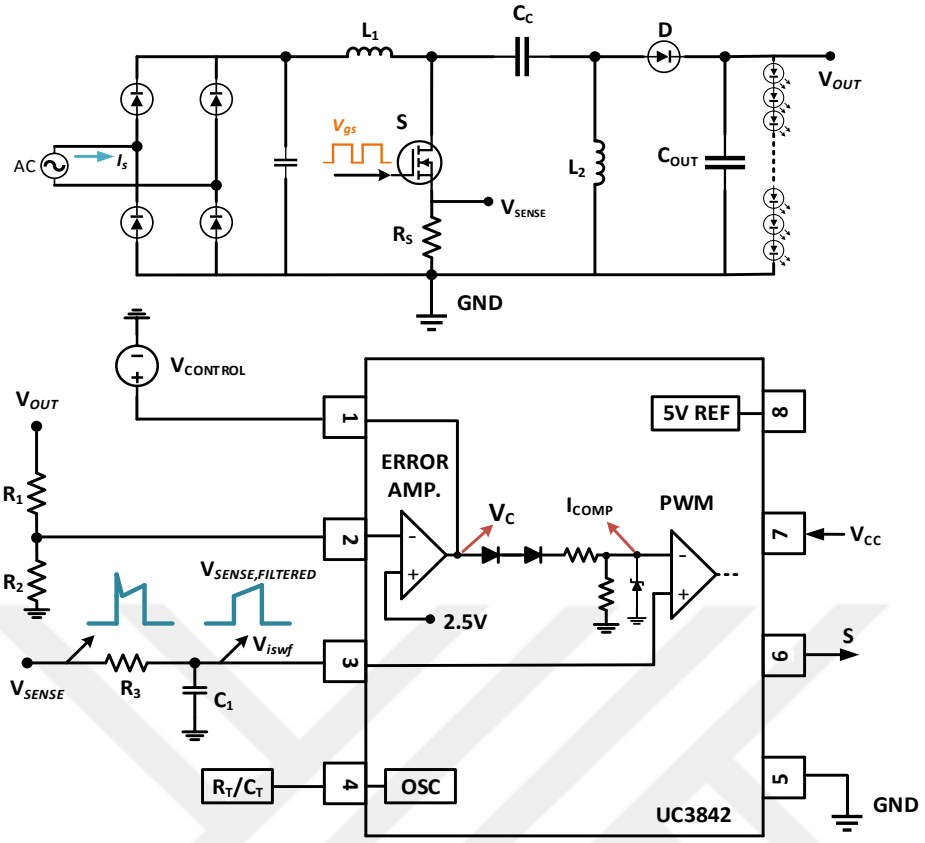

Figure 3.14 : Proposed peak-current-mode controlled SEPIC LED driver without PFC.

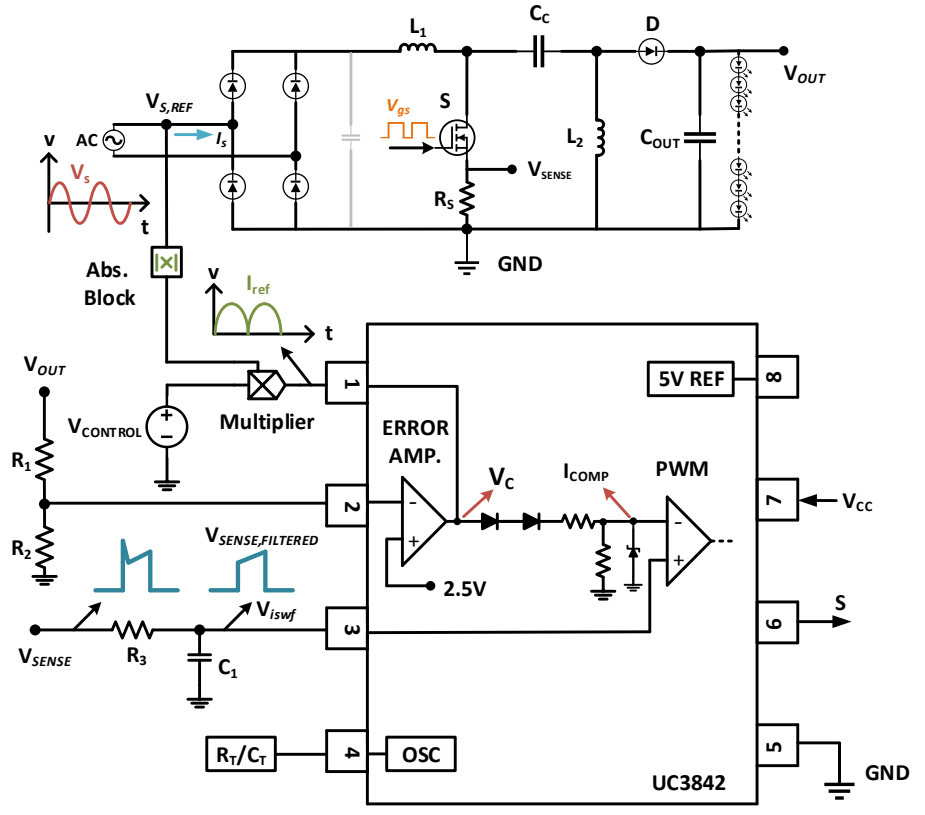

Figure 3.15 : Proposed PCMC SEPIC LED driver with PFC.

4. SIMULATION RESULTS

In this chapter, the proposed control strategy is applied to the LED driver circuit with PFC and without PFC. Circuits are simulated in PSIM software. Output current control of the LED string by proposed control method is validated. Power factor is compared for both circuit. Moreover, flicker metrics are calculated through the simulation, and checked whether the limits stays in recommended operating areas (see Figure 3.9 and Table 3.1) or not under several operation currents.

4.1 Power Stage and Driver Design

Design criteria and goals of the system are given in Table 4.1. SEPIC converter that is assumed to be working in continuous conduction mode is selected as LED driver. Nominal power of the LED is considered as 30 Watt. Required DC voltage at the input of SEPIC converter either can be rectified from AC power supply or directly connected to a DC power supply. Power factor higher than 0.9 is expected for PFC circuit.

Table 4.1 : Design criteria for LED driver.

Parameters	Symbols	Values
Input Voltage	V_{IN}	180V~260V AC 250V~360V DC
Output Voltage	V_{OUT}	100V
Output Current	I_{OUT}	50mA~300mA
Nominal Output Power	P_{OUT}	30 Watt
Line Frequency	f_L	50Hz
Switching Frequency	f_s	100kHz
Peak-to-Peak Current Ripple	ΔI_L	40%
Peak-to-Peak Output Voltage Ripple	ΔV_{OUT}	2%
Power Factor	PF	≥ 0.9

Output of the circuit consists of 37 series connected LED chips with adjustable current levels. Each LED has 2.7 V forward biased voltage and 1Ω internal resistance. The representation of AC-DC LED driver without the control stage is shown in Figure 4.1.

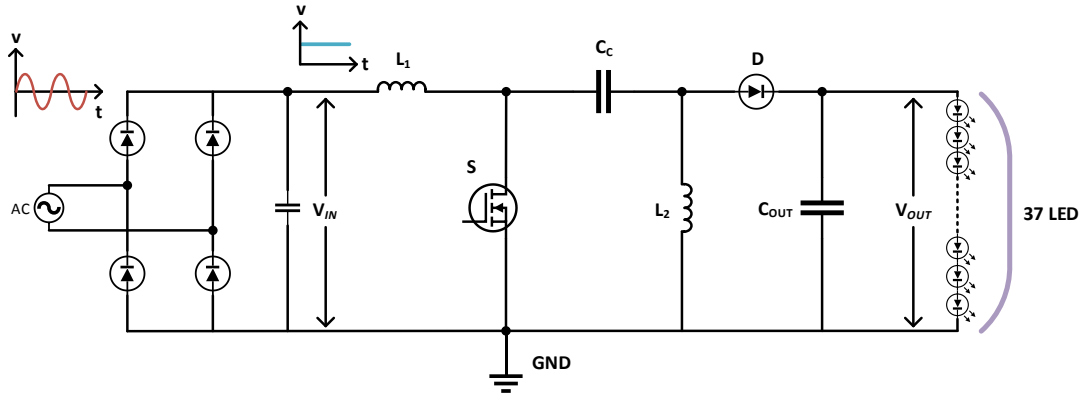

Figure 4.1 : Representation of AC-DC LED driver.

The input voltage of the proposed SEPIC converter can vary between 250 V and 360 V of DC voltage. While the minimum duty cycle occurs at maximum voltage, maximum duty cycle occurs at minimum voltage. Therefore, according to Equation 2.4, the minimum and maximum duty cycles are defined as:

$$D_{min} = 0.2174 \leq D \leq 0.2857 = D_{max} \tag{4.1}$$

The inductance value has been selected from peak-to-peak current ripple that is allowed to be 40% of the average input current for the worst case of operation. Whilst the highest input current occurs at the lowest input voltage value, the change from peak-to-peak current can be defined as:

$$\Delta I_L = I_{in}.40\% = I_{out}\frac{V_{out}}{V_{in(\min)}}40\% = 0.048\ A \tag{4.2}$$

When the switching frequency is selected as 100 kHz, the values of the inductances L_1 and L_2 are calculated as follows:

$$L_1 = L_2 = L = \frac{V_{in(\min)}}{\Delta I_L f_{sw}} D_{max} = 14.88\ mH \tag{4.3}$$

Assuming that the voltage ripple on the coupling capacitor is 10% of the DC input voltage, the value of coupling capacitor is calculated by following formula:

$$C_C = \frac{I_{OUT} D_{max}}{\Delta V_{C_C} f_{sw}} \geq 0.034\ \mu F \tag{4.4}$$

C_C is chosen as 0.1 uF.

In order to prevent the huge output ripple when no bulk capacitor is used for PFC circuit, output capacitor is calculated as follows:

$$C_{OUT} = \frac{I_{OUT}}{\Delta V_{OUT} 2\pi f} = 477\ \mu F \tag{4.5}$$

The driver circuit without controller is shown in Figure 4.2. For both circuit, current is sensed through a resistor in series with MOSFET and 220 V(rms)-50 Hz AC mains is used as input.

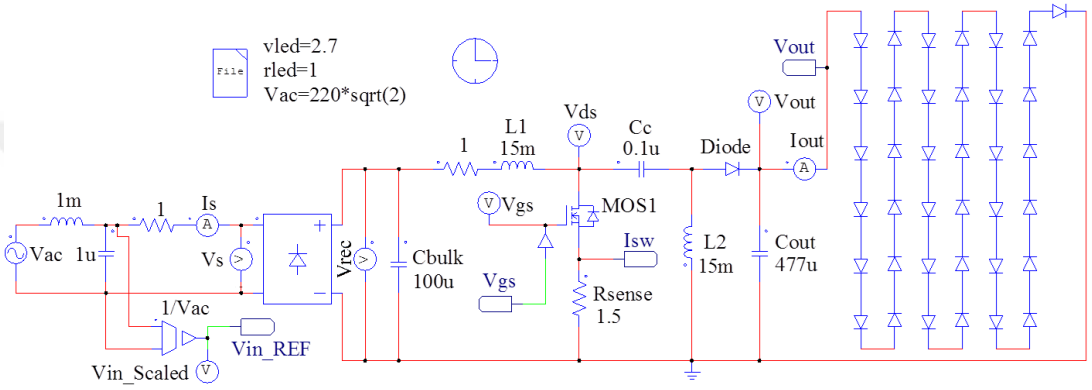

Figure 4.2 : PSIM driver circuit without controller.

The overall driver circuit including two separate controllers are given in Figure 4.3. The controllers are explained in related sections afterwards.

4.2 LED Driver without PFC

The controller circuit without PFC is shown in Figure 4.4. As in the proposed control strategy, a variable dc voltage source is directly connected to pin 1 of IC. Therefore, the control input voltage $V_{CONTROL}$ is the same node as error amplifier output V_c (see Figure 3.14 for notations). A simple RC filter is used to prevent huge spikes in current waveform while sensing the current, oscillator R_T/C_T is arranged that 100 kHz switching frequency is obtained (see R_T/C_T combinations versus oscillator frequency and related circuit for adjusting switching frequency in appendix).

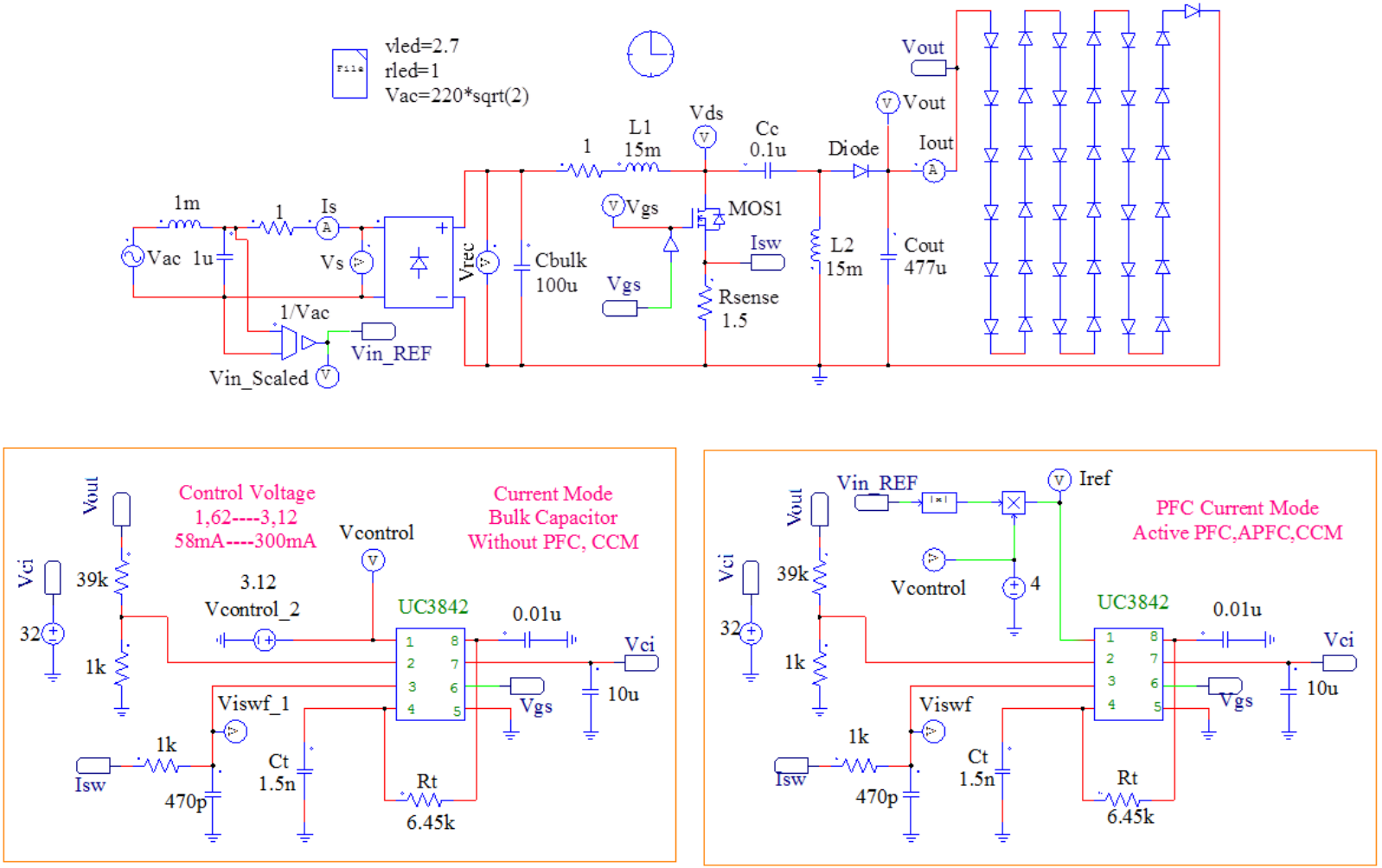

Figure 4.3 : Overall driver circuit.

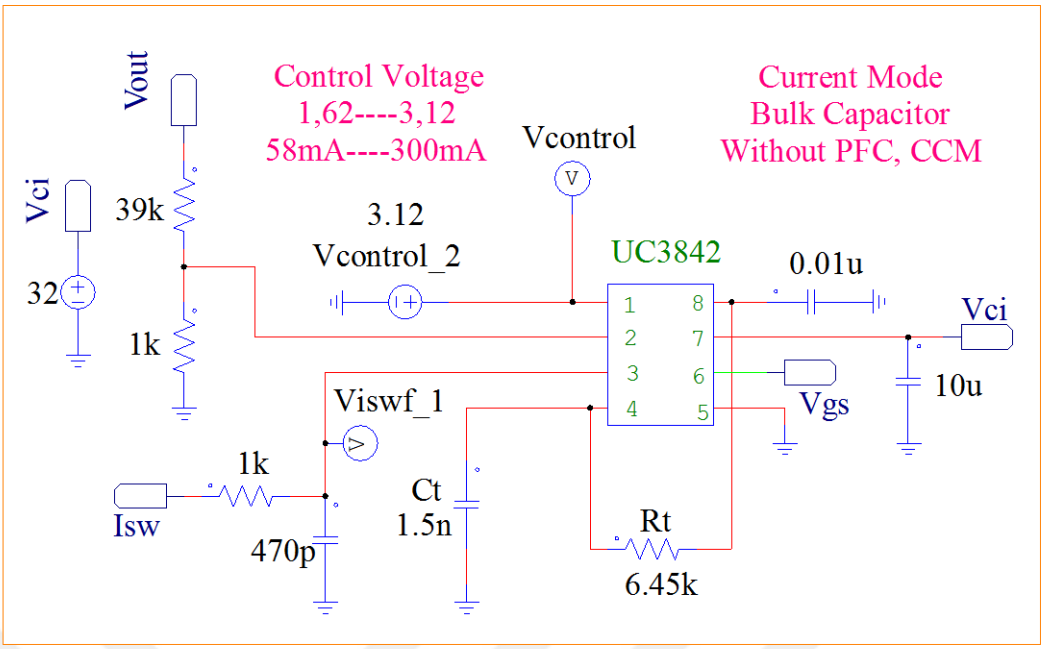

Figure 4.4 : Controller circuit without PFC.

Related waveforms for nominal operation output current 300 mA are given to understand the operation of the LED driver in Figure 4.5, 4.6, 4.7, 4.8, and 4.9.

When the control input voltage is 3.12 V, output current will be adjusted 300mA as shown in Figure 4.5. As can be seen, there is no current flow until the applied voltage reaches 99.9V (37x2.7V) which is the total forward voltage of the LED chips. The total output voltage will be 111V when the internal resistance's voltage drop is added (37Ωx0.3A).

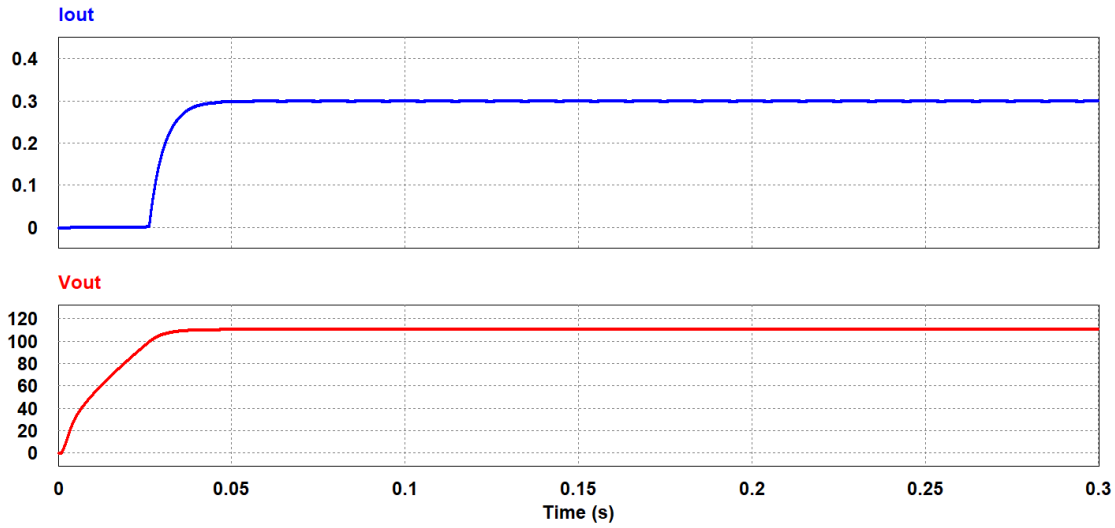

Figure 4.5 : Output current I_{OUT} (A) and output voltage V_{OUT} (V) [V_c at 3.12 V].

Control mechanism and generation of PWM signal are shown in Figure 4.6. 100 kHz clock signal (red), filtered sensed voltage (red) and peak threshold voltage (blue), PWM signal (black) are shown, respectively. Clearly, V_{gs} turned from 1 to 0 when the sensed voltage reaches the peak threshold voltage. V_{gs} is applied to MOSFET gate-source, to switch MOSFET on and off. In Figure 4.6, peak threshold voltage is limited to 0.64V, which can be calculated by the Equation 3.4:

$$V_{R_{SENSE}}(PEAK) = \frac{3.12 - 1.2}{3} = 0.64V \tag{4.6}$$

Where, R_{SENSE} is chosen as 1.5 Ω, two diode voltage drops as 1.2 V.

Peak current on R_{SENSE} is limited to 0.426A, which can be calculated by the Equation 3.5:

$$I_{R_{SENSE}}(PEAK) = \frac{0.64V}{1.5\Omega} = 0.426\ A \tag{4.7}$$

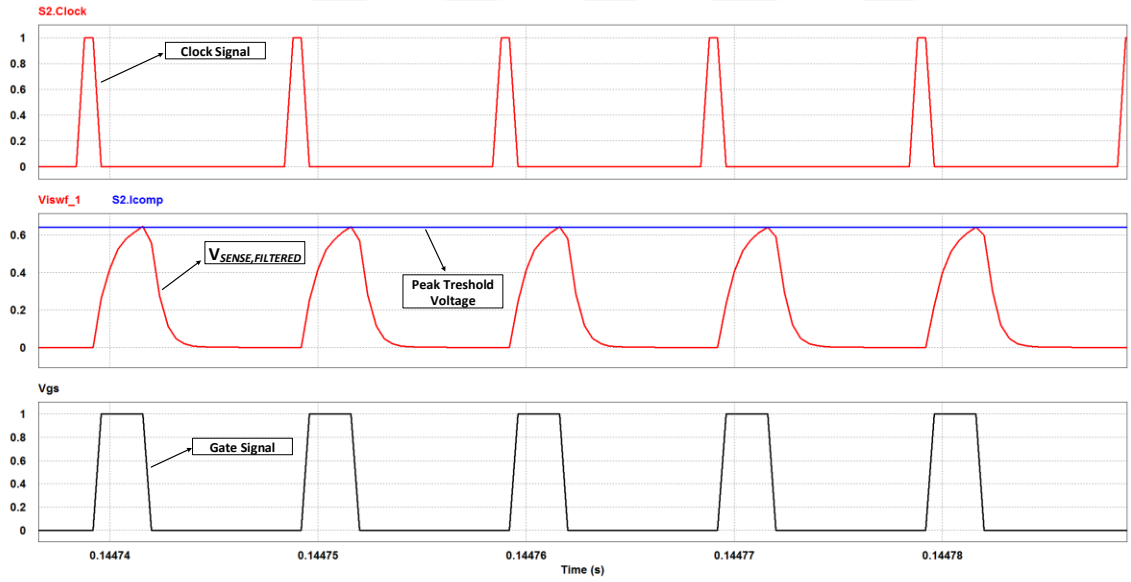

Figure 4.6 : PWM signal generation (V_c at 3.12 V).

Furthermore, RC filter has a significant influence on sensed voltage as shown in Figure 4.7. It suppresses the susceptible noises when sensing current and does not allow undesirable effects on gate signal. The peak current on sensing resistor R_{SENSE} is shown in Figure 4.8 and it is a bit higher than the expected value which is 0.455 A. Poor power factor around 0.42 is obtained in the line as shown in Figure 4.9.

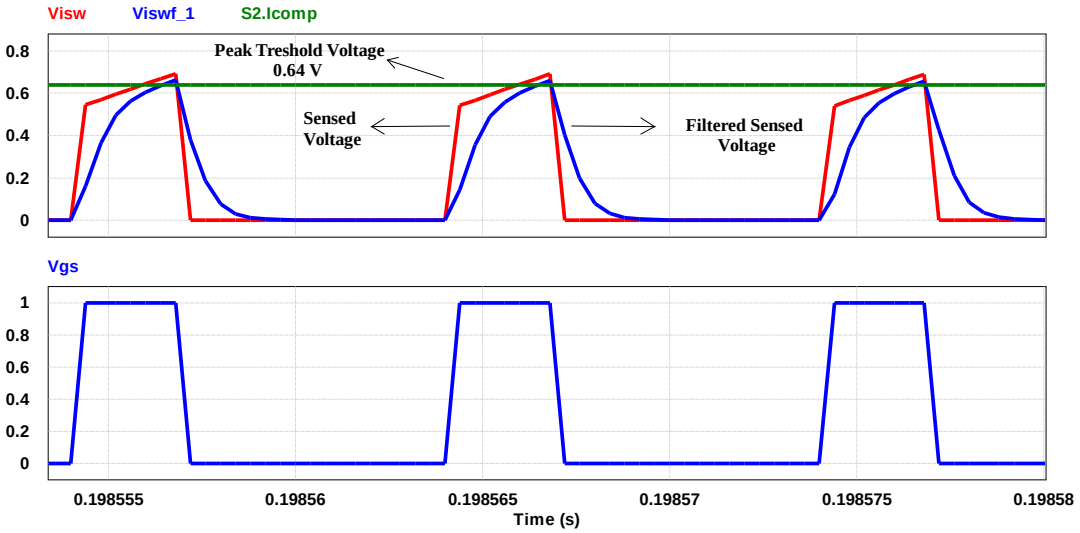

Figure 4.7 : Couple of PWM cycles (V_c at 3.12 V).

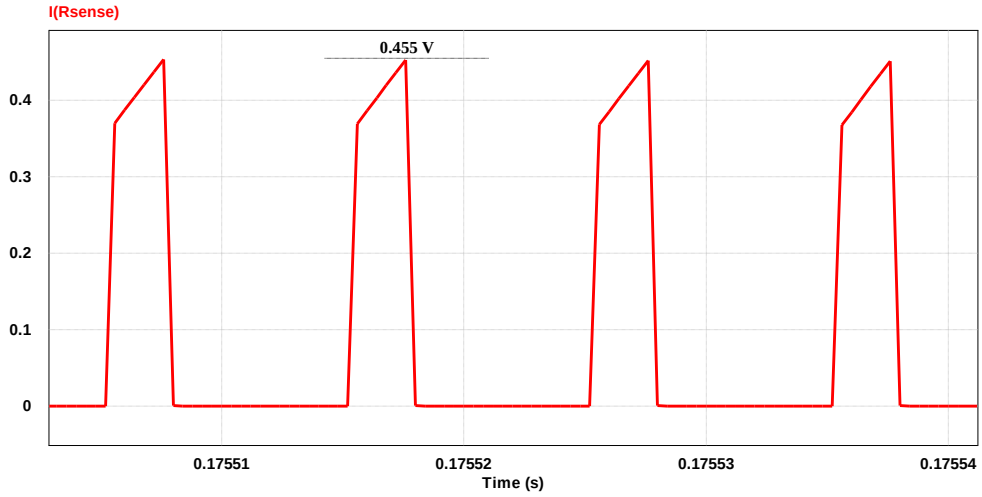

Figure 4.8 : Peak current on R_{SENSE} (V_c at 3.12 V).

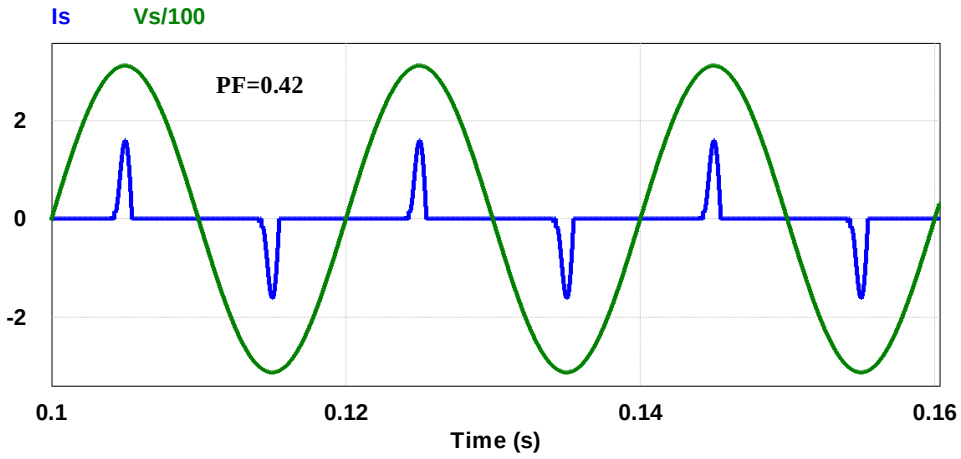

Figure 4.9 : Poor power factor (V_c at 3.12 V).

Four different control input voltage $V_{CONTROL}$ levels are selected to adjust the output current. $V_{CONTROL}$ was initially 3.12 V. Then, it is decreased by 0.5 V at each step. The output current results in 300mA, 221mA, 140mA and 58mA, respectively as shown in Figure 4.10.

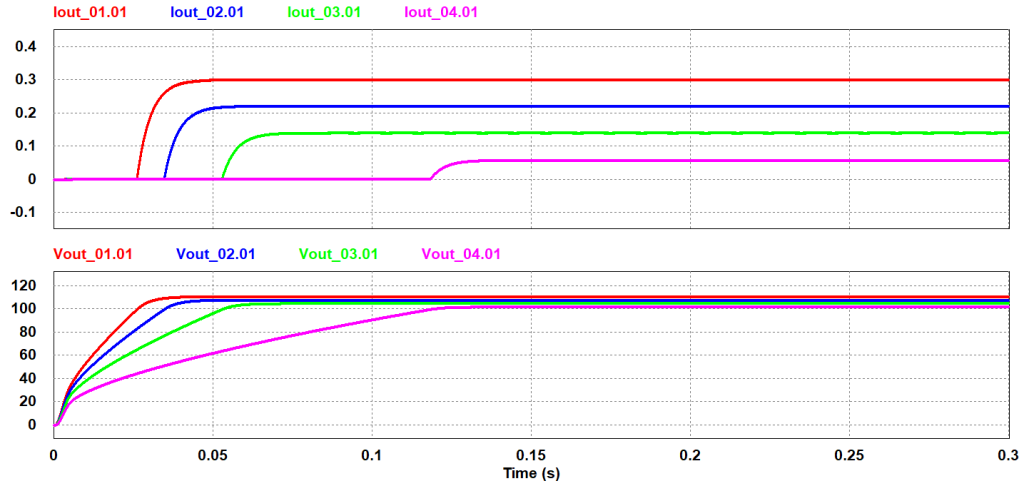

Figure 4.10 : Output currents (A) and output voltages (V) [$V_{CONTROL}$ at 3.12V (Red), 2.62V (Blue), 2.12V(Green) and 1.62V(Pink)].

Hence, the output current is adjusted around 50mA-300mA by changing the control voltage. LED brightness control is achieved. But, even more bad power factors (below 0.42) are obtained as the output current decreases. The output voltage is also decreased regarding the internal resistances of series connected LED's. 111 V peak, around 102 V minimum output voltages are obtained. Moreover, V_c is randomly changed to adjust output current in every 0.3 second while the circuit is running as shown in Figure 4.11.

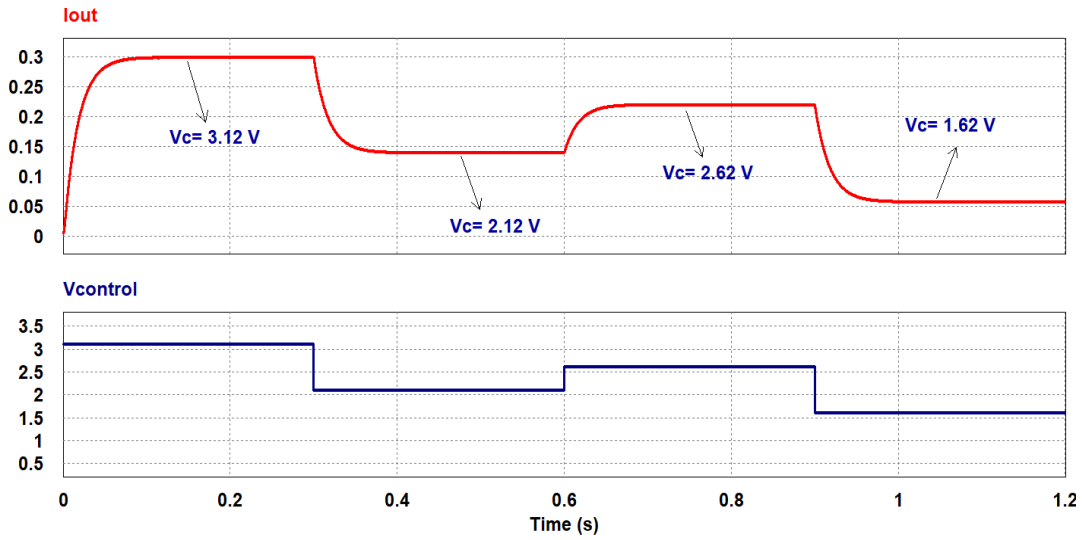

Figure 4.11 : Output current adjustment.

4.3 LED Driver with PFC

The controller circuit with PFC is shown in Figure 4.12. In proposed control strategy, the control input voltage $V_{CONTROL}$ is multiplied by sinusoidal input voltage and connected to pin 1 of IC. Now, the control voltage node V_c denotes as I_{ref} (see Figure 3.15 for notations). The reference current I_{ref} is pushed to follow the line current in order to get high power factor. Additionally, the bulk capacitor at the input of the converter is replaced with a small capacitor (100nF).

Four different control input voltage $V_{CONTROL}$ levels are selected. $V_{CONTROL}$ was initially 6 V. Then, it is decreased by 1 V at each step. The output current results in 305mA, 279mA, 220mA and 130mA, respectively as shown in Figure 4.13. Likewise, $V_{CONTROL}$ is randomly changed to adjust output current in every 0.3 second while the circuit is running as shown in Figure 4.14. The output current ripple is obtained around 16%, while the output voltage ripple is 2V. The ripple frequency is twice the line frequency.

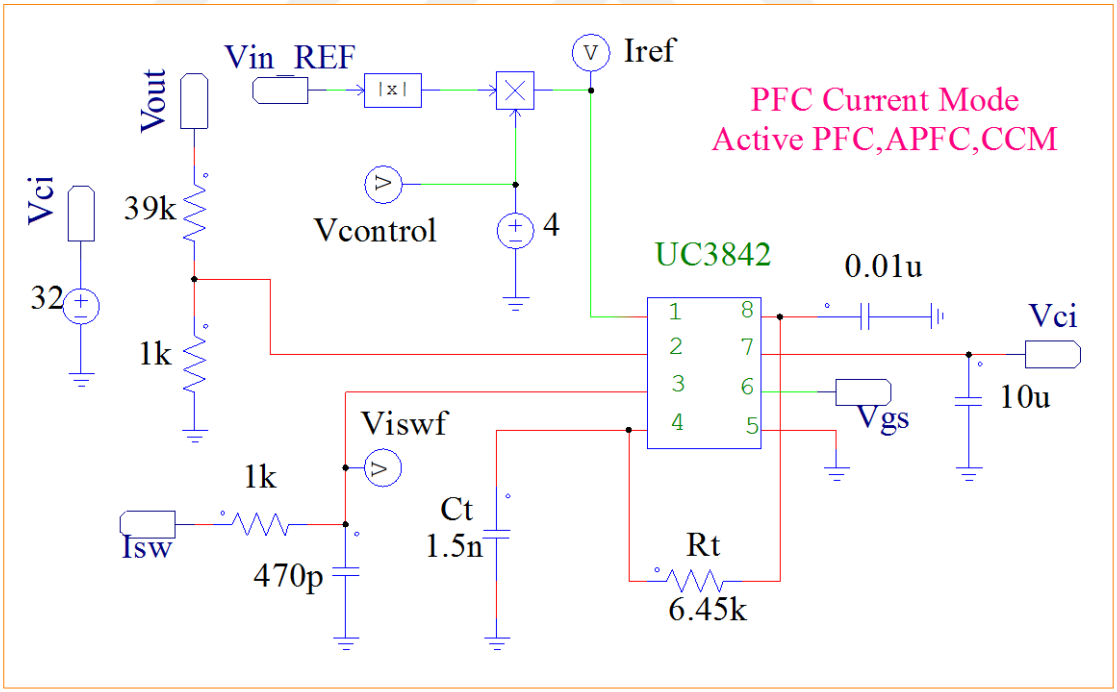

Figure 4.12 : Controller circuit with PFC.

Besides, while adjusting the desired output current level, the line current is always nearly in phase with the line voltage as shown in Figure 4.15.

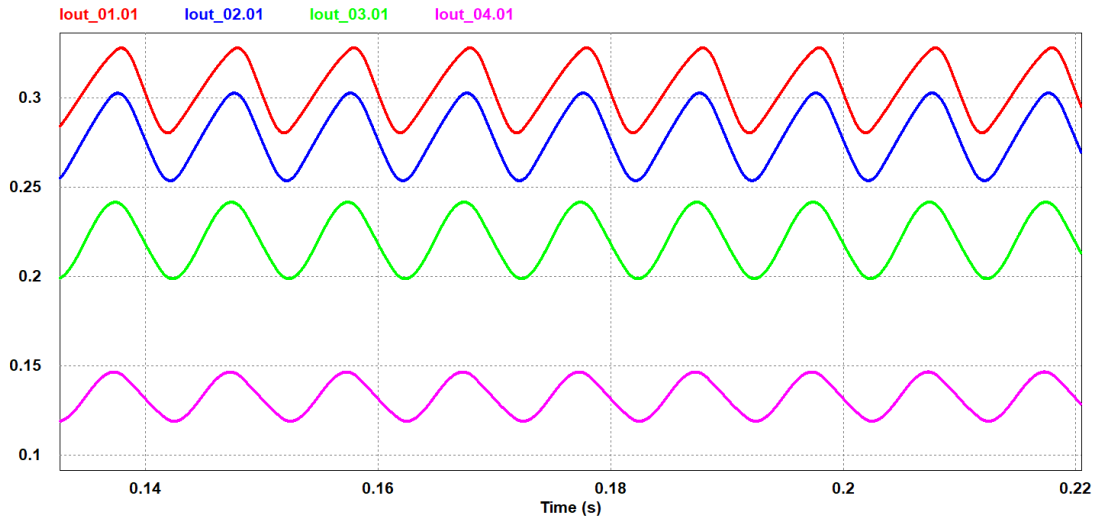

Figure 4.13 : Output currents (A) [$V_{CONTROL}$ at 6V (Red), 5V (Blue), 4V(Green) and 3V(Pink)].

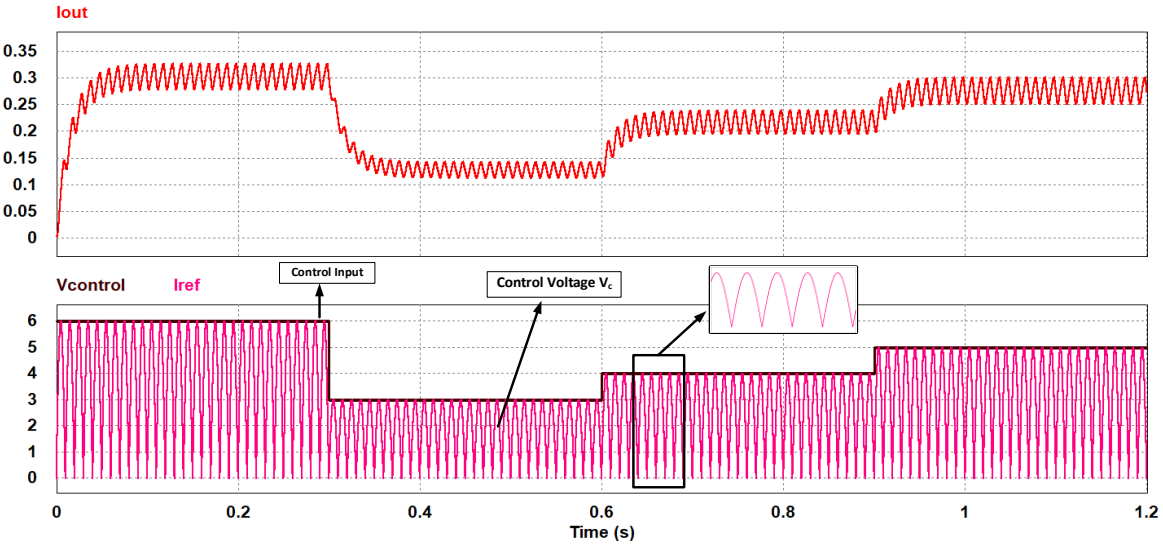

Figure 4.14 : Output current adjustment in PFC driver.

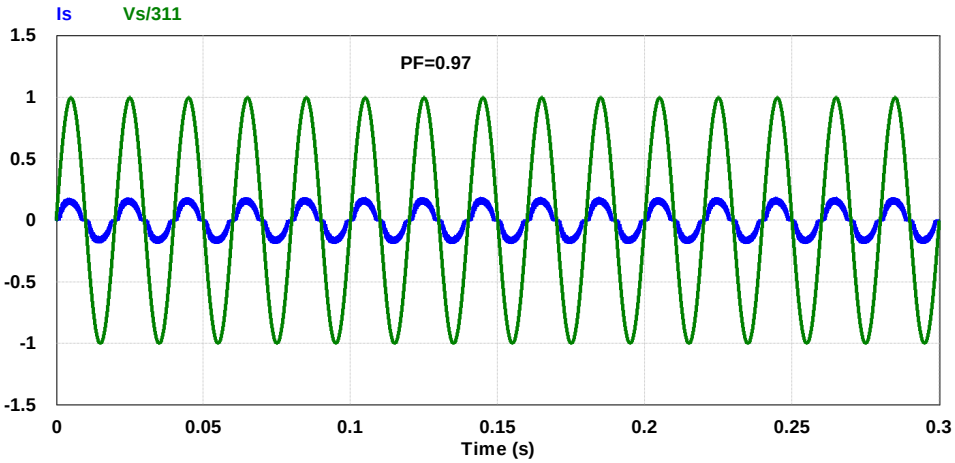

(a)

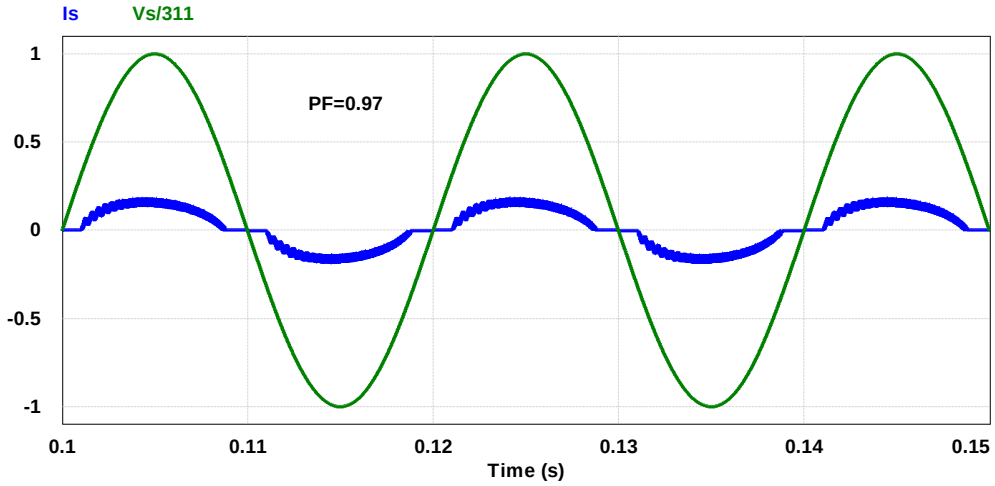

(b)

Figure 4.15 : Input current I_S and input voltage V_s ($V_{CONTROL}\ at\ 4V$): a) Larger time span. b) Shorter time span.

However, the control input voltage is adjusted to 6V to operate at 305 mA output current. When the control input voltage is multiplied by the input voltage, the reference current I_{ref} waveform is shaped like full wave rectified voltage having 6 V peak as shown in Figure 4.16.

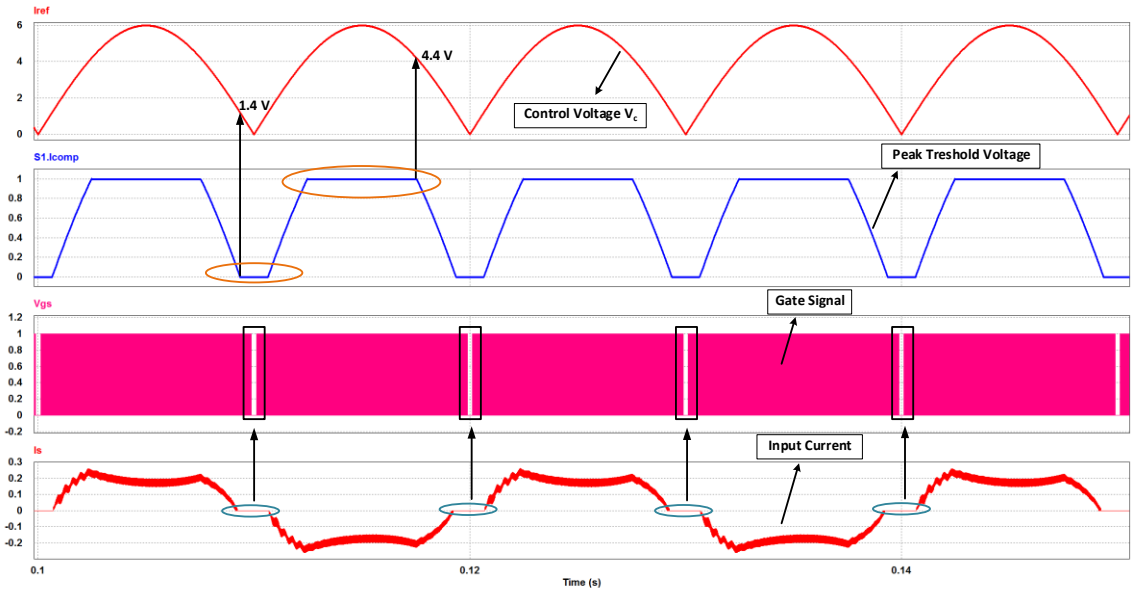

Figure 4.16 : Distorted input current due to control voltage limitations on IC ($V_{CONTROL}\ at\ 6V$).

According to Equation 3.4, minimum control voltage should be greater than 1.4V. So, the control voltage smaller than 1.4V will cause small blank areas on gate signal V_{gs} of MOSFET in each half period of input voltage (10ms). Also, peak threshold voltage is limited to 1V with a zener diode. Therefore, providing that the control voltage is

greater than 4.4V, the reference voltage will not exceed 1V. Eventually, the input current waveform I_s is slightly distorted in these areas.

4.4 Power Factor Comparison

The output current of the LED is successfully controlled by both circuits. High power factor is achieved with power factor correction LED driver. The output current level of the LED versus power factor is plotted in Figure 4.17.

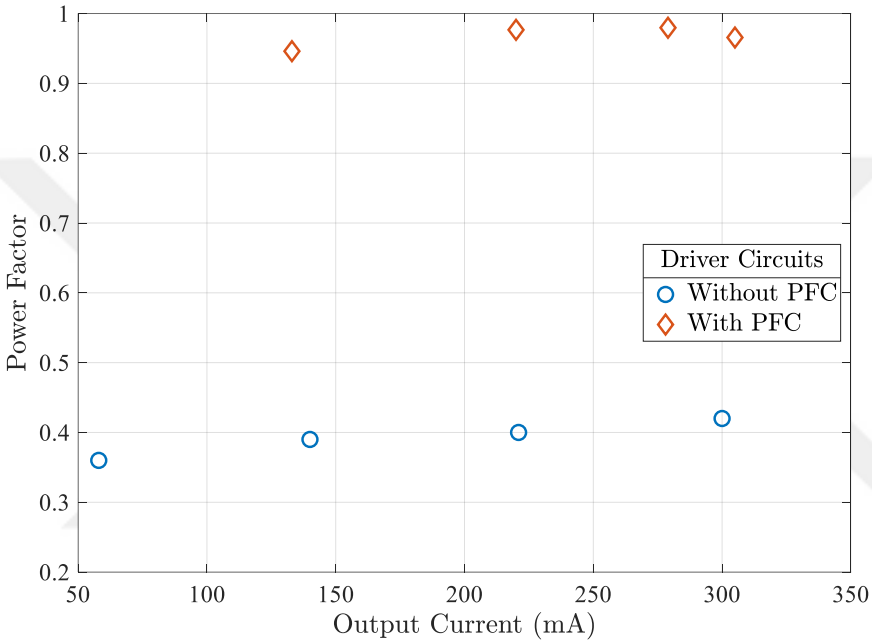

Figure 4.17 : Output current vs. power factor.

Power factor is plotted according to data recorded at different output currents shown in Table 4.2.

Table 4.2 : Power factor and output current data of driver circuits.

	Output Current (mA)	Power Factor
Without PFC	300	0.420
	221	0.400
	140	0.390
	58	0.360
With PFC	305	0.966
	279	0.980
	220	0.976
	133	0.946

4.5 Flicker Comparison

Flicker tests for LED string are held for both circuits in Figure 4.18 and 4.19. Percent flicker and flicker index are measured and calculated by formulas given in related section (See Chapter 3.2).

Low risk region for flicker frequencies above 90 Hz is given by "$Mod\% < 0.08 f_{flicker}$", while no observable effect level (NOEL) is given by "$Mod\% < 0.0333 f_{flicker}$". In our case, modulation in current waveform should be smaller than 8% for low risk level and smaller than 3.33% for NOEL, considering flicker frequency is 100 Hz (See Table 3.1).

It can be seen from Figure 4.18, the modulation also called as percent flicker stays in the limits of NOEL for different output current levels and it is far below the any biological effect region.

However, the modulation in PFC circuit stays in low risk level for nominal operation current 300 mA, while the modulation for below 300 mA output current exceeds the limits for low risk level up to 10.5%.

The flicker index was recommended to be below 0.1 at 100 Hz flicker frequency in general lighting applications. For both circuit, flicker index stays within this limit over the operation region.

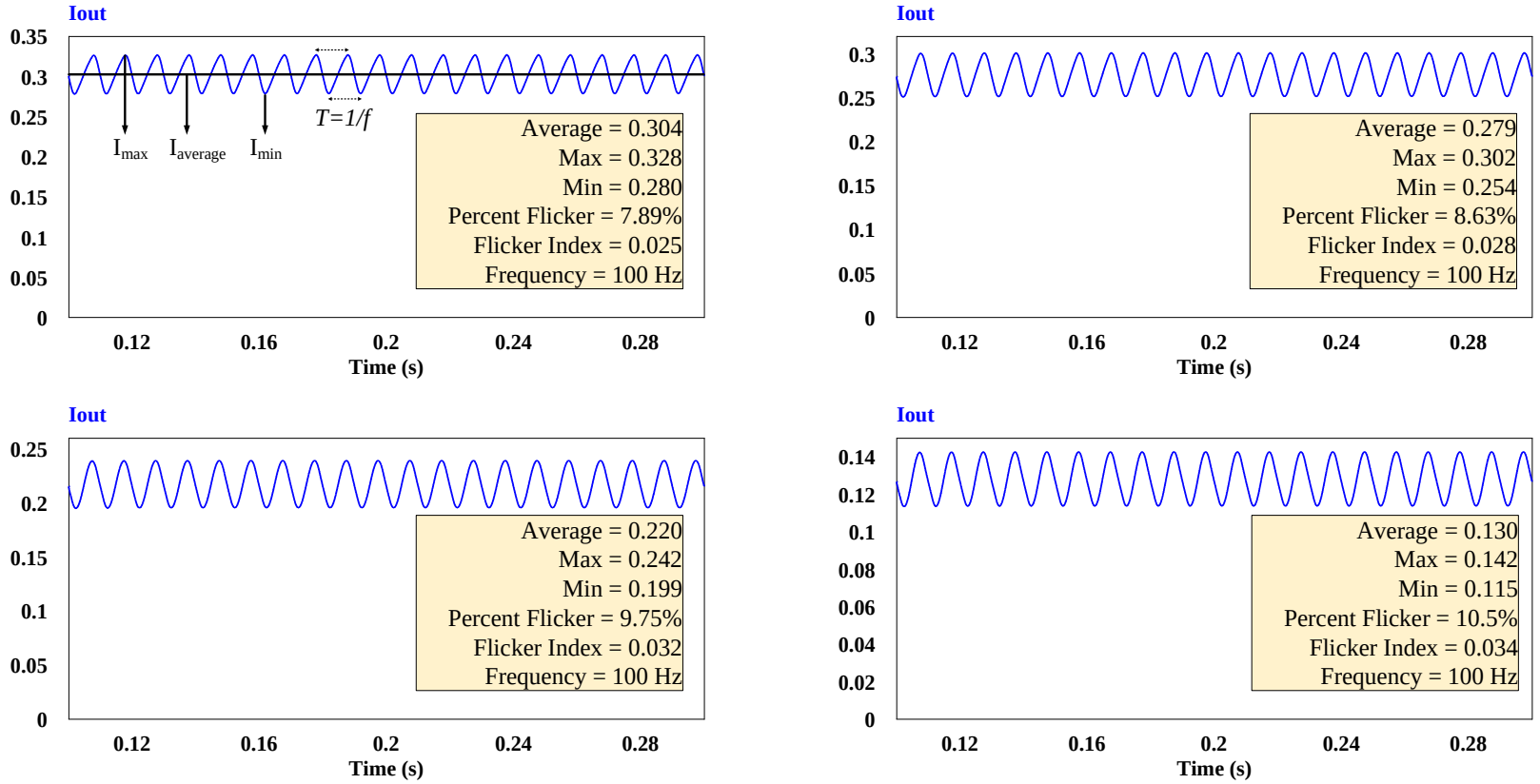

Figure 4.18 : Flicker measurements (With PFC).

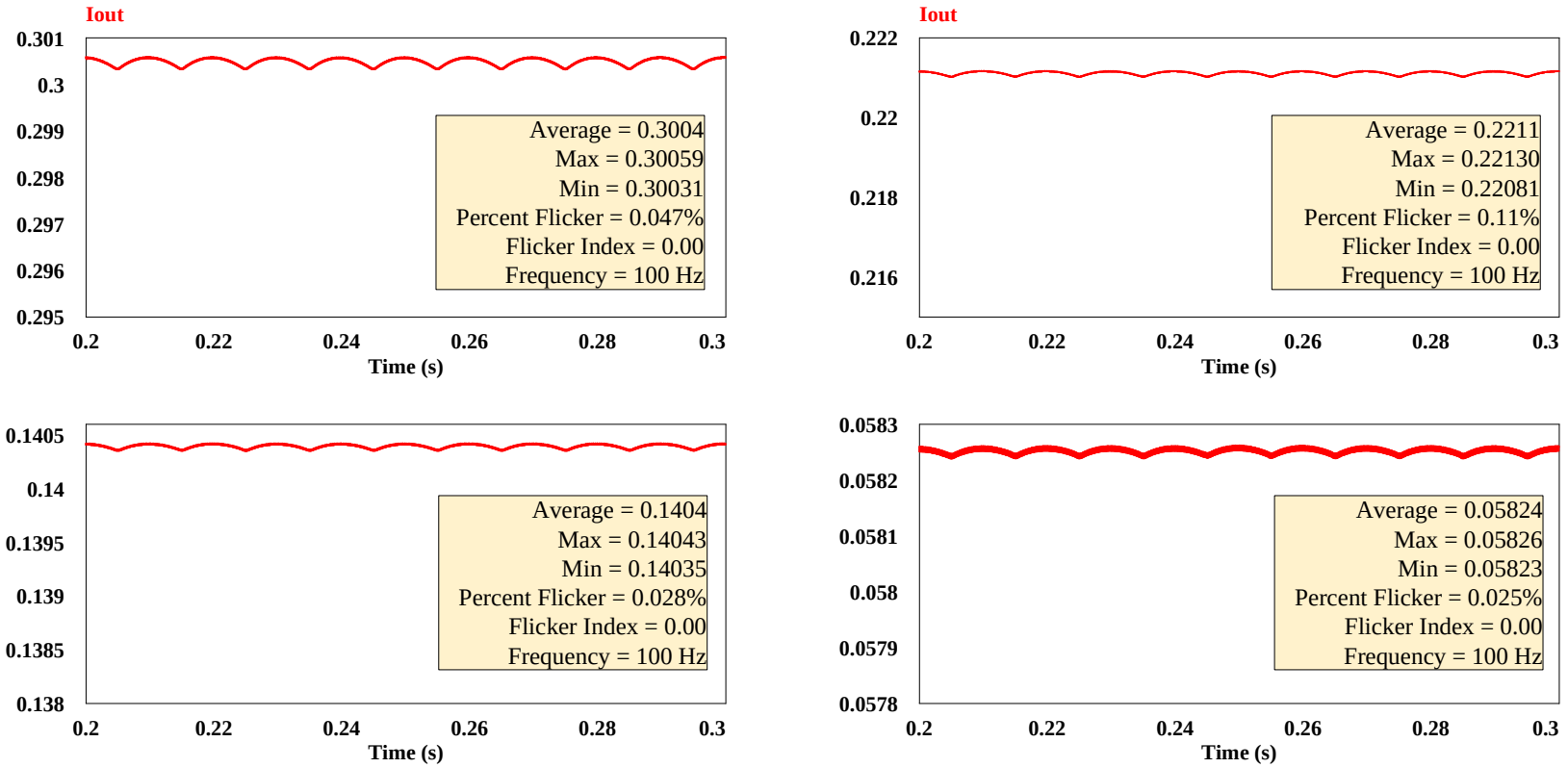

Figure 4.19 : Flicker measurements (Without PFC).

5. EXPERIMENTAL RESULTS

The proposed peak-current-mode-control strategy should be tested experimentally even though the simulation results give many ideas about the operation principle of the LED driver. In this chapter, experimental results of the proposed PCMC SEPIC LED driver without PFC are given. Efficiency of the driver circuit is calculated. Flicker on LED string is measured from the current flowing through the LED.

5.1 Component Selection and Experimental Setup

At first, 30 Watt LED should be chosen according to the design goal in Table 4.1. Therefore, a higher wattage LED is preferred in practice which is shown in Figure 5.1. This LED is actually 70 Watt but it has two 35 Watt LED string. Therefore, only one of the strings will be used.

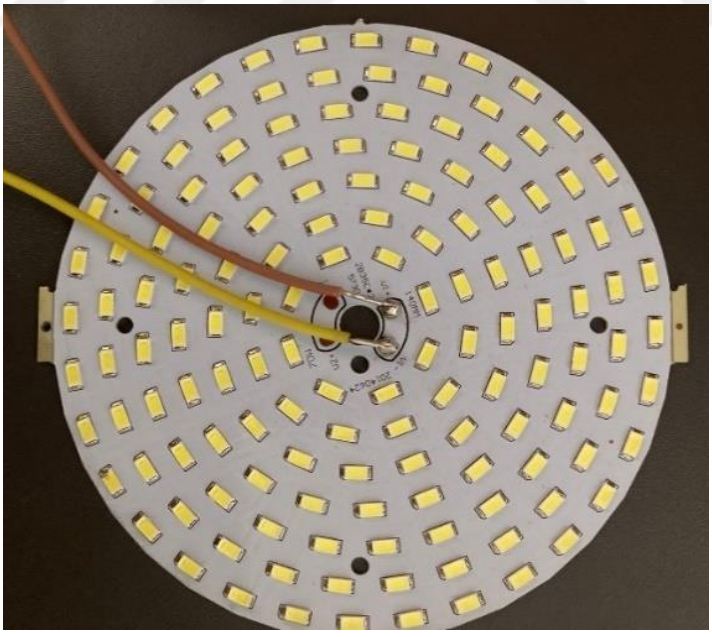

Figure 5.1 : Two 35 Watt LED string.

LED is tested directly from a DC power supply before it is connected to the driver circuit. V-I table of this LED is given in Table 5.1.

Table 5.1 : V-I characteristic of the 35 Watt LED.

Voltage (V)	Current (mA)
91	10
93.4	20
97	50
98	60
99.1	80
100.5	100
103.4	140
106.2	190
107.2	210
108.1	230
108.4	240
109.5	260
110	280
110.8	300

5.1.1 MOSFET and output diode selection

220 VAC (rms) voltage will be rectified by a full wave bridge rectifier with capacitor filter. The rectified voltage at the input of the SEPIC converter can be at max 311.12 V considering the AC signal is not fluctuating and purely sinusoidal. The output voltage of the SEPIC converter according to Table 5.1 is around 110 V. Therefore, the switches must withstand voltage stress of at least 420V (See considerations 2.2.4 in Chapter 2).

- IRF840 MOSFET from International Rectifier company is chosen for this purpose [37]. Maximum Drain-Source Voltage of the MOSFET is 500 V, while the current passes through the MOSFET can be up to 8A that is easily satisfy the current stress on switch in proposed driver circuit.
- As a diode, MUR1560 from ON Semiconductor is preferred [38]. This diode has a 600 V DC blocking voltage, and forward current of the diode can handle current stress higher than the proposed driver circuit up to 15 A.

5.1.2 Inductor and inductor current ripple selection

Let's consider inductor is selected according to aforementioned considerations (See considerations 2.2.2 in Chapter 2). When the MOSFET is closed, the rectified input voltage will be applied to inductor and this voltage is high. According to Equation 2.8, the average current of inductor L_1 is found as:

$$I_{L1} = \frac{110 \cdot 0.3}{311} = 0.106\ A \tag{5.1}$$

When the Peak-to-peak current ripple of L_1 is chosen 40% of the average inductor current, ΔI_L will be 0.0424 A. Duty cycle is calculated as follows:

$$D = \frac{110}{311 + 110} = 0.261 \tag{5.2}$$

If the switching frequency is selected 40 kHz, the inductor value is calculated as:

$$L_1 = L_2 = \frac{V_{in}D}{\Delta i_{L1} f_s} = \frac{311 \cdot 0.261}{0.0424 \cdot 40000} = 0.048H \tag{5.3}$$

As seen in CCM mode, the inductor values found as 48 mH which is not something applicable. To reduce the inductor value, the switching frequency can be increased but that leads another issues related with the noise, switching losses, and EMI. Therefore, 40 kHz switching frequency is selected for the experimental circuit.

What can be done is that operate the converter in Discontinuous Conduction Mode. This can increase current stress on switching device but selected devices can capable of carrying these currents. In addition, the peak current on MOSFET can be limited by the proposed PCMC method. For the above purposes, inductors are selected as 2 mH. The inductor is chosen as SRC1616-102M 1mH fixed inductor from Core Master company [39]. In order to get 2 mH, two 1 mH inductors are connected in series.

5.1.3 Experimental setup

Overall circuit including the controller is drawn to understand layout of the circuit in PSIM and shown in Figure 5.2.

Current-Mode PWM controller TL3845 from the Texas Instruments is used. There are small differences between UC3842 and TL3845 but they are used for the same manner. Maximum duty cycle of the TL3845 is limited by 50% and the start threshold voltage of the controller is 8.4 V [40]. The supply voltage of the TL3845 can be adjusted to gate-to-source voltage of the MOSFET. Because, the supply voltage determines the output voltage of the controller (See pin configuration and functions of the TL3845 in appendix). The LED at the pin 8 is just to indicate that there is power on controller. At pin 1, two external diodes are connected for the technique called “Adjustable

Reduction of Clamp Level" [40]. The diodes compensate the internal diodes voltage drop and peak threshold voltage on sensing resistor becomes easy to calculate. The calculation of the peak current and peak voltage on sensing resistor becomes as:

$$V_{R_{SENSE}}(PEAK) = \frac{V_C - 1.4V + 1.4V}{3} = \frac{V_C}{3} \tag{5.4}$$

$$I_{R_{SENSE}}(PEAK) = \frac{V_C}{3R_{SENSE}} \tag{5.5}$$

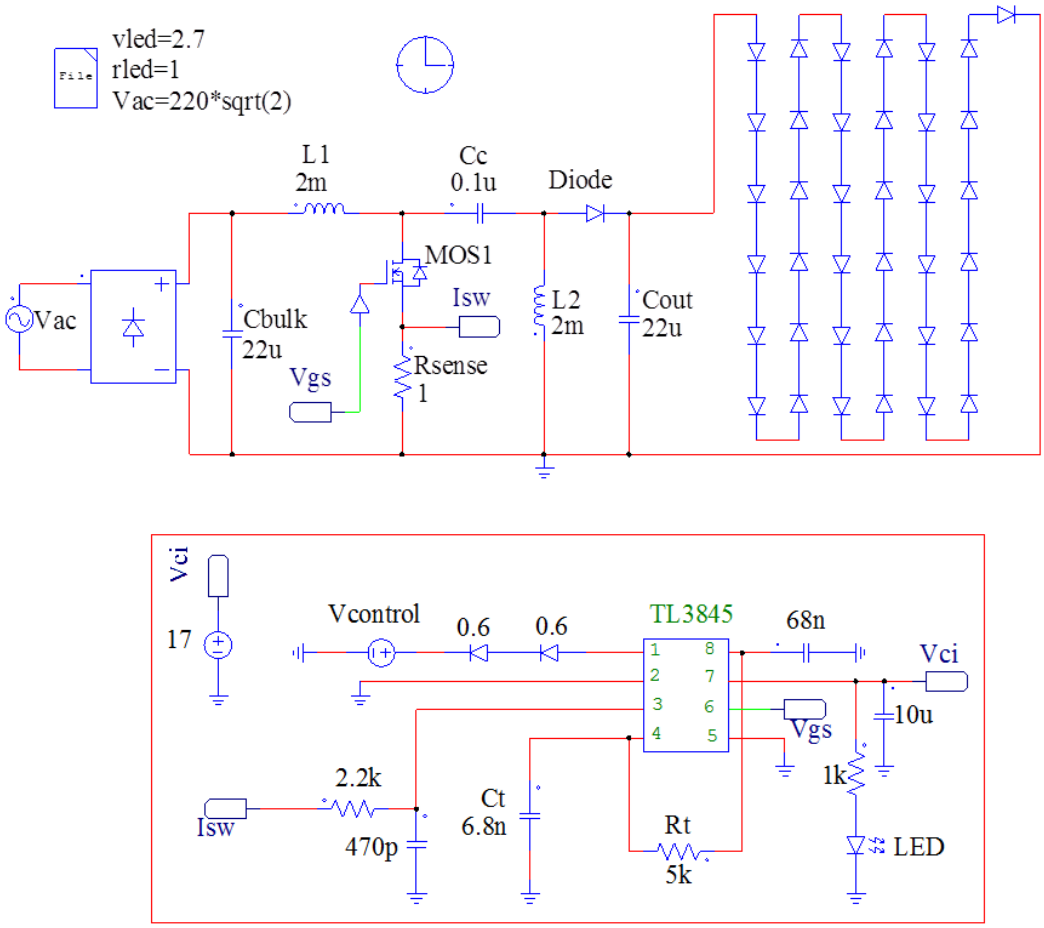

Figure 5.2 : Experimental LED driver circuit.

Elements used in driver circuit are listed in Table 5.2. Experimental setup in laboratory is shown in Figure 5.3. The proposed PCMC SEPIC LED driver is operated at nominal output power which is 33.6 Watt in Figure 5.3 (b). Each equipment is shown with their identifier in Figure 5.4 and given in Table 5.3.

Table 5.2 : Experimental components used in the driver circuit.

Component List	
IRF840	MOSFET
MUR1560	Output Diode
2 mH	Inductors
22 μF	Output Capacitor
0.1 uF	Coupling Capacitor
1 Ω	Sensing Resistor
22 μF	Input Capacitor
35 Watt	LED
10 Ω	Gate Resistor
50 $k\Omega$ Pot - 6.8 nF	Oscillator R_t/C_t
2.2 $k\Omega - 470$ pF	Current Spike Filter
1N4148	Reduction of Clamp Level Diodes
Gw-Instek GPC-3060D	DC Power Supply
Tektronix TDS 1001B	Oscilloscope
Wavetek DM23XT	Digital Multimeter
De Lorenzo- DL1013T1	AC Power Supply
De Lorenzo- DL1031	Wattmeter
De Lorenzo- DL2642	Isolation Amplifier
De Lorenzo- DL 1093	Transformer

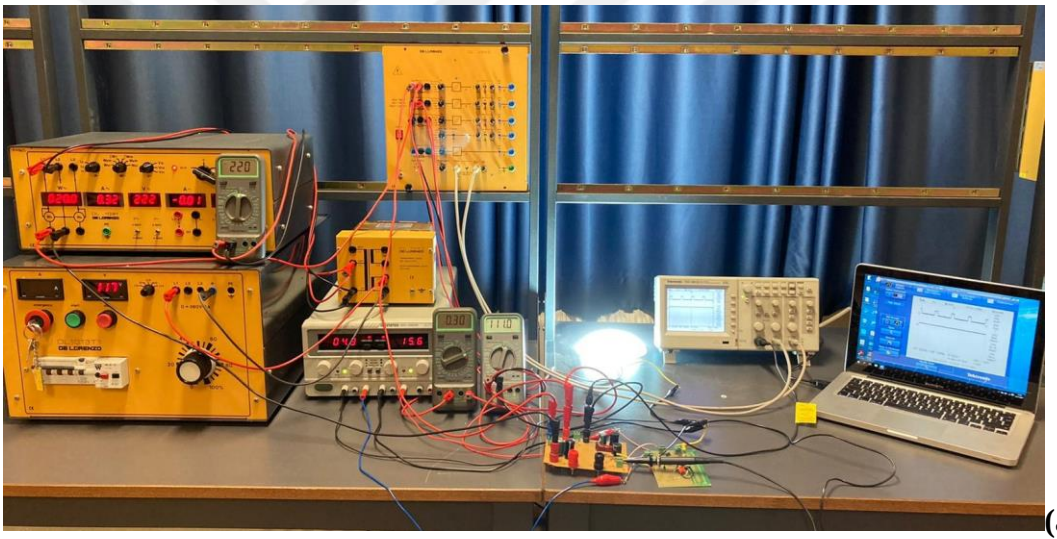

(a)

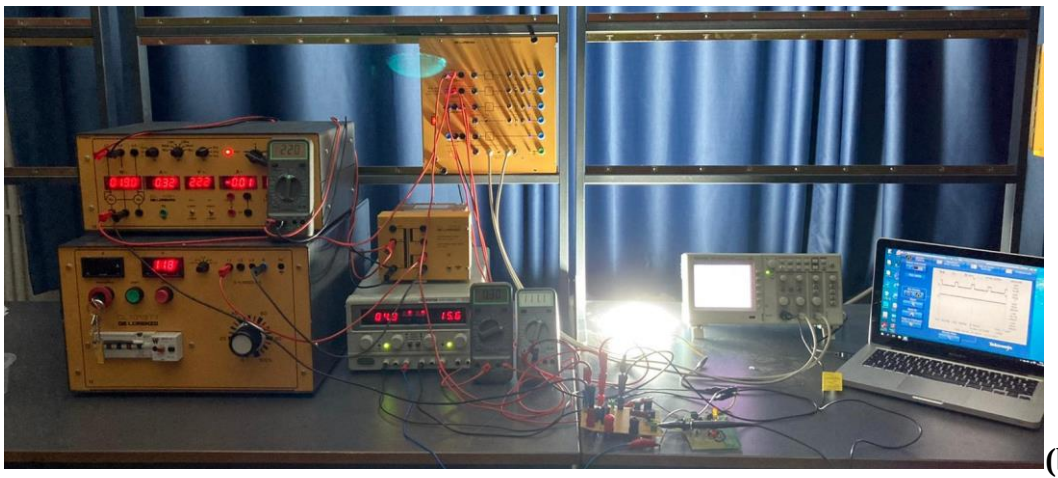

(b)

Figure 5.3 : Experimental setup at nominal output power: a) Laboratory light on. b) Laboratory light off.

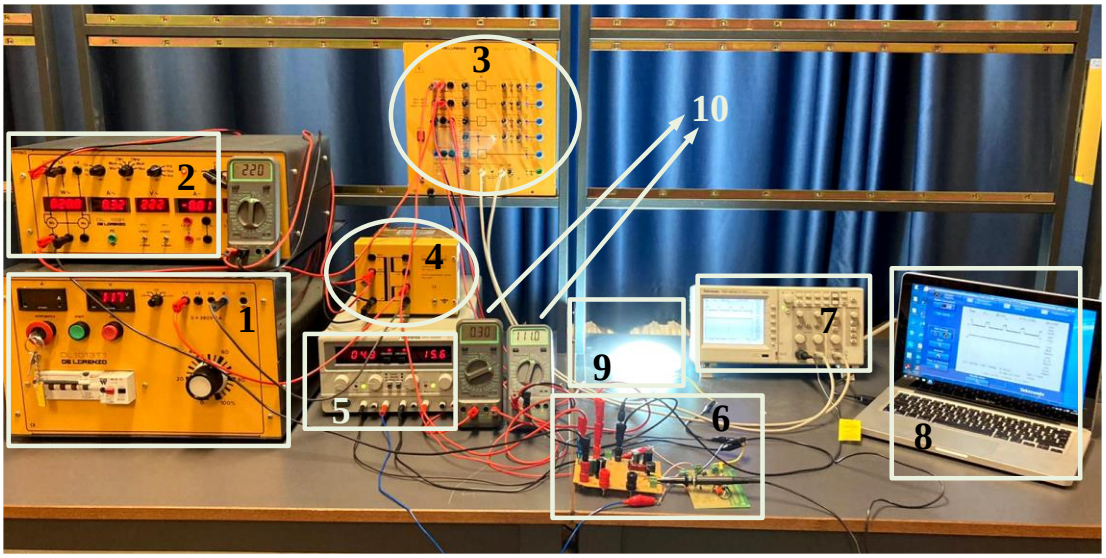

Figure 5.4 : Introduction of laboratory setup.

Table 5.3 : Device identification.

Identifier	Equipment
1	AC Power Supply
2	Wattmeter
3	Isolation Amplifier
4	Transformer
5	DC Power Supply
6	PCMC SEPIC Driver
7	Oscilloscope
8	Computer
9	LED
10	Multimeter

- Right hand side channel of the DC power supply (15.6 V) is used to supply TL3845 controller, while the other channel is to adjust control voltage (4.3 V) which will determine the threshold voltage to turn off the MOSFET. The output current is adjusted from the left hand side channel.
- A variable three-phase power supply from De Lorenzo Company [41] is used to supply AC input of the driver circuit. Single phase will be used for 220V rms. Technical features can be found in datasheet.
- A transformer is used for the isolation between circuit and AC power supply.
- An isolation amplifier connected to the oscilloscope is used for potential-free measurements. Technical features are given in datasheet [42].
- A wattmeter is used to measure the current and active power drawn by the source.

- Digital multimeters are used to measure output current and voltage. Right hand side multimeter is used as a voltmeter for the output voltage (111 V), while the left hand side multimeter is used as an ampere-meter for the output current (0.3 A). Far left multimeter is to measure AC input voltage.
- In addition, a computer is connected to oscilloscope for screenshots of the waveform and waveform data.
- Isolation amplifier has 4 channels A, B, C, and E. Three channels of the isolation amplifier are used. The attenuator is chosen 1 V/A at Channel A for the input current which will be equal to amplitude of the signal seen on oscilloscope screen. As similar, the attenuator is chosen 1 V/A at Channel B for the output current. The Channel C is used for the output voltage. The attenuator of Channel C is chosen as 1/100.

The SEPIC converter and its controller are shown in Figure 5.5, 5.6, and 5.7. The driver circuit can be either connected to AC or DC power supply. In Figure 5.6, the DC output of the SEPIC converter is connected to LED string. In Figure 5.7, the control input will adjust the output current/ brightness of the lighting source.

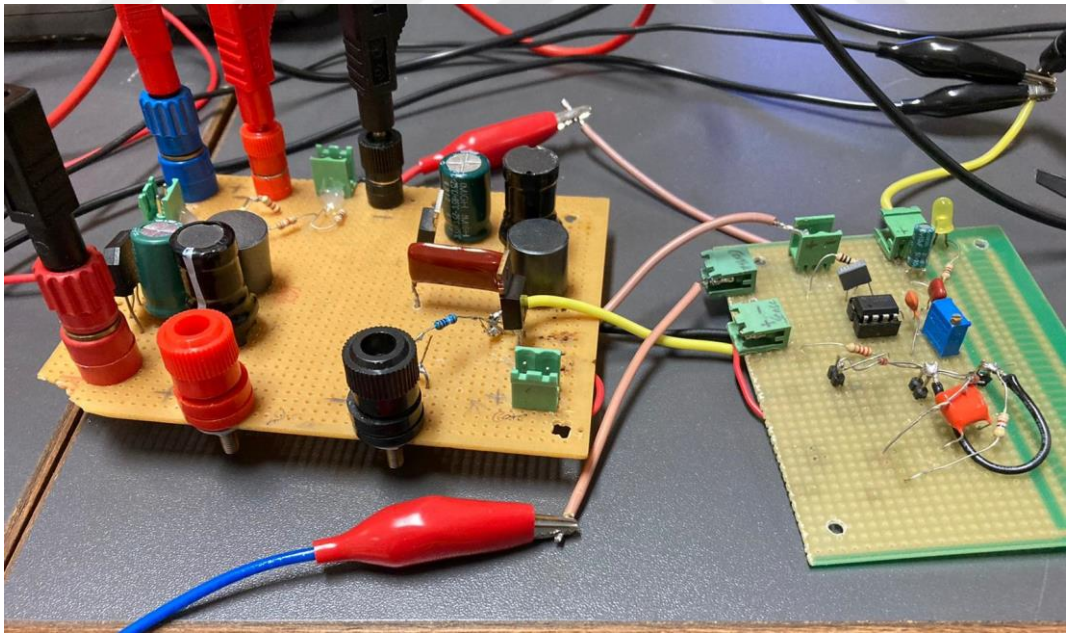

Figure 5.5 : SEPIC converter and proposed peak-current-mode controller.

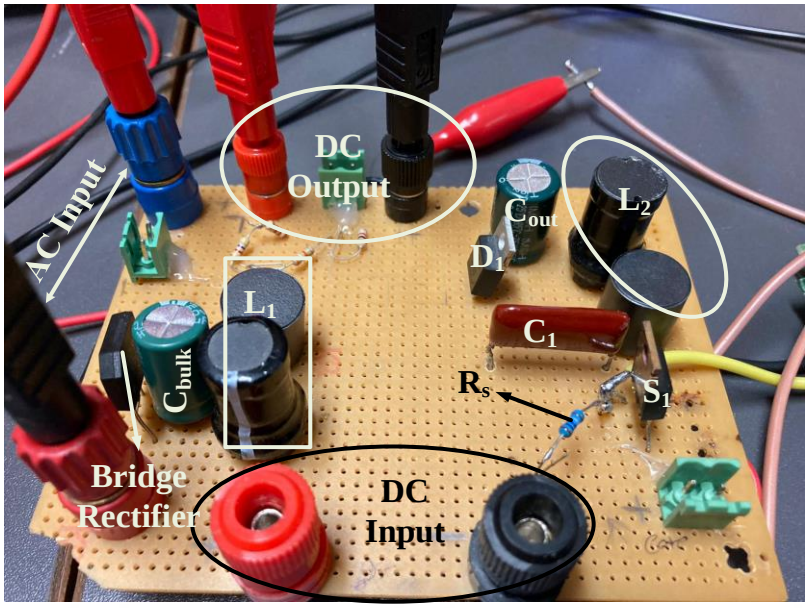

Figure 5.6 : SEPIC converter.

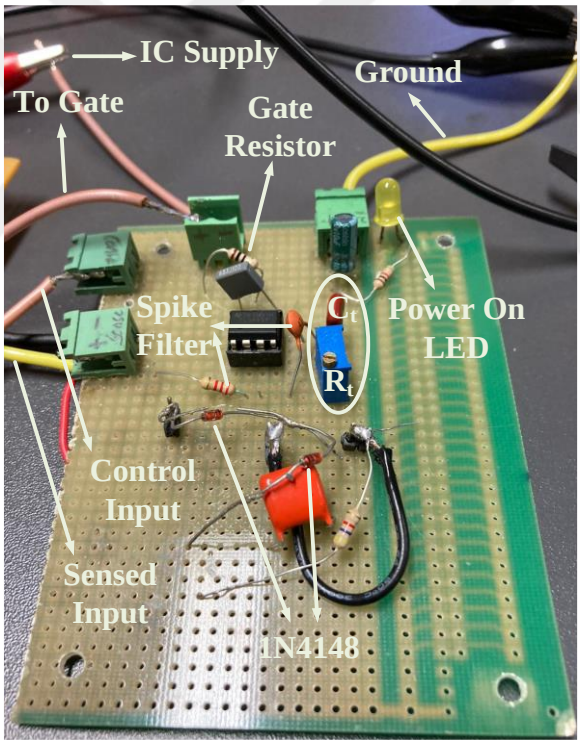

Figure 5.7 : Proposed peak-current-mode controller.

5.2 Experimental Results of the Proposed PCMC SEPIC LED Driver

First, related waveforms such as PWM signal, input current, output current, output voltage, sensed voltage are given when the control voltage is 4.3 V. The waveforms and data are saved via computer connected to oscilloscope. The PWM signal and the output current are shown in Figure 5.8. The average output current is adjusted 307 mA

as seen in Channel 2 mean value. The attenuator of the isolation amplifier for output current channel is chosen as 1V/A. Hence, the mean voltage value of 307 mV is actually 307 mA. Digital multimeter also shows the output current as 300 mA. 40 kHz switching frequency is obtained by adjusting the potentiometer R_t of the oscillator. The duty cycle is recorded as 0.187 (4.687us/25us).

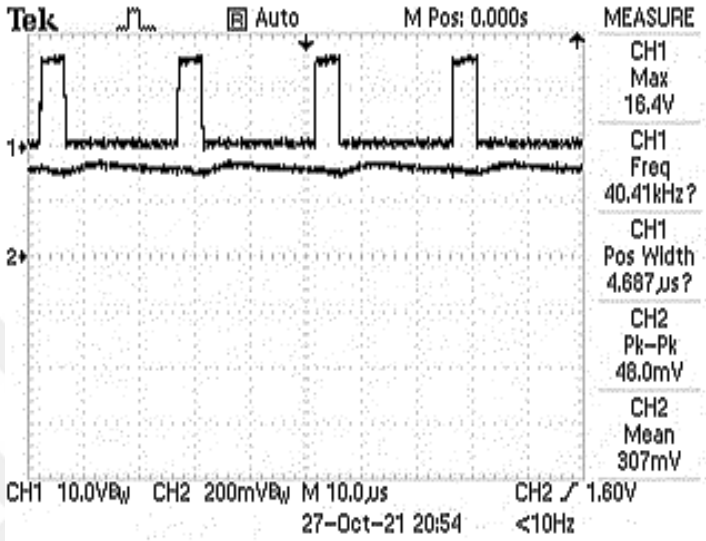

Figure 5.8 : PWM signal and 300 mA output current (Control voltage at 4.3 V).

The PWM signal and the output voltage are shown in Figure 5.9. The output voltage is adjusted 1.14 V as seen in Channel 2 mean value. However, the actual output voltage is 111.4 V since the attenuator of the isolation amplifier for related channel is chosen as 1/100. Digital multimeter also shows the output voltage as 111V. This shows that the measurements are reliable.

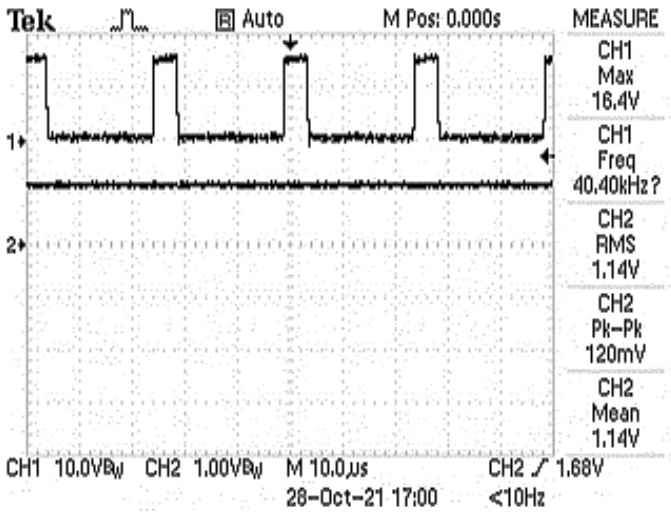

Figure 5.9 : PWM signal and 111 V output voltage (Control voltage at 4.3 V).

The key part of the driver circuit lies on the controller circuit. The switch S_1 current is sensed by R_s in Figure 5.6. Channel 1 of the oscilloscope is directly connected to source of the switch. Choosing the R_s as 1Ω will make the voltage on sensing resistor same as the current flowing through on it. However, tolerance of the resistor should be considered. The sensed current on sensing resistor is given in Figure 5.10. First observation is the noise when sensing the current. The current spikes at the leading edge of the waveform are quite high up to 3.48 V and it should be suppressed. This can cause the switch turn off earlier and whole operation can be ruined.

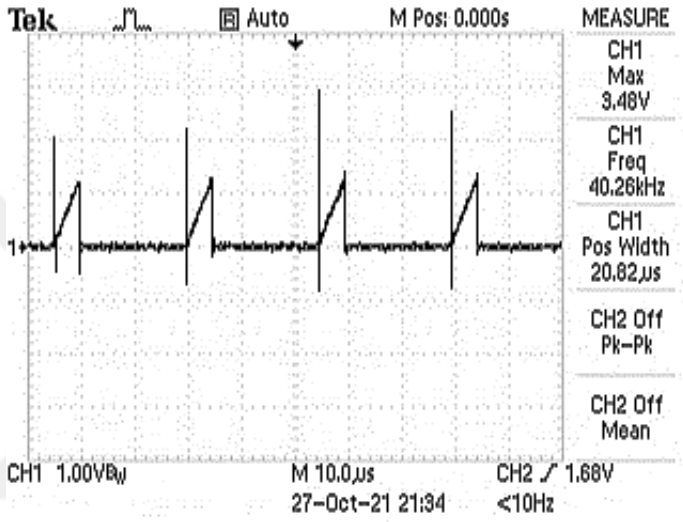

Figure 5.10 : Switch current (Control voltage at 4.3 V).

This spike can be eliminated by a RC spike filter shown in Figure 5.7. The filtered waveform becomes as in Figure 5.11 after the sensed switch current is filtered.

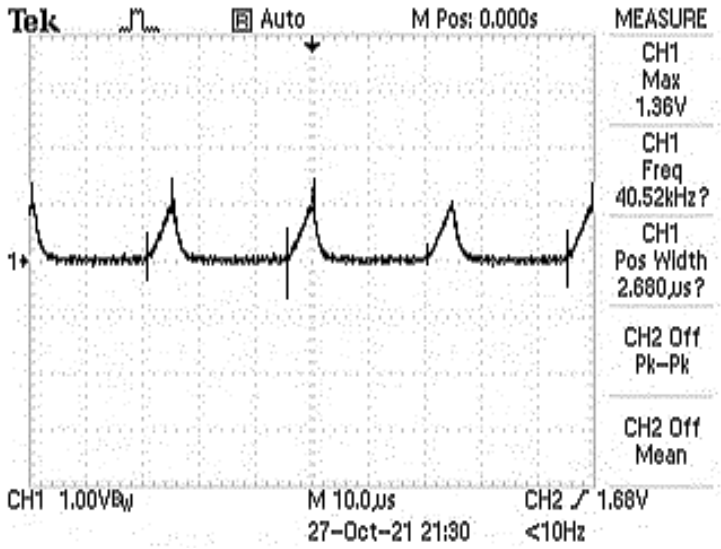

Figure 5.11 : Filtered switch current (Control voltage at 4.3 V).

Second observation is that the switch current raises until 1V since volt/div of Channel 1 is 1 V. Once it reaches the 1V, the switch is closed. According to Equation 5.4, the peak voltage on sensing resistor is calculated as 1.433 V which is greater than the zener diode voltage limitation of 1V. Therefore, the peak threshold voltage is clamped to 1V by zener diode. Then, the peak current of the switch should be 1A theoretically since R_s is 1Ω. So far, the SEPIC LED driver have been working properly with proposed PCMC and theoretical results matches the experimental results.

Third observation is that the input current drawn by AC input shown in Figure 5.12 is similar to waveform in Figure 4.9. This indicates that the power factor will be low. The attenuator of the isolation amplifier for related channel is chosen as 1V/A. Hence, the rms voltage value of 336 mV is actually 336 mA. And, the line frequency is 50 Hz.

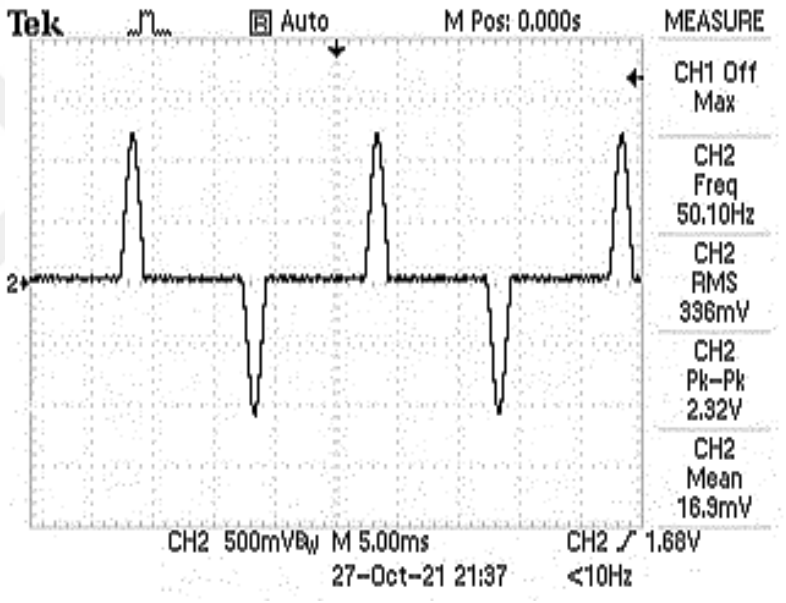

Figure 5.12 : AC input current (Control voltage at 4.3 V).

The control voltage should be reduced from 4.3 V to reduce brightness of the LED. When this threshold voltage reduces, switch will turn off earlier. That means the inductor L_2 stores less energy during the switch turned on position. Hence, the output current will decrease. To verify the output current control, four different control voltage V_c is applied to driver circuit. Output current I_{out}, output voltage V_{out}, input current I_{in}, input voltage V_{in}, active power P_{in} drawn by input are recorded for each control voltage in Table 5.4.

Table 5.4 : Output current adjustment and efficiency calculation for different control voltages.

V_c	I_{out}	V_{out}	P_{out}	I_{in}	V_{in}	S_{in}	P_{in}	Cos φ	η
4.3V	300mA	112.0V	33.60W	0.33A	220V	72.6VA	38W	0.520	88.4%
2.5V	200mA	106.5V	21.30W	0.23A	220V	50.6VA	26W	0.514	81.9%
1.5V	100mA	100.2V	10.02W	0.12A	220V	26.4VA	12W	0.455	83.5%
1.2V	60mA	97.7V	5.862W	0.08A	220V	17.6VA	8W	0.455	73.2%

Output Power $=P_{out} = V_{out} I_{out}$, Apparent Power $=S_{in} = V_{in} I_{in}$, Power Factor = Cos $\varphi = P_{in}/ S_{in}$, Efficiency= $\eta = P_{out}/ P_{in}$

As seen in Table 5.4, at nominal output current, the LED driver efficiency is calculated around 0.88. If the operation output current region is chosen between 100mA-300mA, the SEPIC LED driver by proposed PCMC method is working over 80% efficiency. When the control voltage is 1.2V, the converter efficiency drops. However, there is no need to reduce output power down to 5 Watt. The last case is added just to show the proposed PCMC working properly. Power factor is low around 0.5 for the operation region since the power factor correction technique proposed in Figure 3.15 is not applied.

At 100 mA output current, the PWM signal and the output current are shown in Figure 5.13. As noticed, the duty cycle is smaller than in Figure 5.8. Because, the controller turns off the MOSFET earlier since the control voltage is 1.5 V. The output voltage is nearly hundred volts as shown in Figure 5.14.

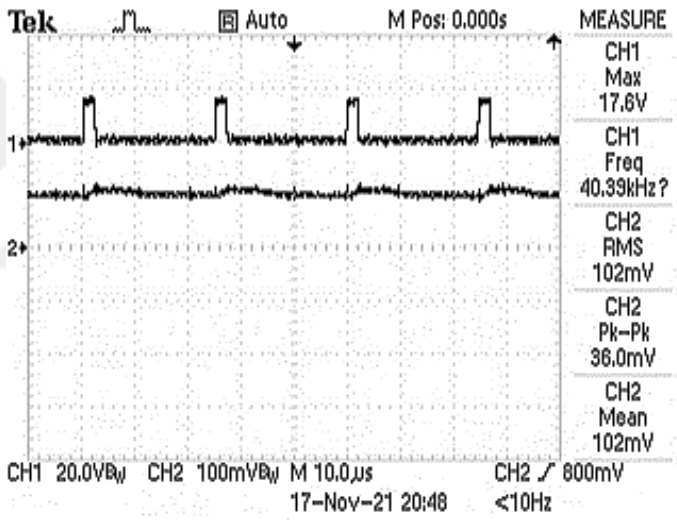

Figure 5.13 : PWM signal and 100 mA output current (Control voltage at 1.5 V).

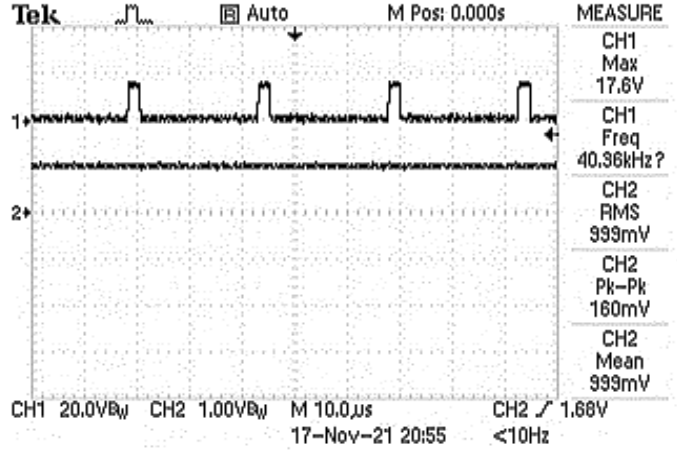

Figure 5.14 : PWM signal and 100 V output voltage (Control voltage at 1.5 V).

The sensed current on sensing resistor and filtered sensed current waveform for 100 mA are shown in Figure 5.15 and 5.16, respectively. According to Equation 5.4, the peak voltage on sensing resistor is calculated as 0.5 V. On the oscilloscope screen of Figure 5.16, volt/div is 500 mV and it is clearly seen that the switch current raises until one division which is equal to 0.5V.

$$V_{R_{SENSE}}(PEAK) = \frac{1.5}{3} = 0.5\,V \tag{5.6}$$

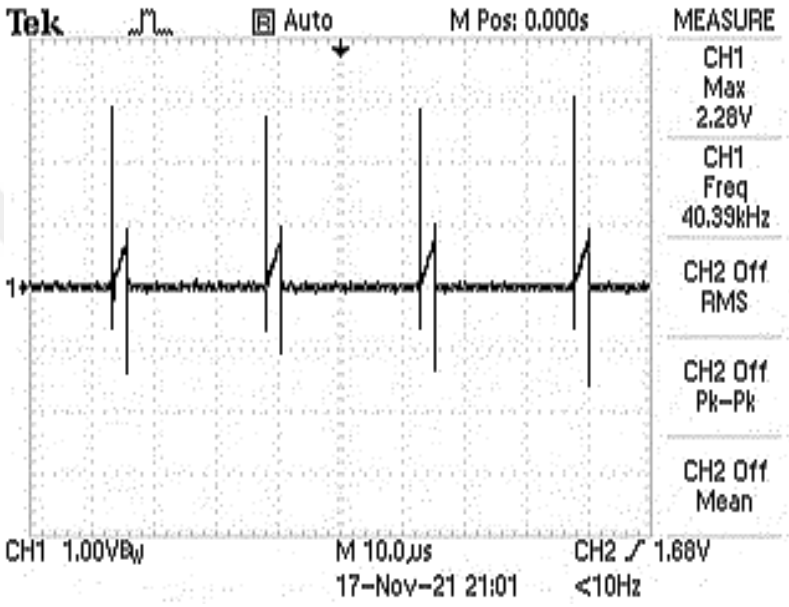

Figure 5.15 : Switch current (Control voltage at 1.5 V).

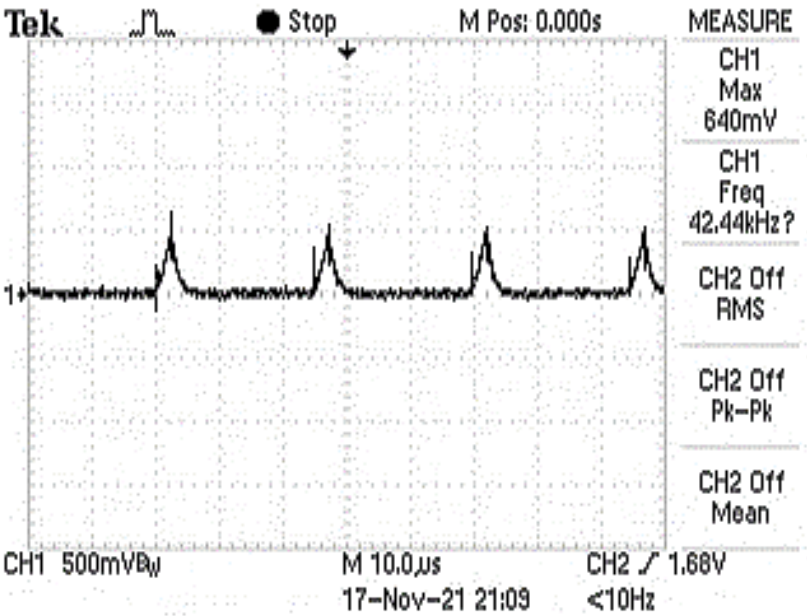

Figure 5.16 : Filtered switch current (Control voltage at 1.5 V).

Power stage and the controller stage of the proposed PCMC SEPIC LED driver are investigated under different conditions. The output current of the circuit can be adjusted by this control method. Output current control is proved in experimental setup. For each output current, the measurements are taken from the experimental setup and efficiency of the converter is calculated. In Figure 5.17 (a), output current vs converter efficiency is plotted. As seen from the Figure 5.17 (a), LED driver is working near to 90% efficiency at nominal output. Except for the 60 mA, the converter efficiency is higher than 80%. Output current is given as a function of control voltage in Figure 5.17 (b).

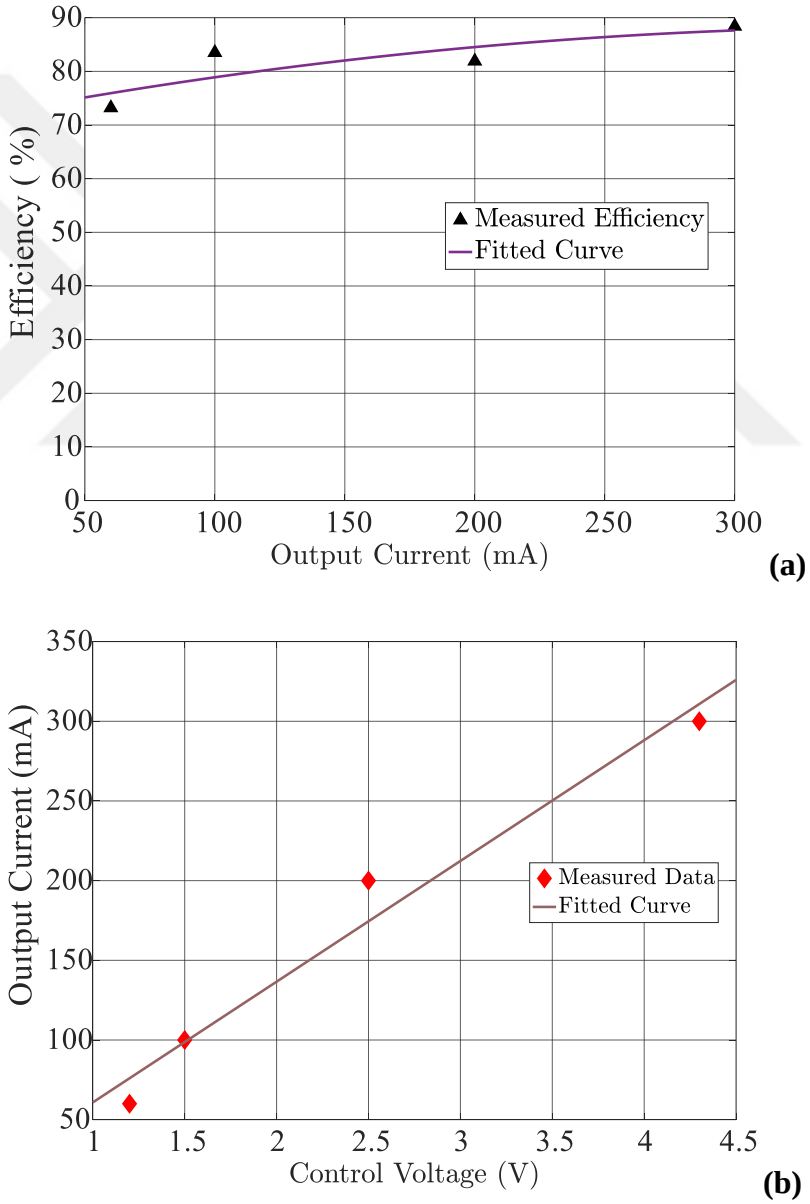

Figure 5.17 : Experimental results of the proposed driver circuit: a) Output current vs. efficiency. b) Control voltage vs. output current.

5.3 Flicker Metrics of the Lighting Source and Its Limitations

With the assumption of LED current is approximately proportional to luminous flux output of the LED, the flicker metrics are calculated from the output current curve. When the line frequency is 50 Hz, there will be 100 Hz ac ripple at the output of the driver because of the full wave rectification. The line period is 20ms, while the output ripple period is 10ms. 300 mA output current is shown in Figure 5.18. Time/division of the Channel 2 is chosen as 5ms. As seen from the Figure 5.18, the period of the AC component can be calculated as 10ms. Only the AC component of the output current is shown Figure 5.19. Here, peak-to-peak current ripple is recorded as 54 mV on the Channel 2 screen. Even though the maximum and minimum value can be calculated via oscilloscope screen, the peak-to-peak current ripple can be misleading because of the noise. To be precise, the output current data is taken to computer and plotted in MATLAB as in Figure 5.20. The record length includes 2500 data. When the noises are ignored, the maximum and minimum values of the output current are 0.328 A and 0.292 A, respectively. Percent flicker or Mod% is easy to calculate from this curve. The maximum and minimum values of the output current are enough to calculate this metric.

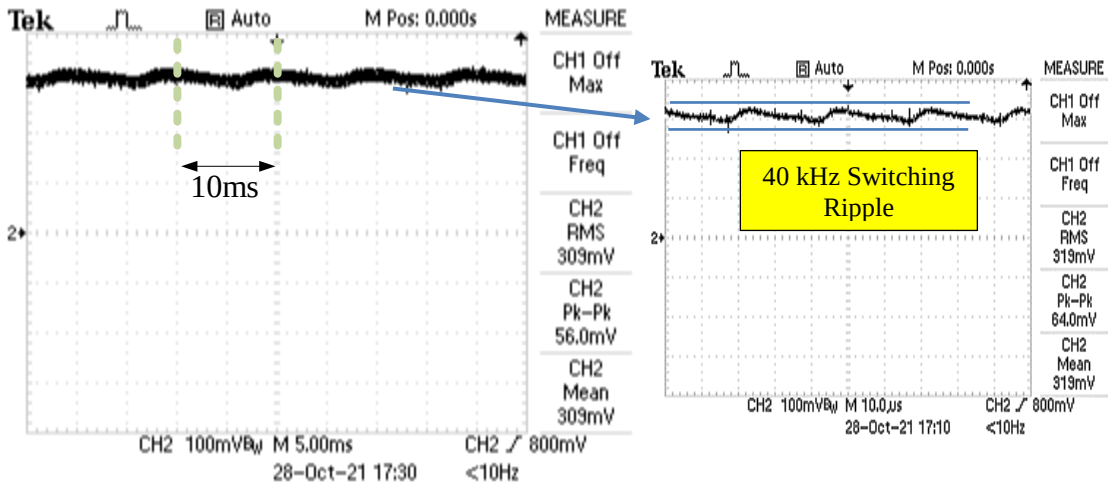

Figure 5.18 : 300 mA output current (DC + 100 Hz AC component).

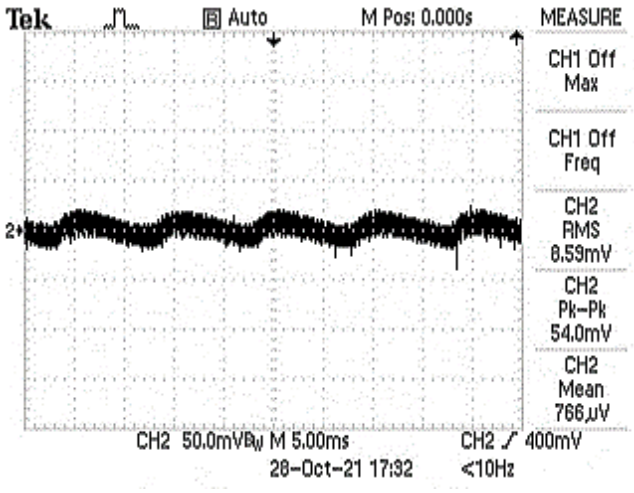

Figure 5.19 : 300 mA output current (100 Hz AC component).

When the Equation 3.3 is applied in Figure 5.20, percent flicker is calculated as 5.806% for the LED at 300 mA. This is acceptable since the Mod% is lower than 8% and stays in low-risk level region. Recommended Percent Flicker at 100 Hz for human health has already shown in Table 3.1.

$$Mod\% = 100\frac{0.328 - 0.292}{0.328 + 0.292} = 5.806\% \tag{5.7}$$

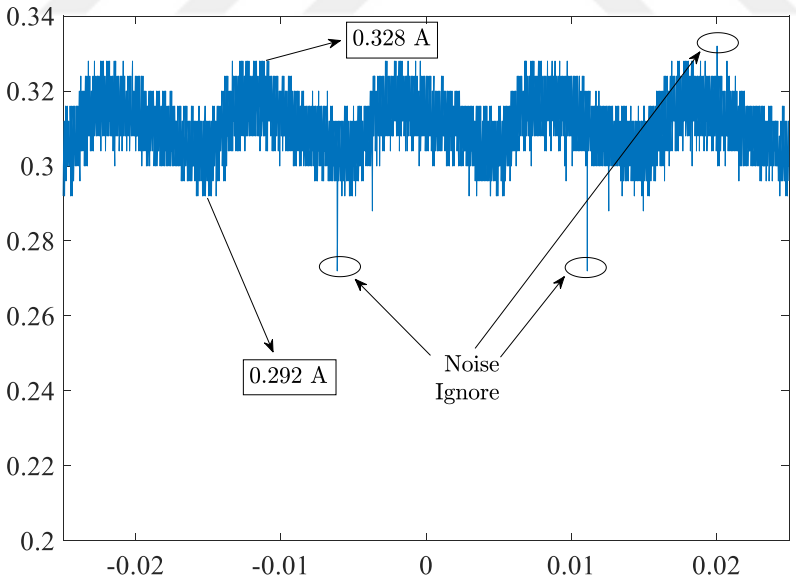

Figure 5.20 : 300 mA output current plotted in MATLAB.

Flicker index is required more complex calculations. Neither from the oscilloscope screen or from the data set, it is hard to calculate this metric. Therefore, there will be some assumptions on output current curve when calculating flicker index as follows:

1. The ac ripple at 40 kHz switching frequency is ignored.

2. The ac ripple at 100 Hz is purely sinusoidal.
3. Maximum and minimum values are 0.328A and 0.292A, while the average value is 0.310A.

With these assumptions, the output current is plotted in Figure 5.21. The MATLAB code is given below for the estimated curve.

```
------------------------------------------------------------------------
dt=1/10000;                         % seconds per sample
Stoptime=0.025;                     % seconds
t=(-0.025:dt:Stoptime);             % seconds
dc= 0.310;                          % DC component
Maximum=0.328;                      % Amp
Minimum=0.292;                      % Amp
ripple=Maximum-Minimum;             % Amp
ac=(ripple/2)*cos(2*pi*100*t);      % AC component
Iout=dc+ac;                         % AC+DC component
plot(t,Iout)                        % Output current vs time
------------------------------------------------------------------------
```

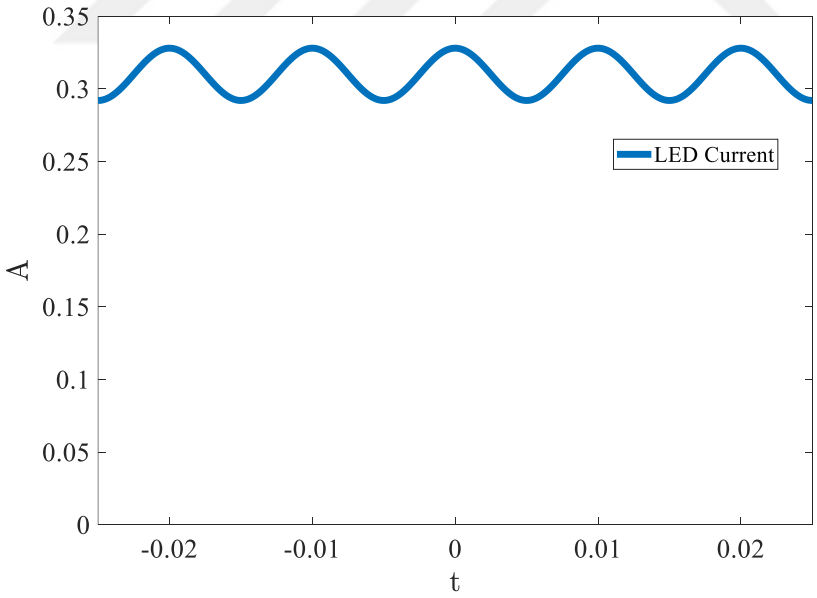

Figure 5.21 : Estimated 300 mA output current curve for calculating flicker index and mod%.

To calculate flicker index, area above the average output current and the total area of the output current curve are needed in a single period. These areas are illustrated in Figure 5.22.

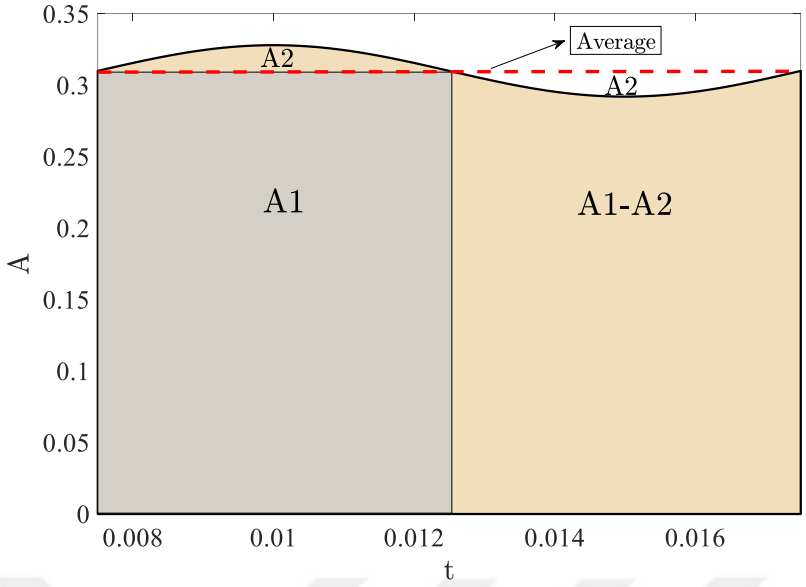

Figure 5.22 : Flicker index calculation for 300 mA.

In Figure 5.22, area above the average output current is A2 and the total area of the output current curve for a single cycle is the summation of A2, A1 and A1-A2 which gives us 2xA1. Then, flicker index can be calculated according to Equation 3.2 as follows:

$$Flicker\ Index = \frac{A2}{2A1} \tag{5.8}$$

A1 is the area of rectangular shape which is calculated as:

$$A1 = 0.310 \cdot (0.0125 - 0.0075) = 1.55 \cdot 10^{-3} = 0.00155 \tag{5.9}$$

A2 has a sinusoidal shape which can be calculated as:

$$A2 = \int_{0.0075}^{0.0125} \left(I_{max} - I_{average}\right) cos\left(2pif_{flicker}t\right) dt \tag{5.10}$$

$$A2 = \int_{0.0075}^{0.0125} (0.018) cos(2pi100t) dt = 0.0000572958 \tag{5.11}$$

$$Flicker\ Index = \frac{0.0000572958}{2 \cdot 0.00155} = 0.0185 \tag{5.12}$$

The percent flicker and flicker index will be calculated also for 100 mA output current. First, 100 mA output current at the flicker frequency is shown in Figure 5.23. The plotted 100 mA output current in MATLAB is shown in Figure 5.24. There will be

similar assumptions on output current curve as before in 300 mA to calculate flicker index and percent flicker. Estimated 100 mA curve is plotted in Figure 5.25 by following assumptions.

1. The ac ripple at 40 kHz switching frequency is ignored.
2. The ac ripple at 100 Hz is purely sinusoidal.
3. Maximum and minimum values are 0.114 A and 0.100A, while the average value is 0.107A.

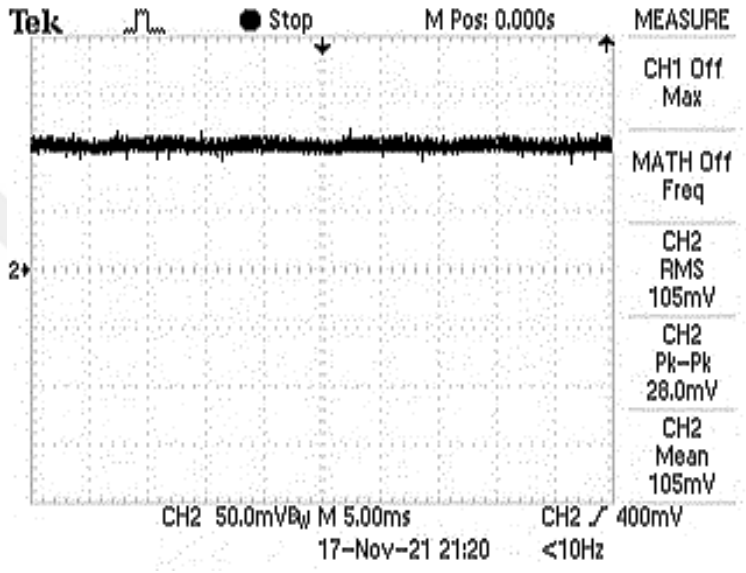

Figure 5.23 : 100 mA output current (DC + 100 Hz AC component): a) Without cursor measurements. b) With cursor measurements.

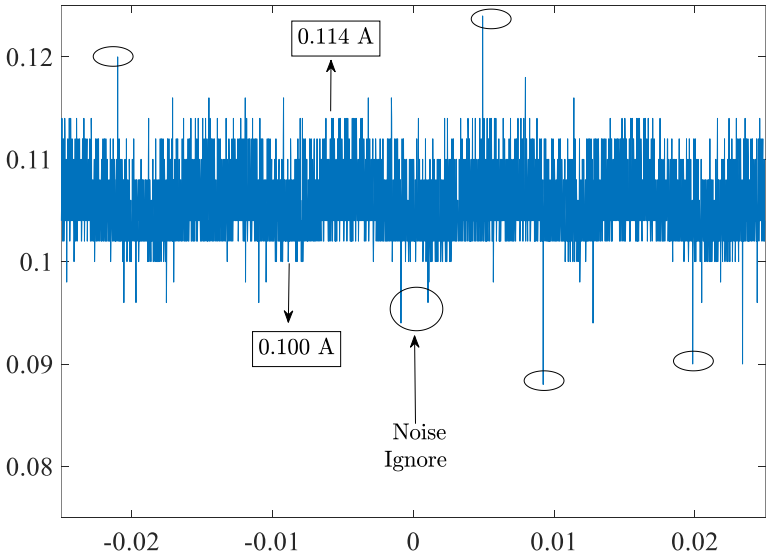

Figure 5.24 : 100 mA output current plotted in MATLAB.

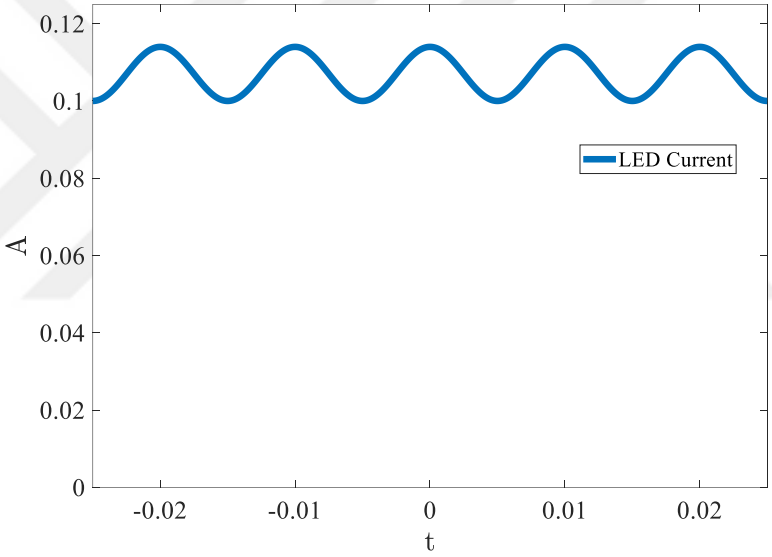

Figure 5.25 : Estimated 100 mA output current curve for calculating flicker index and mod%.

According to Equation 3.3, percent flicker or mod% is calculated as

$$Mod\% = 100\frac{0.114 - 0.100}{0.114 + 0.100} = 6.54\% \tag{5.13}$$

while operating at 100 mA output current. This 6.54% is also lower than recommended percent flicker at 100 Hz. The flicker index can be calculated by Equation 5.8 which is shown for 300 mA. It is an easy calculation method. When this formula applied to one period of the 100 mA estimated curve shown in Figure 5.26, the flicker index can be calculated as in Equation 5.17.

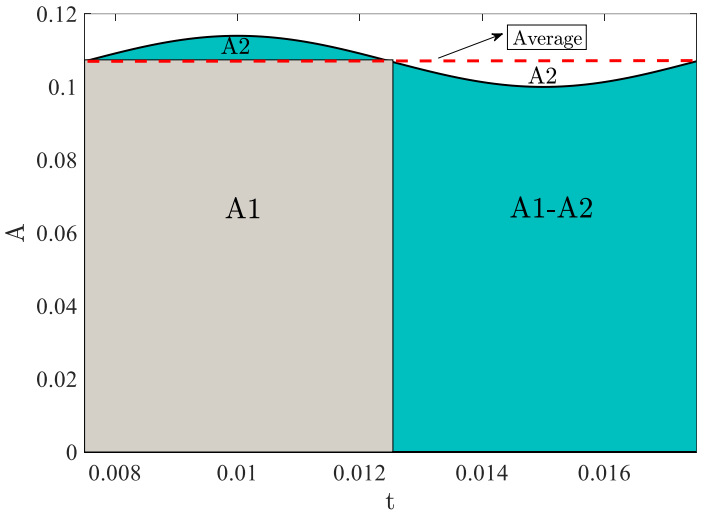

Figure 5.26 : Flicker index calculation for 100 mA.

A1 is the area of rectangular shape which is calculated as:

$$A1 = 0.107 \cdot (0.0125 - 0.0075) = 5.35 \cdot 10^{-4} = 0.000535 \tag{5.14}$$

A2 has a sinusoidal shape which can be calculated as;

$$A2 = \int_{0.0075}^{0.0125} (I_{max} - I_{average}\ ) cos(2pif_{flicker}t) dt \tag{5.15}$$

$$A2 = \int_{0.0075}^{0.0125} (0.007) cos(2pi100t) dt = 0.0000222817 \tag{5.16}$$

$$Flicker\ Index = \frac{0.0000222817}{2 \cdot 0.000535} = 0.0208 \tag{5.17}$$

To sum up, flicker metrics of the LED at the 300 mA and 100 mA output current are calculated from the estimated curves and represented in Figure 5.27. It should be reminded that average values of the estimated output currents are 310 mA and 107 mA. However, these values can be rounded as 300 mA and 100mA considering measurement device tolerance and laboratory conditions. Also, the flicker measurements taken from the output current of the LED requires confirmation from the light output curve of the LED. There is a benefit to remind this, even though the LED current is proportional to light output. In addition, peak-to-peak output current ripple is obtained as 11.6% at nominal output current, while it is obtained as 13.7% at 100 mA.

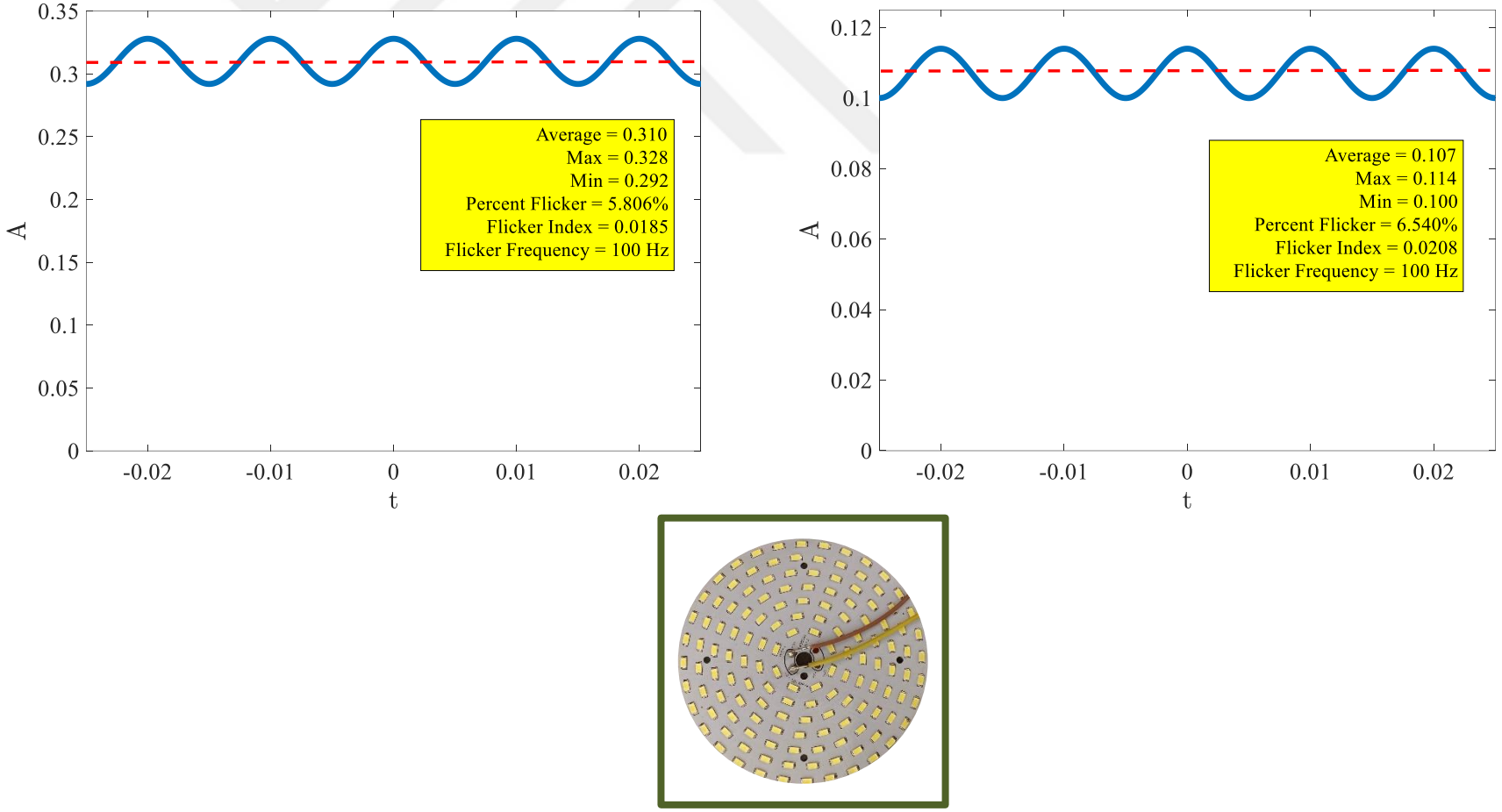

Figure 5.27 : Flicker metrics of the LED at 300 mA and 100 mA output current.

5.4 LED Driver Tester

The driver circuit is also tested by LT-101A LED driver analyzer from EVERFINE company. This device is designed to analyze input and output electrical performance of LED drivers. The prototype driver circuit is tested at 300 mA and 210 mA output current.

Table 5.5 : Results of the LED driver tester.

I_{out}	V_{out}	P_{out}	I_{in}	V_{in}	P_{in}	Cos φ	η
300mA	110.3V	33.40W	0.294A	220V	36.97W	0.568	90.3%
210mA	106.5V	22.34W	0.209A	220V	25.12W	0.545	88.9%

Efficiency of the driver is obtained around 90.3% and 88.9%, while operating at 300 mA and 210 mA, respectively.

6. CONCLUSIONS

In this thesis, the single-ended primary inductor converter (SEPIC) that can be designed for a wide range of input and output ratios is chosen as adjustable current LED driver. As for the control technique, a peak current mode control method is proposed to control LED brightness. Besides, flicker on LED string are measured for different output current levels and tested whether it is harmful or not for human health. A SEPIC LED driver by the proposed method is carried out in practice. To see findings clearly and emphasis key points, conclusions of this thesis are sorted out one by one as follows:

1) A modified peak-current-mode control method is proposed for 30-Watt SEPIC LED driver.
2) In proposed control method, LED current is adjusted by a control voltage. Switch current is sensed by a resistor in every switching period, and controller turns off the switch when this current reaches peak threshold value determined by the control voltage. Hence, LED brightness is controlled by changing this control voltage. Simply, LED brightness can be increased by increasing the control voltage, or can be decreased by decreasing the control voltage in proposed control method.
3) Driver circuits; with PFC and without PFC are simulated in PSIM environment. In simulation, DC-DC SEPIC converter is designed to operate in continuous conduction mode. Required DC voltage at the input of the SEPIC converter is rectified from AC mains. For the controller, a current-mode-control IC UC3842 is used. 100 kHz switching frequency is selected for the simulations.
4) In simulation, driver circuit without PFC has focused on a robust output current control from 50mA up to 300 mA, and low level of flicker. However, the power factor is obtained significantly low because of the input capacitor filter. Also, the driver circuit suffers from this bulk capacitor which increases the volume of the driver and cost. On the other hand, percent flicker on LED lamp is

measured very low at No Observable Effect Level (NOEL) meaning that no health risk is concerned. According to our findings, flicker index and percent flicker will be far below any biological effect region if the LED is driven by this circuit. The major disadvantage of this circuit is the bad power factor at the AC side.

5) In simulation, driver circuit with PFC aims to improve power factor. Bulk capacitor at the input is removed. Output current control from 90 mA up to 300 mA has been achieved. The output current ripple is obtained around 16%, while the output voltage ripple is 2%. Output current and voltage ripple are obtained higher than in the first circuit but kept within acceptable levels. One of the drawbacks of this circuit is the limitations mentioned earlier that distorts the input current shape in Figure 4.16. However, high power factor is kept above 0.9 for operation region between 100mA-300mA. The highest power factor is recorded as 97.97% when the output current is 279 mA. Unfortunately, the percent flicker on LED is slightly higher than the limits for low risk level while operating below 300 mA. According to our findings, output capacitor filter can be enlarged to reduce output current ripple which leads to reduce the percent flicker. Nevertheless, flicker index has been kept below 0.1 that is the limit allowed to be used in general lighting applications.
6) In practice, a current-mode PWM Controller TL3845 that has a similar operation to UC3842 is used for the controller. The switching frequency is selected as 40 kHz. At this switching frequency, 48 mH inductors were required to operate in CCM. This inductor values were not applicable and not found in the market. To reduce the inductor values and still operate in CCM, the switching frequency could be increased. However, higher switching frequencies are related with the noise, switching losses, and EMI issues. Also, TL3845 used in driver is limited by 500 kHz operation. Therefore, it is preferred to operate SEPIC converter in discontinuous conduction mode. This allows to select inductor values much lower than 48 mH. In DCM, it was known that currents stress on components will be higher but there was no problem since the peak current on switching device could be controlled by proposed control method.
7) In practice, outer voltage feedback is removed since the current reference is determined directly by the control voltage. Therefore, there is no need to use

voltage feedback loop and related pin is connected to ground. Overvoltage protection on LED is accomplished by controlling the output current. As long as the current flowing through the LED is controlled, the over-voltage on LED will be prevented. This is proved by the experimental results for different currents. When operating the driver at nominal output and minimum output current for a while, the LED voltage is kept constant. In addition, a proper heat sink can be added for over-heating.

8) In practice, calculation of the peak current on sensing resistor has become much easier by adding two Schottky Diodes at pin 1 of the controller. This technique is called as "Reduction of the Clamp Level" which compensates the internal voltage drops at related pin. This technique is adapted to our proposed control method. Furthermore, a new formula that decides when the switch should be turned off is given. In Figure 5.15, at 100 mA output current, it is seen that switch current raises until the same value calculated by this formula. Also, once the switch current reaches this threshold value, the switch is turned off. Moreover, 1V zener diode voltage limitation that keeps the maximum current at 1 A can be seen in Figure 5.11. Therefore, theoretical background of the peak current control is confirmed in experimental setup.
9) In practice, LED current has been controlled from 60 mA up to 300 mA by adjusting the control voltage. Hence, LED brightness is controlled. Converter efficiency is calculated at each output current: 300 mA, 200 mA, 100 mA, 60 mA. Highest energy efficiency is recorded as 88.4% at 300 mA. Results shows that the converter can be operated over 80% efficiency between 100 mA and 300 mA output current. Owing to proposed PCMC method, adjustable output current and high efficiency SEPIC LED driver is prototyped.
10) In practice, however, any power factor correction technique is not applied for the experimental driver circuit. As expected, power factor is obtained low around 0.5 over the operation region. As for the power rating, output power varies roughly from 5 Watt to 35 Watt. Hence, consumers can adjust output power just as required.
11) In practice, the flicker produced by lighting source is measured from the output current curve. Flicker index and percent flicker are the most commonly used flicker metrics when measuring flicker. Therefore, both metrics are measured for output current of 100mA and 300 mA. Results from the lighting source

show that the percent flicker at the minimum and nominal output current satisfies the limits for low-risk level region. Moreover, the flicker index at 100 Hz is also less than 0.1 which is unlikely to produce harmful effects on human health. Flicker metrics have been showed that this LED can be used in general lighting applications by the proposed PCMC SEPIC LED driver.

In conclusion, LED driver circuits have become much important by the increasing demand on LED technology. Therefore, the driver circuit design is an essential task. The SEPIC driver circuit by the proposed peak current mode control strategy in this thesis offers LED brightness control for the consumer comfort, a high efficient system, and finally human health friendly lighting source with low level of flicker.

For future work, the proposed peak current mode controlled SEPIC LED driver with PFC will be applied experimentally. Moreover, the flicker measurements of LED will be taken from the light output curve to verify measurements taken from the output current curve.

REFERENCES

[1] **Chiu, H. J., Lo, Y. K., Chen, J. T., Cheng, S. J., Lin, C. Y., and Mou, S. C.** (2010). A high-efficiency dimmable LED driver for low-power lighting applications, *IEEE Transactions on Industrial Electronics*, vol. 57, no. 2, pp. 735–743, doi: 10.1109/TIE.2009.2027251.

[2] **Yadav, A., Pachauri, R. K., and Chauhan, Y. K.** (2016). Power quality improvement using PFC SEPIC converter for LED bulb adaptable for universal input voltage. In *2016 IEEE 1st International Conference on Power Electronics, Intelligent Control and Energy Systems (ICPEICES)*, pp. 1–6, doi: 10.1109/ICPEICES.2016.7853725.

[3] **Ye, Z., Greenfeld, F., and Liang, Z.** (2008). Design considerations of a high power factor SEPIC converter for high brightness white LED lighting applications. In *PESC Record - IEEE Annual Power Electronics Specialists Conference*, pp. 2657–2663, doi: 10.1109/PESC.2008.4592343.

[4] **Wang, Y., Alonso, J. M., and Ruan, X.** (2017). A Review of LED Drivers and Related Technologies. *IEEE Transactions on Industrial Electronics*, vol. 64, no. 7, pp. 5754–5765, doi: 10.1109/TIE.2017.2677335.

[5] **Wang, S., Ruan, X., Yao, K., Tan, S., Yang, Y., and Ye, Z.** (2012). A Flicker-Free Electrolytic Capacitor-Less AC – DC LED Driver. *IEEE Transactions on Power Electronics*, vol. 27, no. 11, pp. 4540–4548.

[6] **Şehirli, E., Altınay, M., Üstün, Ö., and Çakır, B.** (2017). Comparison of single phase buck-boost and sepic LED driver. *Light and Engineering*, vol. 25, no. 4, pp. 92–98.

[7] **Hayirli, I. H., Kelleci, B., Kivanc, O. C., Ozturk, S. B., Tuncay, R. N., and Citci, M. O.** (2019). Design and Analysis of 240 Watt SEPIC Converter for LED Applications. In *2019 IEEE 28th International Symposium on Industrial Electronics (ISIE)*, pp. 804–809, doi: 10.1109/ISIE.2019.8781396.

[8] **Kouzou, A.** (2018). Power Factor Correction Circuits. In *Power Electronics Handbook*, 4th ed., no. d, Elsevier Inc., pp. 529–569.

[9] **IEEE Power Electronics Society.** (2015). IEEE Recommended Practices for Modulating Current in High-Brightness LEDs for Mitigating Health Risks to Viewers, *IEEE Std 1789-2015*, pp. 1–80, doi: 10.1109/IEEESTD.2015.7118618.

[10] **Energy Focus.** (2017). Optical Flicker in Lighting, whitepaper.

[11] **Lamar, D. G., Zúñiga, J. S., Alonso, A. R., González, M. R., and Álvarez, M. M. H.** (2009). A very simple control strategy for power factor correctors driving high-brightness LEDs, *IEEE Transactions on Power*

Electronics, vol. 24, no. 8, pp. 2032–2042, 2009, doi: 10.1109/TPEL.2009.2020900.

[12] **Şehirli, E., and Üstün, Ö.** (2016). Design and Application of High Power Factor SEPIC LED Driver. In *2016 National Conference on Electrical, Electronics and Biomedical Engineering (ELECO)*, 2016, pp. 115–119.

[13] **Wang, Y., Huang, J., Shi, G., Wang, W., and Xu, D.** (2016). A single-stage single-switch LED driver based on the integrated SEPIC circuit and class-E converter, *IEEE Transactions on Power Electronics*, vol. 31, no. 8, pp. 5814–5824, 2016, doi: 10.1109/TPEL.2015.2489464.

[14] **Mahadeokar, S., and Sardeshmukh, M.** (2015). Energy efficient PWM Dimmable Smart Digital LED driver. In *International Conference on Energy Systems and Applications, ICESA 2015*, pp. 306–311, doi: 10.1109/ICESA.2015.7503361.

[15] **Fang, P., Liu, Y., and Sen, P. C.** (2015). A Flicker-Free Single-Stage Offline LED Driver, *IEEE Journal of Emerging and Selected Topics in Power Electronics*, vol. 3, no. 3, pp. 654–665.

[16] **Chen**, **R.** (2015). Analysis and design of DCM SEPIC PFC with adjustable output voltage (Master's Thesis). Virginia Polytechnic Institute and State University, Virginia.

[17] **Zhang, D.** (2013). AN-1484 Designing A SEPIC Converter. Texas Instruments Incorporated, Application Report, SNVA168E.

[18] **Kesik, E. P.** (2018). Design and Implementation of a SEPIC Battery Charger for Automotive PV Applications (Master's Thesis). Istanbul Technical University, Istanbul.

[19] **Hayirli, I. H.** (2019). Design and Analysis of High Power SEPIC Converter (Master's Thesis). Istanbul Okan University, Istanbul.

[20] **Karaarslan, A.** (2019). Bilgisayar Sistemlerinde SEPIC Dönüştürücü Uygulaması ve Benzetim Çalışması, *Bilişim Teknolojileri Dergisi*, vol. 12, no. 2, pp. 111–117, doi: 10.17671/gazibtd.540127.

[21] **Erickson, R. W., and Maksimovic, D.** (2004). *Fundamentals of Power Electronics*, 2nd ed. New York: Kluwer Academic Publishers.

[22] **Eng, V., Pinsopon, U., and Bunlaksananusorn, C.** (2009). Modeling of a SEPIC converter operating in continuous conduction mode. In *2009 6th International Conference on Electrical Engineering/Electronics, Computer, Telecommunications and Information Technology*, pp. 136-139, doi: 10.1109/ECTICON.2009.5136982..

[23] **Nishat, M. M., Oninda, M. A. M., Faisal, F., and Hoque, M. A.** (2018). Modeling, Simulation and Performance Analysis of SEPIC Converter Using Hysteresis Current Control and PI Control Method. In *2018 International Conference on Innovations in Science, Engineering and Technology*, pp. 7–12, doi: 10.1109/ICISET.2018.8745619.

[24] **Kircioğlu, O., Ünlü, M., and Çamur, S.** (2016). Modeling and analysis of DC-DC SEPIC converter with coupled inductors. In 2016 International Symposium on Industrial Electronics, doi: 10.1109/INDEL.2016.7797807.

[25] **Kotecha, R. M.** (2010). Analysis and Comparison of Popular Models for Current-Mode Control of Switch Mode Power Supplies (Master's Thesis). Wright State University.

[26] **Mammano, R.** (1999). Switching Power Supply Topology Voltage Mode vs. Current Mode. Texas Instruments Incorporated, Design Note, DN-62.

[27] **Dixon**, **L.** (1990). Average current mode control of switching power supplies. Unitrode Power Supply Design Seminar Handbook, Unitrode Corporation.

[28] **S. T. Microelectronics.** UC3842 Provides Low-Cost Current-Mode Control. Application Note, AN246.

[29] **Ali, M., Orabi, M., Ahmed, M. E., and El-Aroudi, A.** (2010). A single stage SEPIC PFC converter for LED stage lighting applications. In *2010 IEEE International Conference on Power and Energy*, pp. 501–506, doi: 10.1109/PECON.2010.5697634.

[30] **Ali, M., Orabi, M., Ahmed, M. E., and El-Aroudi, A.** (2011). Design considerations of a single-stage LED lamp driver with power factor correction. In *2011 2nd International Conference on Electric Power and Energy Conversion Systems (EPECS)*, pp. 1–6, doi: 10.1109/EPECS.2011.6126799.

[31] **Avago Technologies.** (2010). Driving High Power and High Brightness LEDs. Application Note 5310.

[32] **DiLaura, D. L., Houser, K. W., Mistrick, R. G., and Steffy, G. R.** (2011). *The lighting handbook*, 10th ed. New York: Illuminating Engineering Society.

[33] **Chen, P., Chen, Y. H., Marquez, J. C. J. S., Wang, R. T., Chen, J. J., and Hwang, Y. S.** (2020). Low Flicker Dimmable Multichannel LED Driver with Matrix-Style DPWM and Precise Current Matching, *IEEE Transactions on Very Large Scale Integration (VLSI) Systems.* vol. 28, no. 11, pp. 2233–2242, doi: 10.1109/TVLSI.2020.3003520.

[34] **Poplawski, M., and Miller, N.** (2013). Flicker in Solid-State Lighting: Measurement Techniques, and Proposed Reporting and Application Criteria. In Proceedings of CIE Centenary Conference "Towards a new century of light".

[35] **Van Roy, R.** (2014). Minimizing Light Flicker in LED Lighting Applications. Richtek Application Note, AN022.

[36] **Texas Instruments.** Uc3842/3/4/5 Provides Low-Cost Current-Mode Control. Unitrode Application Note, U-100A.

[37] **International Rectifier**. IRF 840 Power MOSFET, Datasheet.

[38] **On Semiconductor.** (2006). Switchmode™ Power Rectifiers, MUR1560 Datasheet, Feb. 2006.

[39] **Core Master.** Filter Choke / SRC Type, Inductor Datasheet.

[40] **Texas Instruments. (2016).** TLx84x Current-Mode PWM Controllers, TL3845 Datasheet, 2016.

[41] **De Lorenzo.** DL 1013T1 Variable Three-Phase Power Supply, Datasheet.
[42] **De Lorenzo.** DL 2642 Isolation Amplifier, Datasheet.

APPENDICES

APPENDIX A: Measured V-I data of 9 Watt LED string.

APPENDIX B: Measured V-I data of 15 Watt LED string.

APPENDIX C: Internal Structure of UC3842 (Data sheet).

APPENDIX D: Pin Configuration and Functional Diagram of TL3845 (Data sheet).

APPENDIX E: PSIM model for UC3842.

Table A.1 : Measured V-I data of the 9 Watt LED string.

Voltage (V)	Current (mA)
0	0
18	0
20.5	3.1
20.9	8.6
21.1	12.8
21.6	26.9
21.9	37
22.1	45
22.8	72
23	90
23.5	113
24.2	157
24.6	180
24.8	220
24.9	250
25.2	260
25.3	280
25.9	300
26.1	340
26.3	360

Table A.2 : Measured V-I data of the 15 Watt LED string.

Voltage (V)	Current (mA)
0	0
36	0
42.5	50
44.4	100
44.6	120
45	130
45.3	150
45.7	160
46.2	180
46.8	200
47.6	240
47.9	260
48.5	280
48.9	300
49	310
49.3	320
49.7	350

APPENDIX C

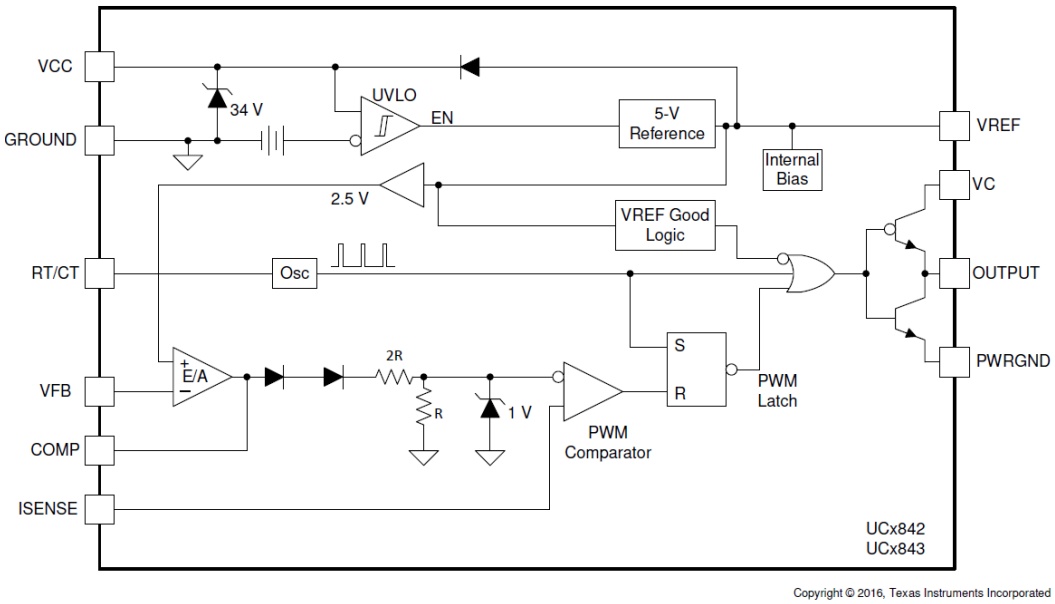

(a)

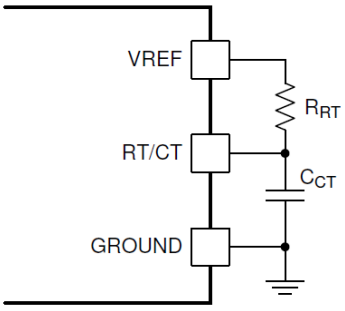

(b)

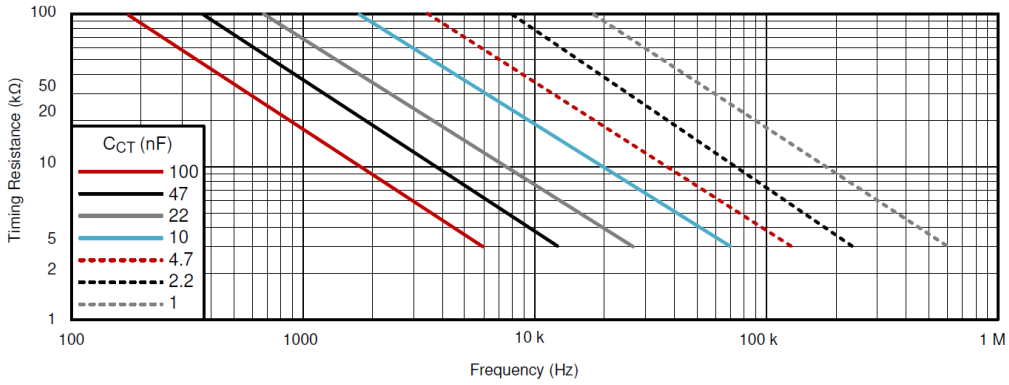

(c)

Figure C.1 : Internal structure of UC3842: a) UC3842 functional block diagram. b) Oscillator circuit. c) Timing resistance vs oscillator frequency.

APPENDIX D

Pin Configuration and Functions

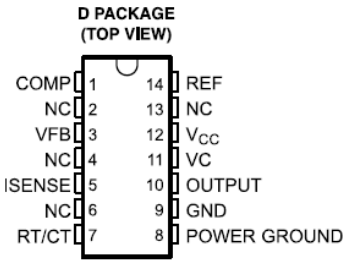

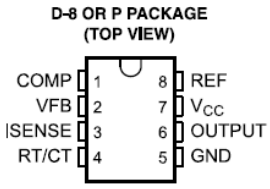

NC – No internal connection

Pin Functions

PIN			TYPE	DESCRIPTION
NAME	D	D-8 or P		
COMP	1	1	I/O	Error amplifier compensation pin
GND	9	5	—	Device power supply ground terminal
ISENSE	5	3	I	Current sense comparator input
NC	2, 4, 6, 13	-	—	Do not connect
OUTPUT	10	6	O	PWM Output
POWER GROUND	8	-	—	Output PWM ground terminal
REF	14	8	O	Oscillator voltage reference
RT/CT	7	4	I/O	Oscillator RC input
VC	11	-	—	Output PWM positive voltage supply
V_{CC}	12	7	—	Device positive voltage supply
VFB	3	2	I	Error amplifier input

Functional Block Diagram

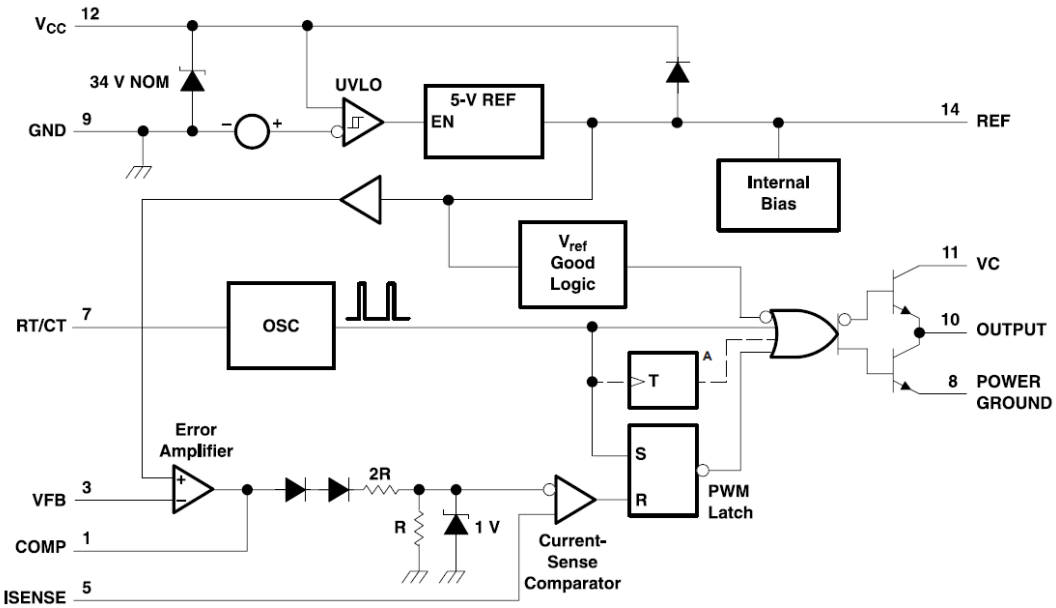

A. The toggle flip-flop is present only in TL2844, TL2845, TL3844, and TL3845. Pin numbers shown are for the D (14-pin) package.

Figure D.1 : Pin configuration and functional diagram of TL3845.

APPENDIX E

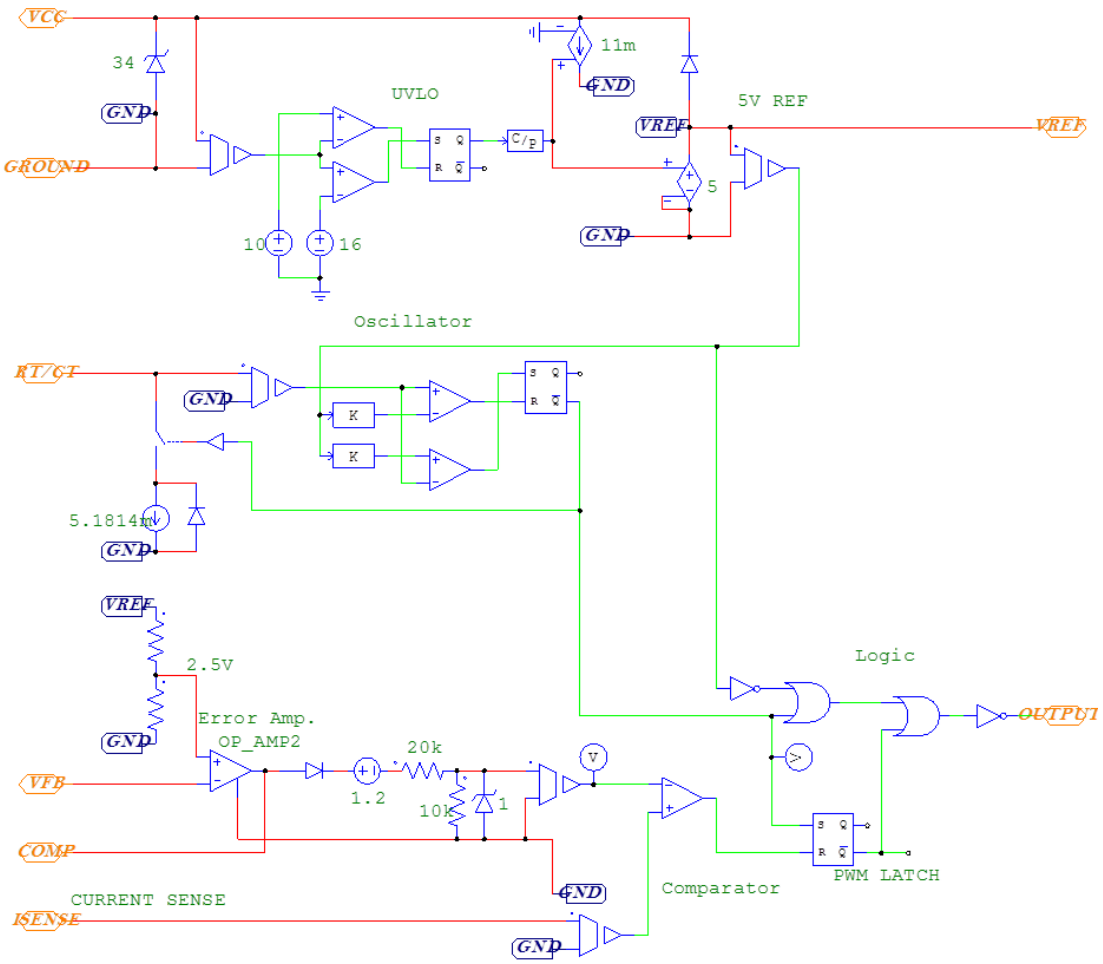

Figure E.1 : PSIM model for UC3842.

CURRICULUM VITAE

Name Surname **:** Kerim ÖRÜKLÜ

EDUCATION **:**

- **B.Sc.** **:** 2018, Ondokuz Mayis University, Engineering Faculty, Department of Electrical and Electronics Engineering

PROFESSIONAL EXPERIENCE:

- 2020-Present, Research Assistant, Eskisehir Technical University, Department of Electrical and Electronics Engineering.

PUBLICATIONS, PRESENTATIONS AND PATENTS ON THE THESIS:

OTHER PUBLICATIONS, PRESENTATIONS AND PATENTS:

- **M. Lordoglu, U. Polat, K. Oruklu, and D. Yildirim**. 2021. Half-Bridge LLC Resonant Converter Design for High Voltage Battery to Low Voltage Battery Conversion in Electric Vehicles, *13th International Conference on Electrical and Electronics Engineering*, Nov. 25-27, 2021 Bursa, Turkey.